Title
Imaging thoughts - an investigation of neural circuits encoding changes in behavior in zebrafish

Author
Oldfield, Claire Sylvie

Publication Date
2016

Peer reviewed|Thesis/dissertation

Imaging thoughts - an investigation of neural circuits encoding changes in behavior in zebrafish

by

Claire Oldfield

A dissertation submitted in partial satisfaction
of the requirement for the degree of

Doctor of Philosophy

in

Neuroscience

In the Graduate Division of the
University of California, Berkeley

Committee in charge:

Professor Ehud Y. Isacoff, Chair
Professor Dan E. Feldman
Professor Marla Feller
Professor Craig Miller

Summer 2016

Abstract

Imaging thoughts - an investigation of neural circuits encoding changes in behavior in zebrafish

By Claire Oldfield

Doctor of Philosophy in Neuroscience

University of California, Berkeley

Professor Ehud Isacoff, Chair

Experience influences how we perceive the world, how we interact with our environment, and how we develop. In fact, almost all animals can modify their behavior as a result of experience. Psychologists have long distinguished between different forms of learning and memory, and later determined that they are encoded in distinct brain areas. Neuroscientists dating back to Santiago Ramón y Cajal suggested that learning and memory might be encoded as changes in synaptic connections between neurons, but it wasn't until the second half of the 20th century that experimental evidence corroborated this idea. Specific firing patterns of neurons during learning results in strengthening or weakening of synapses, and morphological modifications that can lead to long lasting changes in neural circuits. The molecular mechanisms that drive these changes are remarkably conserved across vertebrates. However, understanding how synaptic plasticity is integrated at a network level remains a big challenge in neuroscience. Relatively few studies have focused on how neural circuits encode changes in behavior in a natural context.

In this dissertation I present two such examples using calcium imaging and optogenetic techniques in larval zebrafish. First, in collaboration with others, I studied neural activity that drives the onset of the very first behavior of the fish, tail coiling. We characterized the transition of spontaneous activity in the spinal cord from a sporadic, uncorrelated state, to a regular and synchronized state. We determined that this transition occurred through coalescence of local microcircuits, and that inhibiting the early sporadic activity impaired normal development of the central pattern generator network. Second, I studied how experience of prey affects hunting behavior and underlying neural activity. I developed a paradigm to assess the effect of prior hunting on prey capture behavior and showed that experienced fish initiate more captures than their naïve counterparts. I next established that experience does not affect the ability of the fish to see prey. Rather, experience increases the probability that activity in visual areas will evoke a capture initiation. This is accomplished by increasing the impact of information transfer from visual to motor areas, possibly due to increased activity in forebrain areas for experienced fish.

Dedication

To my family and friends,

Thank you for your continued support.

Table of Contents

Acknowledgements

The work presented in this dissertation would not have been possible without the scientific and personal support I received throughout my PhD research.

I would first like to thank Udi Isacoff for welcoming me in his lab, and being a great advisor for the past five years. Udi gave me scientific freedom to pursue the project that most interested me, even though it was outside the scope his lab research. The opportunity to drive one's own project is daunting at the beginning of a PhD, but it is certainly justified by how much I learned along the way, and the immense satisfaction of seeing the work come together. Udi slowly but surely guided me through designing experiments, taught me to find patterns in data regardless of the nature of the data, and showed me how to present a compelling scientific argument. It has been a pleasure working with him on the manuscript, his excitement in fitting scientific puzzle pieces together is contagious! Udi was very supportive of my career choice following grad school, for which I am grateful.

Second, I would like to thank Claire Wyart, my second unofficial advisor. Claire did her post-doctoral work in Udi's lab before starting her own lab at the ICM in Paris around the same time I started my PhD. Claire's guidance has been invaluable throughout the years. She first invited me to give presentations in her lab in the early stages of my project, giving me feedback and suggestions when direction was unclear. We later started a collaboration with the Chateaubriand fellowship we applied for together. She introduced me to Mario Chavez from her institute with whom we worked on functional connectivity analysis. Claire's enthusiasm for my project and passion for science were key elements in keeping me motivated through the dark middle years of the PhD. She is an inspiration to me as a strong woman in science, and I am extremely grateful for her mentorship.

Of course, the long road to scientific discoveries is never travelled by a single person. Huge leaps were made in my research project when I started collaborating with Mario Chavez, a mathematician from the ICM in Paris, and Alex Huth, a computational neuroscientist from UC Berkeley. Both were extremely generous with their time, and by sharing their expertise with me, I got a glimpse into how modelling methods can be used in systems neuroscience. I also received help from numerous people in the Isacoff lab. Beth Carroll taught me not to be afraid of taking microscopes apart, and adapting them to my experiment, Adam Hoagland helped set up initial image analysis pipelines, and Tony Qu, my undergraduate research assistant, diligently assisted with experiments and analysis. Finally, Andy Prendergast from Claire Wyart's lab made the beautiful transgenic zebrafish line that was used in all my imaging experiments.

I am grateful for the personal support I received from lab members, and people from the neuroscience community who shared moments of joy when experiments were working, and who were encouraging when they were not. In particular, I'd like to thank Drew Friedman and Zach Newman, my co-graduate students in the Isacoff lab, for being fun and helpful as we embarked on our journey as budding scientists. Erica Warp mentored

me when I rotated in the Isacoff lab, she introduced me to working with zebrafish, and to calcium imaging. Erica was a wonderful instructor, and she is one of the reasons I joined the Isacoff lab. Holly Aaron and Jen Lee from the Molecular Imaging Center were always available for imaging advice. Holly and Alden Conner supported me by being unwavering companions for our Tequila Tuesday nights. Ariane Baudhuin-Kessel from the Ngai lab, Cathy O'Hare from the Isacoff lab, Matar Haller from Bob Knight's lab were great friends who listened to much frustration when I was losing against the fish. I would like to thank them for their wise advice.

I was fortunate to do my graduate work in the very friendly and welcoming community of the Helen Wills Neuroscience Institute at UC Berkeley. I would like to thank administrative staff, Kati Markowitz, Tony Leonard, Candace Groskreutz, and Natalie Terranova for making sure students were always well taken care of. My fellow graduate students were always helpful with advice on experiments and analysis, and many of them have become good friends. My thesis committee Dan Feldman, Marla Feller, and Craig Miller also gave me invaluable feedback over the years, and I appreciate their time and support.

Graduate school was an opportunity to learn how to be a good scientist, but it was also an opportunity for broader professional development. I received a fellowship from the Boehringer Ingelheim Fonds, which provided not only financial support, but also communication training and career education. BIF fellows and alumni are a wonderful professional network to be a part of, and I look forward to staying in touch with them as I move on into management consulting. Another organization on campus which furthered my professional development was the Beyond Academia group. I co-organized the Beyond Academia conference for two years, and the experience opened my eyes to what gets accomplished when a motivated group of people from different academic backgrounds works together. My experience with Beyond Academia was a determining factor in securing a job after graduate school. I would especially like to thank fellow Beyond Academia organizers Els Van Der Helm and Sahar Yousef for being inspirational, strong, entrepreneurial women.

Finally, I would like to thank my partner Chris Holdgraf for his unwavering support since my 3rd year in graduate school. Chris always looks at problems as a learning opportunity, and I learned from his confidence that each incremental step of progress in research eventually leads to a completed project. I really appreciate his patience and optimism. In no small part thanks to him, I will look back on graduate school with fond memories.

Chapter 1:

Introduction: Larval zebrafish as a model for understanding how experience is encoded in the brain

1. How do neurons encode behavior and changes in behavior?

The adult human brain contains about 86 billion neurons[1], most of which are already present at birth. Similar to other vertebrates, neurons in the human brain are organized in regions that specialize in different roles, from controlling vital functions, to perceiving the environment, or generating sensations of hunger of fear. Neurons within and across brain areas form circuits that integrate information about the external world and the internal state of the brain to generate behavior. First, animals must gather information about their environment, using their senses to see food, hear a predator, or smell conspecifics. Second, sensory information is progressively sent up to higher levels of the brain where it is "interpreted" to extract relevant cues. Finally, they must choose an appropriate behavioral response (e.g. to hunt prey or escape predators), that requires a specific motor output. Even this simplified description of the chain of events that lead to behavior involves multiple neurons in different brain areas, whose activity might be greatly influenced by small variations in the environment and prior experience. One of the ultimate goals of neuroscientists is to understand how complex, seemingly hard-wired circuits change with experience, making adjustments to behavior necessary to adapt to different environments, but without disrupting the basic ability to perform a given task.

Starting in the 1950s, studies of patients with localized brain lesions suggested that different types of memories were encoded in different brain areas. The most famous case Henry Gustav Molaison (or patient HM) was an epilepsy patient who had bilateral removal of his hippocampal formation, amygdala and parts of his temporal cortex. While HM still had normal short-term memory, and could recall long-term memories formed before the operation, he could no longer commit new events to his long-term memory[2]. On the other hand, HM retained the ability to acquire new motor skills (such as drawing a star while looking at his hand in a mirror). Studying the case of HM was one of the first times that the hippocampal formation was pinpointed in the formation of long-term memories, but not in other types of memories.

Psychologists now distinguish between different types of learning and memory: the two overarching categories are explicit memory (the conscious recollection of facts and experiences) and implicit memory (unconscious habits, reflexes etc), and implicit memory can further by subdivided in priming (when exposure to a stimulus influences the response to another stimulus), procedural memory (improved performance of a motor or cognitive skill through repetition), associative learning (association between two stimuli or a behavior and a stimulus), and non-associative learning (habituation and sensitization). The anatomical seat of these different types of memories is consistent across species: for example, explicit memory is thought to be encoded in neocortical areas, procedural learning relies on the striatum, and associative fear learning is driven by the amygdala.

Having pinpointed regions responsible for memory, neuroscientists started looking for the cellular and molecular changes that encode memory and experience.

Cellular and molecular mechanisms of memory were first studied in invertebrates by examining simple forms of implicit learning: habituation, sensitization and classic condition. In the 1940s, Donald Hebb hypothesized that if a cell A repeatedly excited a cell B, metabolic changes would take place in both cells to increase efficiency of cell A in firing B[3]. It wasn't until the 1960s that experimental evidence emerged to support this idea, with Eric Kandel and colleagues' work on the gill withdrawal reflex in the mollusk *Aplysia*. While an innocuous tactile stimulus delivered to the siphon of Aplysia elicits withdrawal of both siphon and gill, with repeated stimulation animals habituate and respond less often. By dissecting the neural circuit underlying this reflex, researchers realized that the basic organization of the circuit did not change during habituation. Rather, the strength of synaptic connections between sensory neurons that detected touch, and motor neurons that drove the withdrawal movement, was decreased. They determined this was due to a decrease in neurotransmitter released at the presynaptic terminal[4]. Similarly, during sensitization, an aversive stimulus to a different part of the body makes a mild touch stimulus more likely to evoke a gill withdrawal reflex, and this is driven by an increase in synaptic strength between sensory and motor neurons[5]. Kandel and colleagues dove deep into understanding the molecular mechanisms that underlie long-term habituation and sensitization.

In the 1970s, Timothy Bliss and colleagues were studying how learning was encoded in the hippocampus, which had been established as a fundamental component in forming long term explicit memories. The hippocampal circuit comprises a trisynaptic loop: 1) The entorhinal cortex projects to the dentate gyrus of the hippocampus via the perforant pathway. 2) Neurons in the dentate gyrus synapse on pyramidal cells in the CA1 region via the mossy fiber pathway. 3) CA3 neurons activate CA1 neurons via Schaffer collaterals. Studying the perforant pathway, researchers found that a high-frequency train of stimuli delivered to pre-synaptic neurons in the entorhinal cortex resulted in an increase in excitability of post-synaptic granule cells in the dentate gyrus[6], a process called long-term potentiation (LTP). Potentiation lasted several hours after the conditioning trains. LTP and its counterpart LTD (long-term depression) have since been established as more general mechanisms for increasing (or decreasing) excitability of synapses all over the brain[7].

From the large body of work identifying molecular mechanisms of synaptic plasticity, it has emerged that multiple different signaling pathways can mediate potentiation and depression. For example, LTP in the perforant pathway originally studied by Bliss and colleagues was shown to depend on post-synaptic activation of N-methyl-D-aspartate receptors (NMDAR)[6], whereas in the mossy fiber pathway, LTP expression is presynaptic and is c-AMP dependent[8]. For the NMDAR-dependent form of LTP, coincidence of presynaptic and post-synaptic depolarization activates NMDARs, letting calcium flow into the dendritic spine. Calcium activates CaMKII and other protein kinases[7], depending on the synapse at which LTP is being expressed, triggering intracellular signaling cascades that result in potentiation of the synapse: the number of α-amino-3-hydroxy-5-methyl-4-

isoxazolepropinioc acid receptors (AMPAR) trafficked to the plasma membrane is increased[9], and AMPARs are phosphorylated which increases their conductance[10]. Maintenance of long-term LTP depends on local protein-synthesis[11], possibly increasing AMPAR translation as well as scaffolding proteins that modify spine structure. The variety of LTP and LTD-inducing mechanisms that have been described in the literature is matched only by the variety of neuronal subtypes in the brain at different developmental time points.

In most original studies, LTP was induced using a sustained high-frequency presynaptic stimulation, however in the late 1990s, a different firing pattern was employed that was based on the timing of individual spikes rather than the presence of high frequency bursts[12]. It was shown that if a presynaptic neuron A consistently fires right before a postsynaptic neuron B in a 20 millisecond window, the synapse from neuron A to B is strengthened, however if neuron B consistently fires in a 20 millisecond window before neuron A, that synapse is weakened[13]. It was later shown that this spike-timing dependent plasticity (STDP) can be induced *in vivo.* For example, in *Xenopus* electrical stimulation of retinal ganglion cells paired with tectal neuron depolarization potentiates that synapse[14], and this potentiation can be achieved by presenting the animal with repetitive visual stimuli[15]. STDP has also been observed in mammals, for example pairing visual stimulation with electrical cortical activation in cats leads to changes in orientation-tuning maps[16]. Today, spike timing is thought to be a strong driver of plasticity at some synapses, while firing rate or depolarization state of the post-synaptic neuron are more important at other synapses[17].

Understanding the factors that drive synaptic plasticity provides a framework for explaining how memories might be encoded in the brain. Complex animal behaviors often involve multiple brain areas and circuits, from sensory areas, to decision making areas, to motor areas. Recent work has started to examine how experience is distributed across neural circuits. A well-studied example is auditory fear conditioning, a form of associative learning, in rodents: a tone (conditioned stimulus) is paired with an aversive stimulus (a mild electric shock, the unconditioned stimulus), and after learning animals have a physiological reaction of fear (in rodents, freezing) to the tone alone. The amygdala has long been identified as an essential region that associates sensory stimuli (a tone for example) with the sensation of pain (from the electric shock) during learning[18]. Injecting an NMDAR antagonist in the amygdala impairs fear conditioning which indicates that amygdala circuits undergo NMDAR-dependent LTP to encode association between tone and pain[19]. However, the amygdala is not the only place to undergo conditioning-associated changes in synaptic strength. The hippocampus plays a role in associating contextual information with fear because inhibiting NMDARs in the hippocampus impairs consolidation of fear conditioning[20]. Even primary auditory cortex (A1), which was considered to be a simple information processing site with no role in fear learning, has been shown to re-organize so that more neurons are tuned to the shock-associated tone[21]. It has recently been shown that A1 plasticity during fear conditioning is modulated by cholinergic inputs from the basal forebrain[22]. Moreover the dorsal-medial prefrontal cortex is thought to be involved in fear expression, possibly contributing to the selection of the appropriate response[23]. This brief summary of circuits underlying fear-conditioning

illustrates the complexity, and distributed nature of one of the simplest forms of learning. It is no wonder relatively little is known about how complex tasks and experiences are encoded in the brain.

One of the times in an organism's life when experience is the most important is during development: for example, children learn their mother-tongue during a critical period between 0 and 7 years through experience of people around them, past that point they will never achieve native fluency[24]. Similarly, at the level of neural circuits, sensory experience is necessary for normal development. For example, depriving a young cat of vision in one eye leads to atrophy of neurons in the thalamus[25], and disrupts ocular dominance in primary visual cortex[26]. Interestingly, before developing organisms receive any sensory input from the outside work, neural circuits already undergo a period of synaptic strengthening and weakening as a result of their spontaneous activity. This spontaneous neural activity has been observed in the retina[27], the spinal cord[28], and many other brain areas[29], and is thought to guide the development of neural circuits by interacting with genetic programs[30]. In the case of the zebrafish spinal cord, emergence of spontaneous correlated activity in motor neurons leads to spontaneous tail coiling[28], the first behavior of the fish. Strikingly, it has been shown that experience of light inhibits coiling, an effect driven by the unexpected presence of a light-sensing opsin in motor neurons[31]. In turn, photoinhibition regulates the development of the spinal cord central pattern generator. These examples demonstrate the importance of the environment and experience for the developing organism, and illustrate some mechanisms by which it is encoded.

2. Zebrafish, a small vertebrate with big potential in neuroscience

Zebrafish are native to the southeastern Himalaya region and live in slow-moving or stagnant bodies of fresh water. Adults are about three centimeters long, and have characteristic blue and silver stripes on their sides. They are diurnal, social animals that live in shoals, and feed on zooplankton and phytoplankton. Zebrafish became a model in developmental biology in the 1970s because of their external development that can be easily observed and perturbed, and their ease of reproduction in a laboratory setting. With the advent of modern genetics and the mapping of the zebrafish genome, it was established that 70% of human genes share at least one zebrafish orthologue, consolidating the position of zebrafish as a solid model for biomedical research[32].

Zebrafish are part of the teleost bony fish family, and as such share a common general organization of their nervous system with other vertebrates. By 5 dpf, zebrafish larvae have ~ 100,000 neurons and all the major areas found in the mammalian brain. They also share the same neurotransmitters, such as glutamate, GABA, and neuromodulatory systems (dopamine, serotonin, histamine, noradrenaline and acetylcholine). The most notable difference between zebrafish and mammals is the absence of neocortex in the former, however structures homologous to the hippocampus, piriform cortex and amygdala have been identified in the zebrafish telencephalon. Of interest to the study of predation, sensory systems, and in particular vision, are highly conserved in zebrafish. Retinal ganglion cells send projections in 10 arborization fields to the pretectum and the optic tectum[33]. The optic tectum is homologous to the superior colliculus in mammals and

is particularly large in zebrafish, presumably because it accomplishes a lot of computations that occur in the neocortex in mammals.

During their first 7 days, zebrafish develop a wide range of behaviors that are studied to understand the neural basis of sensory processing, and motor control, as well as to assess gene function in behavioral screens. Young larvae's first display of behavior occurs at about 17 hours post fertilization when zebrafish start coiling their tails spontaneously while still in their egg (Chapter 2). Around 2 dpf, they break free of their chorion and stay relatively inactive a part from escaping from touch stimuli, and the occasional burst of swimming. When their swim bladder inflates at 4 dpf, they develop more elaborated behaviors: they maintain themselves upright in the water (instead of being on their sides), they swim in a more coordinated fashion, and they display robust escape behaviors from touch, sound, sudden changes of light and big looming predator-like stimuli.

Similar to other diurnal vertebrates, zebrafish rely heavily on their sense of vision to guide their behavior. At 4 dpf, a large stimulus moving repeatedly in front of the fish will cause their eyes to saccade in that direction (opto-kinetic reflex). By 5 dpf a whole-field moving stimulus evokes swimming in the direction of stimulus motion (the opto-motor reflex), which presumably allows fish to counter the effect of water current on their position (Rock and Smith 1986). By 5 dpf, zebrafish also display a circadian rhythm in their swimming activity, resting more at night, in what is believed to be sleep / wake patterns. At the same age, they start hunting small moving prey such as paramecia, or prey-like objects (Chapter 3). Thanks to their rich behavioral repertoire at an early developmental stage, zebrafish are used in drug screens[34], as well as in the study of neurological diseases such as epilepsy.

In the past decade, advances in microscopy combined with the development of optogenetics, the ability to measure and control neural activity with light, have opened the doors to understanding how neural activity encodes behavior. Zebrafish have emerged as a prime model for using these tools. First, larvae have small brains and are transparent which is ideal for imaging neural activity and manipulating it optically in a living animal. Second, transgenic zebrafish lines are easy to generate, enabling researchers to efficiently genetically target neural activity sensors and actuators to neurons. The most common activity reporters are calcium sensors that fluoresce when intracellular calcium increases via calcium influx, a good proxy for detecting bursts of action potentials.

The GCaMP family of calcium indicators, which was used in all chapters of this thesis, was created from a fusion of circularly-permutated green fluorescent protein (GFP), calmodulin (CaM) and M13, a peptide sequence that binds to CaM. When calcium concentration increases, it binds to CaM which in turn interacts with M13 to induce a conformational change in the GFP. This conformational change in the fluorophore leads to an increase in emitted fluorescence which can be detected using fluorescence microscopy. The most common activity manipulators are the opsins channelrhodopsin2 (ChR2) and halorhodopsin (NpHR), endogenous to green algae and archaea respectively. ChR2 is an ion channel permeable to cations which opens upon absorption

of blue (480 nm) light, depolarizing the neuron. NpHR is a chloride pump that is activated by yellow (590 nm) light, and has a hyperpolarization effect on the membrane potential.

Zebrafish are relative newcomers as a learning and memory animal model. While adults display most of the learning abilities studied in mammals (from visual discrimination learning in a T-maze[35] to olfactory conditioning[36]), there are currently only a handful of publications that describe learning paradigms in larval fish below 8 dpf[37,38]. In a classical conditioning paradigm, larval zebrafish can learn to associate a visual stimulus (conditioned stimulus) with an aversive touch (unconditioned stimulus)[37], and similar to mammals[39], the cerebellum is necessary for the acquisition of this memory. Larval zebrafish can also be place-conditioned: they learn to pair a distinct visual environment with the sight of conspecifics, a social reward. They exhibit spatial preference for the rewarded location for up to 36 hours, and this memory is NMDAR and protein synthesis-dependent[38]. To take full advantage of the interesting characteristics of zebrafish as an animal model (optogenetics in a transparent organism, amenable genetics etc) in the field of learning of memory, one challenge will be characterizing what motivates fish to make them "learn"[40]. For the main project of my dissertation I focused on a crucial behavior for survival, feeding, to study how hunting experience affects predation in larval zebrafish.

3. Neuroethology of predation

Throughout the animal kingdom, animals have developed elaborate strategies to feed themselves, and distinguish between things they can eat and things that would harm them. How individuals start feeding during development is a combination of innate skill and practice and/or social learning. Some species actively feed their newborns, for example mammals provide milk and birds bring food back to the nest. Their offspring often stay with one or both of the parents until they are able to forage and/or hunt by themselves, and benefit from social influences, learning from their conspecifics to feed[41]. In contrast, in other species newborns have to feed themselves immediately. For example, archer fish develop a highly specialized hunting technique, spitting at land-based prey in a "ballistic attack" to dislodge the prey and capture it when it hits the water. This behavior is innate but remarkably, archer fish can learn to shoot moving targets just by watching their conspecifics[42]. Another instance of refining predation technique with practice is the barn owl strike. Barn owls can hunt based purely on auditory skills, however the neural circuit underlying auditory-based predation is calibrated using visual feedback[43]. When a mismatch between sound and visual localization is induced experimentally using prisms, visual input instructs topographic projections within the inferior colliculus to re-target until incoming sensory information from eyes and ears concur once again. These examples illustrate the complex strategies animals have evolved to feed themselves, and how innate behavior and experience interplay to ensure adaptability.

Clawed frogs (*Xenopus*) have been of particular interest for the study of the neural circuitry of predation. Early studies with adult frogs showed these animals reliably attack small prey-like objects, but avoid large predator-like objects, even when the objects in question are moving pieces of cardboard in a laboratory setting[44]. This finding is part of a larger body of work describing the concept of key stimuli, introduced in the 1930s, and

that suggests the right combination of visual stimuli (usually a combination of speed, size and direction) releases an innate behavioral sequence resulting either in predation or avoidance. It has been shown that the retino-tecto / tegmento-bulbar / spinal circuit is sufficient to evoke a prey capture response in frogs, and that recognition of a prey vs non-prey stimulus is established in the pretectum. Similar to archer fish, and to barn owls, predation in frogs is also modulated by attention, motivation and experience. Forebrain structures have been shown to modulate directed attention, and mediate associative learning and prey recognition when new stimuli are presented. Dopaminergic circuits modulate prey capture strategy, determining if frogs actively hunt for prey of if they wait for prey[45].

From an evolutionary point of view, organisms must adapt to changes to their environment to survive, and in particular to changes to their food sources. The accomplishment of predation is therefore highly flexible, and modulated by experience in animals as phylogenetically distant as mammals (the Etruscan shrew relies on tactile experience to develop efficient predation[46]) and mollusks (*Limax* learn to avoid a food if they become sick after eating it[47]). Studies of animals across genera point to common themes in the development and maintenance of predation. Key stimuli, whether they be visual, auditory, somatosensory, or a combination thereof, trigger a prey capture behavioral sequence. This response is modulated by attention, motivation and experience, and can also be triggered by new stimuli as a result of associative learning. Prey capture is a complex behavior usually controlled by several brain areas that act together to produce the behavioral output. Little is known about how natural experience affects prey capture circuits during development. My main thesis work project focused on understanding how experience affects predation and the underlying neural circuitry in larval zebrafish.

4. Prey capture circuitry in larval zebrafish

Prey capture has emerged as a popular behavioral model to study a goal-directed behavior in larval zebrafish. Larvae start hunting at 5 dpf after their swim bladder has inflated. They detect their prey, reorient their body towards the prey with a series of unilateral tail flicks (J-Bends), and swim forward until they reach a proximal striking zone. Finally, they dart ahead to engulf the prey in a final capture swim[48–51]. Predation is generally thought to be an innate behavior because zebrafish can successfully capture prey as early as their first attempts. No prior work suggests this behavior might be influenced by experience. As such, neural circuits that detect the prey, identify it as food, and launch the predatory motor sequence, are in place by 5 dpf.

Prey capture is visually mediated because fish in the dark, and blind mutant fish are severely impaired in their hunting abilities[52]. Information flows from the retinal ganglion cells (RGCs) of the retina to the pretectum and the optic tectum. RGCs send projections in 10 distinct arborization fields (AFs), and it is thought that a subset of them, those that project to AF7, respond specifically to prey-like objects[53]. A group of pretectal neurons with dendrites in AF7 project to the optic tectum, and to the nucleus of the medial longitudinal fasciculus (nMLF)[53], however the exact nature of the information carried is not known. The optic tectum, which receives direct inputs from the retinal ganglion cells

and from the pretectum, was the first region to be implicated in controlling prey capture. While the optic tectum is not necessary for the fish to display OKR and OMR behaviors[54], it is necessary for them to capture prey[52]. Local circuits within the optic tectum are thought to filter visual information flowing in from the retina to extract relevant prey cues: it has been shown that a population of inhibitory interneurons responds preferentially to large stimuli, thereby promoting responses to small, prey-like objects in their target neurons[55]. Similarly it has been shown that tectal neurons are tuned to stimulus size[56], and that a subpopulation of them are necessary for pursuing prey-like stimuli[57]. Finally calcium-imaging has revealed that assemblies of tectal neurons fire specifically before a prey capture is initiated[58], leading to the hypothesis that these neurons are the seat of prey recognition that initiate the hunting behavior. It is currently unclear how information filtered in the pretectum and from the optic tectum are integrated. Relatively little is known about the motor circuits that control prey capture behavior downstream of the visual areas. The nMLF sends projections form the midbrain to the spinal cord and appears to be important for controlling the motor sequence of prey capture[52]. The mesencephalic reticular formation, a region controlling eye movements and convergence in goldfish[59], might also be important for initiating hunting. There are currently two papers in the zebrafish literature that investigate the effect of experience on hunting: first it has been shown that juvenile fish can learn to hunt in the dark using their lateral line[60], and that hunger modulates responses to ambiguous stimuli through the dopaminergic system[61].

5. Thesis summary

For my PhD research, I focused on two examples of how changes in neural activity lead to changes in behavior in larval zebrafish. First, I contributed to a study of circuit activity in spinal cord motor neurons, looking at the transition of spontaneous activity from unsynchronized to synchronized (Chapter 2). This transition drives the first behavior of the fish, tail coiling. We showed that the emergence of correlated activity was important for normal development of the central pattern generator. For my main project, I studied how experience affects prey capture behavior and underlying neural activity (Chapter 3). It was previously assumed that learning played no part in the development of prey capture, because it is an innate behavior. However, my work demonstrated that larvae get better at prey capture with experience by increasing their capture initiation frequency, calling into question the belief that larval zebrafish cannot learn. I then asked how prior experience of prey was encoded in neural activity, and found that experience increases the likelihood of the sight of prey evoking a capture attempt. This effect appears to be due to signaling from the forebrain regions that enhances the impact of visual area activity on motor area activity and behavior. Thus, I discovered that larval zebrafish are capable of learning, and pinpointed neural circuits that changed their activity as a function of experience.

References

1. Azevedo, F. A. C. *et al.* Equal numbers of neuronal and nonneuronal cells make the human brain an isometrically scaled-up primate brain. *J. Comp. Neurol.* **513,** 532–541 (2009).
2. Scoville, W. B. & Milner, B. Loss of recent memory after bilateral hippocampal lesions. *J. Neuropsychiatry Clin. Neurosci.* **12,** 103–113 (1957).
3. Hebb, D. O. *The Organization of Behavior*. *Organ. Behav.* **911,** (1949).
4. Castellucci, V., Pinsker, H., Kupfermann, I., and Kandel, E., Castellucci, V., Pinsker, H., Kupfermann, I. & Kandel, E. R. Neuronal Mechanisms of Habituation and dishabituation of the gill withdrawal reflex in Aplysia. *Science (80-.).* **167,** 1745–1748 (1970).
5. Pinsker, H. M., Hening, W. A., Carew, T. J. & Kandel, E. R. Long-term sensitization of a defensive withdrawal reflex in Aplysia. *Science (80-.).* **182,** 1039–42 (1973).
6. Bliss, T. V & Lømo, T. Long-lasting potentiation of synaptic transmission in the dentate area of the anaesthetized rabbit following stimulation of the perforant path. *J. Physiol.* **232,** 331–56 (1973).
7. Malenka, R. C. & Bear, M. F. LTP and LTD: Review An Embarrassment of Riches. *Neuron* **44,** 5–21 (2004).
8. Nicoll, R. A. & Schmitz, D. Synaptic Plasticity at Hippocampal Mossy Fibre Synapses. *Nat. Rev. Neurosci.* **6,** (2005).
9. Anggono, V. & Huganir, R. L. Regulation of AMPA receptor trafficking and synaptic plasticity. *Curr. Opin. Neurobiol.* **22,** 461–469 (2012).
10. Song, I. & Huganir, R. L. Regulation of AMPA receptors during synaptic plasticity. **25,** 578–588 (2002).
11. Sutton, M. A. & Schuman, E. M. Dendritic Protein Synthesis , Synaptic Plasticity , and Memory. *Cell* **127(1),** 49–58 (2006).
12. Markram, H., Lubke, J., Frotscher, M. & Sakmann, B. Regulation of synaptic efficacy by coincidence of postsynaptic APs and EPSPs. *Science (80-.).* **275,** 213–215 (1997).
13. Bi, G. Q. & Poo, M. M. Synaptic modifications in cultured hippocampal neurons: dependence on spike timing, synaptic strength, and postsynaptic cell type. *J. Neurosci.* **18,** 10464–10472 (1998).
14. Zhang, L. I., Tao, H. W., Holt, C. E., Harris, W. A. & Poo, M. A critical window for cooperation and competition among developing retinotectal synapses. *Nature* **395,** 37–44 (1998).
15. Engert, F., Tao, H. W., Zhang, L. I. & Poo, M. Moving visual stimuli rapidly induce

direction sensitivity of developing tectal neurons. *Nature* **419,** 470–475 (2002).

16. Schuett, S., Bonhoeffer, T. & Hübener, M. Pairing-induced changes of orientation maps in cat visual cortex. *Neuron* **32,** 325–337 (2001).

17. Feldman, D. E. The Spike-Timing Dependence of Plasticity. *Neuron* **75,** 556–571 (2012).

18. Fanselow, M. S. & Poulos, A. M. The neuroscience of mammalian associative learning. *Annu. Rev. Psychol.* **56,** 207–34 (2005).

19. Miserendino, M. J., Sananes, C. B., Melia, K. R. & Davis, M. Blocking of acquisition but not expression of conditioned fear-potentiated startle by NMDA antagonists in the amygdala. *Nature* **345,** 716–718 (1990).

20. Shimizu, E., Tang, Y.-P., Rampon, C. & Tsien, J. Z. NMDA Receptor: Dependent Synaptice Reinforcement as a Crucial Process for Memory Consolidation. *Science (80-.).* **290,** 1170–1174 (2000).

21. Rutkowski, R. G. & Weinberger, N. M. Encoding of learned importance of sound by magnitude of representational area in primary auditory cortex. *Proc. Natl. Acad. Sci. U. S. A.* **102,** 13664–9 (2005).

22. Letzkus, J. J. *et al.* A disinhibitory microcircuit for associative fear learning in the auditory cortex. *Nature* **480,** 331–335 (2011).

23. Senn, V. *et al.* Long-range connectivity defines behavioral specificity of amygdala neurons. *Neuron* **81,** 428–437 (2014).

24. Johnson, J. S. & Newport, E. L. Critical period effects in second language learning: The influence of maturational state on the acquisition of English as a second language. *Cogn. Psychol.* **21,** 60–99 (1989).

25. Wiesel, T. N. & Hubel, D. H. Effects of Visual Deprivation on Morphology and Physiology of Cells in the Cats Lateral Geniculate Body. *J. Neurophysiol.* **26,** 978–93 (1963).

26. Wiesel, T. N. & Hubel, D. H. Single-Cell Responses in Striate Cortex of Kittens Deprived of Vision in One Eye. *J. Neurophysiol.* **26,** 1003–1017 (1963).

27. Meister, M., Wong, R. O., Baylor, D. A. & Shatz, C. J. Synchronous bursts of action potentials in ganglion cells of the developing mammalian retina. *Science* **252,** 939–43 (1991).

28. Saint-Amant, L. & Drapeau, P. Synchronization of an embryonic network of identified spinal interneurons solely by electrical coupling. *Neuron* **31,** 1035–46 (2001).

29. Blankenship, A. G. & Feller, M. B. Mechanisms underlying spontaneous patterned activity in developing neural circuits. *Nat. Rev. Neurosci.* **11,** 18–29 (2010).

30. Spitzer, N. C. Coincidence detection enhances appropriate wiring of the nervous

system. *Proc. Nat. Acad. Sci* **101,** 5311–5312 (2004).

31. Friedmann, D., Hoagland, A., Berlin, S. & Isacoff, E. Y. A spinal opsin controls early neural activity and drives a behavioral light response. *Curr. Biol.* **25,** 69–74 (2015).

32. Howe, K. *et al.* The zebrafish reference genome sequence and its relationship to the human genome. *Nature* **496,** 498–503 (2013).

33. Burrill, J. D. & Easter, S. S. Development of the retinofugal projections in the embryonic and larval zebrafish (Brachydanio rerio). *J Comp Neurol* **346,** 583–600 (1994).

34. Rihel, J. *et al.* Zebrafish Behavioral Profiling Links Drugs to Biological Targets and Rest/Wake Regulation. *Science (80-.).* **327,** 348–351 (2010).

35. Colwill, R. M., Raymond, M. P., Ferreira, L. & Escudero, H. Visual discrimination learning in zebrafish (Danio rerio). *Behav. Processes* **70,** 19–31 (2005).

36. Braubach, O. R., Wood, H. D., Gadbois, S., Fine, A. & Croll, R. P. Olfactory conditioning in the zebrafish (Danio rerio). *Behav. Brain Res.* **198,** 190–198 (2009).

37. Aizenberg, M. & Schuman, E. M. Cerebellar-Dependent Learning in Larval Zebrafish. *J. Neurosci.* **31,** 8708–8712 (2011).

38. Hinz, F. I., Aizenberg, M., Tushev, G. & Schuman, E. M. Protein Synthesis-Dependent Associative Long-Term Memory in Larval Zebrafish. **33,** 15382–15387 (2013).

39. Thompson, R. F. & Steinmetz, J. E. The role of the cerebellum in classical conditioning of discrete behavioral responses. *Neuroscience* **162,** 732–755 (2009).

40. Gerlai, R. *Learning and memory in zebrafish (Danio rerio)*. *Methods Cell Biol.* **134,** (Elsevier Ltd, 2016).

41. Galef, B. G. & Giraldeau, L.-A. Social influences on foraging in vertebrates: causal mechanisms and adaptive functions. *Anim. Behav.* **61,** 3–15 (2001).

42. Schuster, S., Wöhl, S., Griebsch, M. & Klostermeier, I. Animal cognition: How archer fish learn to down rapidly moving targets. *Curr. Biol.* **16,** 378–383 (2006).

43. Knudsen, E. I. Instructed learning in the auditory localization pathway of the barn owl. *Nature* **417,** 322–328 (2002).

44. Ewert, J. P. Advances in vertebrate neuroethology. *Trends Neurosci.* **5,** 141–143 (1982).

45. Ewert, J. P. *et al.* Neural modulation of visuomotor functions underlying prey-catching behaviour in anurans: Perception, attention, motor performance, learning. *Comp. Biochem. Physiol. - A Mol. Integr. Physiol.* **128,** 417–461 (2001).

46. Anjum, F. & Brecht, M. Tactile experience shapes prey-capture behavior in Etruscan shrews. *Front. Behav. Neurosci.* **6,** 1–8 (2012).

47. Elliott, C. J. H. & Susswein, a J. Comparative neuroethology of feeding control in molluscs. *J. Exp. Biol.* **205,** 877–896 (2002).

48. Borla, M. A., Palecek, B., Budick, S. & O'Malley, D. M. Prey capture by larval zebrafish: Evidence for fine axial motor control. *Brain. Behav. Evol.* **60,** 207–229 (2002).

49. McElligott, M. B. & O'Malley, D. M. Prey tracking by larval zebrafish: Axial kinematics and visual control. *Brain. Behav. Evol.* **66,** 177–196 (2005).

50. McClenahan, P., Troup, M. & Scott, E. K. Fin-tail coordination during escape and predatory behavior in larval zebrafish. *PLoS One* **7,** 1–11 (2012).

51. Patterson, B. W., Abraham, A. O., MacIver, M. a & McLean, D. L. Visually guided gradation of prey capture movements in larval zebrafish. *J. Exp. Biol.* **216,** 3071–83 (2013).

52. Gahtan, E. Visual Prey Capture in Larval Zebrafish Is Controlled by Identified Reticulospinal Neurons Downstream of the Tectum. *J. Neurosci.* **25,** 9294–9303 (2005).

53. Semmelhack, J. L. *et al.* A dedicated visual pathway for prey detection in larval zebrafish. *Elife* **4,** 1–19 (2014).

54. Roeser, T. & Baier, H. Visuomotor behaviors in larval zebrafish after GFP-guided laser ablation of the optic tectum. *J. Neurosci.* **23,** 3726–3734 (2003).

55. Del Bene, F. *et al.* Filtering of visual information in the tectum by an identified neural circuit. *Science (80-.).* **330,** 669–673 (2010).

56. Preuss, S. J., Trivedi, C. A., Vom Berg-Maurer, C. M., Ryu, S. & Bollmann, J. H. Classification of object size in retinotectal microcircuits. *Curr. Biol.* **24,** 2376–2385 (2014).

57. Barker, A. J. & Baier, H. Sensorimotor decision making in the Zebrafish tectum. *Curr. Biol.* **25,** 2804–2814 (2015).

58. Bianco, I. & Engert, F. Visuomotor Transformations Underlying Hunting Behavior in Zebrafish. *Curr. Biol.* **25,** 831–846 (2015).

59. Luque, M. A., Perez-Perez, M. P., Herrero, L. & Torres, B. Involvement of the optic tectum and mesencephalic reticular formation in the generation of saccadic eye movements in goldfish. *Brain Res. Rev.* **49,** 388–397 (2005).

60. Carrillo, A. & McHenry, M. J. Zebrafish learn to forage in the dark. *J. Exp. Biol.* **219,** 582–589 (2016).

61. Filosa, A., Barker, A. J., Dal Maschio, M. & Baier, H. Feeding State Modulates Behavioral Choice and Processing of Prey Stimuli in the Zebrafish Tectum. *Neuron* 1–13 (2016). doi:10.1016/j.neuron.2016.03.014

CHAPTER 2

Emergence of Patterned Activity in the Developing Zebrafish Spinal Cord

Current Biology (2012) 22, 93-102

LINKER STATEMENT

In collaboration with others, the following study was done to observe the formation of the early spinal CPG and understand the transition from sporadic spontaneous activity to synchronized network activity. Using neural activity imaging to monitor many cells simultaneously, this was the first study to observe the onset of spinal cord spontaneous activity and its transition at the network level *in vivo*. My contribution to this project consisted of setting up the chronic inhibition experiments in which we used halorhodopsin to reduce global network activity. Using the protocol I developed, we were able to show that activity patterns do not mature properly when motor network activity is inhibited.

Emergence of Patterned Activity in the Developing Zebrafish Spinal Cord

This work has been published in the following article and is reprinted in full with permission:

Warp E, Agarwal G, Wyart C, Friedmann D, Oldfield CS, Conner A, Del Bene F, Arrenberg AB, Baier H, and Isacoff EY, Current Biology, Jan , 2012.

Author contributions: For this work, E.W., G.A., C.W., H.B., and E.Y.I. designed the experiments and analytical approaches. E.W. performed the time lapse, heptanol, and the acute and chronic NpHR experiments. D.F. and C.S.O. contributed to data collection and analysis of the chronic NpHR experiments. E.W. and G.A. wrote the MATLAB scripts to analyze the calcium imaging movies and performed the analysis. E.W. and C.W. set up the photomanipulation system. E.W. and A.C. performed the BGUG imaging. F.D.B. assisted with experiment set-up, and A.B.A. made the UAS:NpHR-mCherry transgenic line. E.W. and E.Y.I. wrote the manuscript with feedback from the other authors.

Acknowledgements: We thank K. McDaniel, W. Staub, J. Saint-Hillaire, and D. Weinman for fish care; K. McDaniel for assistance with experiment setup; M. Feller for critical reading of the manuscript; and H. Aaron and Intelligent Imaging Innovations for advice and assistance with the optical system. Support for the work was provided by the National Institutes of Health Nanomedicine Development Center for the Optical Control of Biological Function, PN2EY018241 (E.Y.I.), the Human Frontier Science Program, RGP0013/2010 (E.Y.I.), the National Science Foundation (FIBR 0623527) (E.Y.I.), and the National Institute of Health National Research Service Award fellowship (E.W.).

Summary

Background: Developing neural networks display spontaneous and correlated rhythmic bursts of action potentials that are essential for circuit refinement. In the spinal cord, it is poorly understood how correlated activity is acquired and how its emergence relates to the formation of the spinal central pattern generator (CPG), the circuit that mediates rhythmic behaviors like walking and swimming. It is also unknown whether early, uncorrelated activity is necessary for the formation of the coordinated CPG.

Results: Time-lapse imaging in the intact zebrafish embryo with the genetically encoded calcium indicator GCaMP3 revealed a rapid transition from slow, sporadic activity to fast, ipsilaterally correlated, and contralaterally anticorrelated activity, characteristic of the spinal CPG. Ipsilateral correlations were acquired through the coalescence of local microcircuits. Brief optical manipulation of activity with the light-driven pump halorhodopsin revealed that the transition to correlated activity was associated with a strengthening of ipsilateral connections, likely mediated by gap junctions. Contralateral antagonism increased in strength at the same time. The transition to coordinated activity was disrupted by long-term optical inhibition of sporadic activity in motor neurons and ventral longitudinal descending interneurons and resulted in more neurons exhibiting uncoordinated activity patterns at later time points.

Conclusions: These findings show that the CPG in the zebrafish spinal cord emerges directly from a sporadically active network as functional connectivity strengthens between local and then more distal neurons. These results also reveal that early, sporadic activity in a subset of ventral spinal neurons is required for the integration of maturing neurons into the coordinated CPG network.

Introduction

Spontaneous activity is common to developing networks, occurring in the embryo during periods of concentrated axonal growth and synaptogenesis [1]. A hallmark of this activity is correlated population activity. Such correlations are hypothesized to guide the development of neural circuits [2], as demonstrated in the visual system where disruption of correlated retinal waves causes abnormal circuit development in downstream targets [3]. A transition from sporadic, cell-autonomous activity to correlated rhythmic activity has been observed in brain stem [4], cortex [5], and hippocampus [6], reflecting the emergence of connectivity and suggesting that early, sporadic activity may be necessary for the formation of more mature, correlated networks.

Early in the development of the motor system, cell-autonomous spontaneous calcium transients are observed in spinal cord neurons [7] before the maturation of the synaptic network. Later, spinal cord neurons display correlated patterns of spontaneous activity, beginning with bilaterally synchronized bursts of action potentials [8, 9] that convert to alternation between the left and right sides when γ-aminobutyric acid $(GABA)_A$ and

glycine receptor signaling switches during development from depolarizing to hyperpolarizing [10]. In vertebrates, manipulation of correlated spontaneous activity in the spinal cord disrupts axon guidance [11], the balance between excitatory and inhibitory synaptic strength [12], and the formation of the central pattern generator (CPG) [13], which generates oscillatory rhythms for locomotion into adulthood [14]. Though cholinergic activity has been shown to be necessary for the maturation of rhythmic alternation between the two sides of the mammalian spinal cord [13], it is unknown whether activity influences the acquisition of correlations on the same side of the cord and which cell types may mediate this activity dependence.

We investigated the emergence of correlated patterns of spontaneous activity in vivo in the developing zebrafish spinal cord locomotor system using the genetically encoded calcium indicator GCaMP3 [15] to image spontaneous activity noninvasively at single-cell resolution in identified cells. The imaging identified a remarkably rapid transition from sporadic, uncorrelated activity to rhythms characteristic of the locomotor CPG with ipsilateral correlation and contralateral alternation. Acute optical manipulation of activity revealed that the development of functional connectivity underlies the emergence of the coordinated activity. Chronic optical inhibition of activity in motor neurons and ventral longitudinal descending (VeLD) interneurons early in the transition period disrupted the integration of maturing neurons into the correlated network, suggesting that the emergence of the coordinated CPG is activity dependent.

Results

Emergence of Correlated Activity

In vivo calcium imaging with genetically encoded indicators has been used successfully to image neural activity in zebrafish embryos [16] and larvae [17, 18]. We employed GCaMP3 [15, 18] for its high baseline fluorescence and high signal-to-noise ratio [15]. GCaMP3 and the light-gated inhibitory chloride pump halorhodopsin (NpHR) [19, 20], were targeted to neurons of interest using the UAS/Gal4 system.

Spontaneous activity in the zebrafish spinal cord is restricted to ventral neurons of the motor system [21]. We used the Gal4^{s1020t} line developed in an enhancer trap screen [22] to target a subset of these spontaneously active cells (see Figure S1 available online). We have previously characterized this line to contain primary and secondary motor neurons and Kolmer-Agduhr (KA) ascending interneurons in the spinal cord at 5 days post fertilization (dpf) [23]. At 1 dpf, single-cell imaging with Brn3c:GAL4, UAS:mGFP (BGUG) [22] also revealed targeting to descending interneurons (Figures S1C and S1E). The Gal4 insert for this line is near the olig2 gene [23], which exhibits an identical expression pattern and has been shown at 1 dpf to target motor neurons, KA cells, and VeLD interneurons, as well as bromodeoxyuridine (BrdU)-incorporating cells along the midline [24]. We therefore interpret the descending interneurons to be VeLDs.

Single-cell electrophysiological recordings have identified three key neuron types—primary motor neurons, VeLD interneurons, and IC (ipsilateral caudal) descending interneurons—to be always active during spontaneous events in the zebrafish spinal cord at 20–24 hpf [21]. In the Gal4^{s1020t} line, we could image the population dynamics of spontaneous activity in primary motor neurons and VeLDs, two of the three key neuron types.

During embryonic development, zebrafish display spontaneous bursts of action potentials in the spinal cord that are associated with spontaneous contractions of the tail [25, 26, 21]. We imaged spontaneous calcium activity in UAS: GCaMP3/Gal4^{s1020t} fish at 18 hpf, an hour after the onset of spontaneous behavior [25], and at 20 hpf, when electrophysiological correlation between pairs of spinal neurons has been previously observed [21], and when there is evidence for both electrical and chemical synapse formation in the zebrafish spinal cord [26, 21]. Calcium imaging was performed on embryos paralyzed with α-bungarotoxin to eliminate spontaneous contractions, performed from a dorsal view to simultaneously observe cells on the left and right sides, and centered on somites 5 and 6. Spatial regions corresponding to single active neurons (e.g., regions outlined in Figures 1A and 1D) and intensity traces over time (e.g., time series data in Figure 1B and 1E) were extracted from movies using a semi-automated toolbox [27].

Though activity was present at 18 hpf, it was sporadic, with long-duration events (Figures 1A–1C; Movie S1) that were rarely associated with events in other ipsilateral cells and with no obvious relationship between the left and right sides of the cord. We did observe some correlation between ipsilateral cells at 18 hpf, but this was just between small subsets of nearby cells (e.g., Figure 1B, cells 1 and 2). In contrast, at 20 hpf events were shorter lasting, tightly correlated between nearly all ipsilateral cells, and organized in bursts of alternation between the left and right sides (Figures 1D–1F; Movie S2), as observed previously [16]. The left/right rhythmicity is reminiscent of activity patterns observed during swimming but is significantly slower at this early coiling stage that precedes swimming [28]. We also observed fish that exhibited near-continual alternating bursts (Figure S1F).

Time-lapse calcium imaging was used to characterize the transition between the uncorrelated and correlated network states. Calcium imaging movies of 4 min duration were taken every half hour between 17.5 and 21 hpf. To quantify changes in activity patterns, we calculated the correlation of GCaMP traces for all cell pairs in individual movies. Pairwise correlation matrices of single-cell traces in an example fish (Figure 2A) showed little correlation at early time points, and the few cell pairs that were correlated were weakly so. With time, correlations between ipsilateral neurons became stronger, whereas neurons on opposite sides of the cord became anticorrelated.

Pooled correlation data across fish showed that ipsilateral cells went from weak to strong correlation, reaching a maximum at 20 hpf, 3 hr after the onset of spontaneous

behavior [25] (Figures 2B and 2C). During this period, contra-lateral cells became increasingly anticorrelated (Figures 2B and 2C). By 20 hpf, rhythmic oscillations were apparent (Figures 1F and 2B, right), indicating that the components of a CPG are in place. Increases in ipsilateral correlation and decreases in event duration were detected in individual tracked cells that became active early (e.g., starting at 18 hpf, Figure S2A) as well as for cells that became active later (e.g., starting at 19.5 hpf, Figure S2B), suggesting that maturation of the circuit involves the progressive addition of cells, each of which goes from an initial state of uncorrelated slow activity to network-associated fast activity.

Ipsilateral Synchronization through Coalescence of Local Correlated Groups

Spatiotemporal maps of correlated ensembles in most fish (6/9) at early stages showed multiple nonoverlapping correlated groups on the same side of the cord (Figure 3, 18.5 hpf, left side). With time, the correlations between cells strengthened and the correlated groups increased in size, to eventually include virtually all ipsilateral cells in the field of view (Figure 3, e.g., 20 hpf; Figure S3A). Within these correlated ensembles, cells became more precisely time-locked (i.e., shorter lag times) during this early period of spontaneous activity (Figure S3B). In addition, event amplitude variability decreased during this period (Figure S3C).

In younger embryos (17.5–18.5 hpf), the distance between cells participating in a synchronous event was relatively small, (i.e., correlations were seen between small numbers of neigh-boring cells), whereas temporally coupled cells covered a broader spatial region in older embryos (e.g., 20–21 hpf) (Figure S3D). Conversely, temporal spread was broad at younger stages but tight at later stages as events became more accurately time-locked between ipsilateral cells (Figure S3D). Thus, ipsilateral correlation is accomplished through the coalescence of local correlated groups, which converts small events that are weakly correlated in small groups of cells into large events that occur synchronously on the entire side of the spinal cord. Although the zebrafish spinal cord develops in a rostral to caudal sequence [29], ipsilateral correlations do not emerge in a rostral to caudal pattern, at least in the region of cord that we imaged.

Increased Functional Connectivity Accompanies Emergence of Correlated Activity

Both chemical and electrical synapses have been implicated in mediating spontaneous activity in the spinal cord [9]. Paired recordings have shown that gap junctions play an essential role in the connectivity of the embryonic zebrafish spinal cord [21]. Additionally, uncoupling gap junctions with heptanol or by intracellular acidification eliminates spontaneous activity at 19–24 hpf, whereas blockers of chemical transmission do not [26]. In older embryos (20–20.5 hpf), heptanol eliminated spontaneous activity in all but 3.7% ± 1.6% of cells (n = 11 fish; see Figure S4B for example), whereas 34.7% ± 9.9% of cells remained active in younger embryos (17.5–18 hpf, n = 13 fish; p = 0.002,

unpaired Student's t test; see Figure S4A for example). Though these results could be due to off-target effects on calcium or potassium channels, they remain consistent with a model in which gap junctions are important for correlated activity at 20 hpf and younger neurons are more electrically cell autonomous.

To examine this apparent emergence of functional connectivity between ipsilateral cells, we manipulated activity in single cells or in groups of cells and examined the effect on neighboring ipsilateral cells. We used the genetically encoded light-driven chloride pump NpHR, which hyperpolarizes neurons in response to yellow light [19]. GCaMP3 and NpHR were genetically targeted to the same population of ventral spinal neurons in $Gal4^{s1020t}$/UAS:GCaMP3/UAS:NpHR-mCherry [20] fish (Figure S5A). Spatial targeting of NpHR-activating light was accomplished using a digital micromirror device (DMD). Its spatial resolution was tested by photoconversion of the fluorescent protein Kaede, and light could be restricted to single cells (Figure S5E).

Because NpHR-activating 593nm light does not overlap with the excitation or emission spectrum of GCaMP3 [15], calcium events could be imaged simultaneously during NpHR activation. Spontaneous calcium events imaged with GCaMP3 in NpHR-expressing fish were blocked successfully by illumination of 593 nm light at 19 mW/mm^2 (Figures S5B–S5D). As seen earlier, including in other zebrafish neurons [19, 20], light offset triggered rebound excitation (Figures S5C and S5D), al-lowing us to excite as well as inhibit with a single tool.

We observed striking differences in network responses to NpHR activation between younger and older embryos. Illumination of single cells in younger animals (18–18.5 hpf) caused robust inhibition in the illuminated cell and a rebound excitation upon light-off (Figure 4A) but had no effect on other ipsilateral cells, suggesting low connectivity, where individual cells are functionally independent. In contrast, single-cell illumination at 20–20.5 hpf did not significantly affect activity in either the illuminated cell or in other ipsilateral cells (Figure 4B). However, illumination of a group of cells in a region encompassing two hemi-somites strongly suppressed activity during illumination and evoked rebound excitation upon light-off in both the illuminated cells and nonilluminated ipsilateral neighbors (Figure 4C). Connectivity through electrical synapses can explain the ineffectiveness of NpHR single cell manipulation in the older embryo (Figure 4B), because spread to neighbors of chloride current pumped into an individual cell would reduce the efficacy of the hyperpolarization in that cell. The bidirectionality of electrical synapses can also explain why the inhibition and activation spread to nonilluminated cells in both the rostral and caudal directions (Figure 4D) even though the only spontaneously active ipsilaterally projecting interneurons—the VeLD and IC cells—both have descending axons during this period of development [21, 30, 31]. In summary, our data suggest that increased functional connectivity underlies the emergence of ipsilateral correlation observed between 17.5 and 20 hpf (Figure 2C).

Triggered Rhythmic Oscillation with NpHR Reveals Acquisition of Contralateral Antagonism

Supraspinal activation of the spinal CPG is bilateral for forward swimming but triggers an alternating response in downstream spinal targets [32, 28]. This behaviorally relevant coordinated firing relies on robust inhibitory connections between the two sides of the cord [14]. We tested whether the left and right sides of the cord were functionally antagonistic in the embryo by assessing network responses to bilateral stimulation evoked by NpHR rebound excitation that was confined to the neuronal cell types expressing in the $Gal4^{s1020t}$ line. $Gal4^{s1020t}$/ UAS:GCaMP3/UAS:NpHR-mCherry embryos were illuminated bilaterally over a four-somite region for 15 s, a duration that reliably triggered rebound excitation at light-off (Figures S5C and S5D; Figures 5A and 5B). At 18 hpf, bilateral rebound activation triggered calcium events on the left and right sides of the cord with the initial wave of activity occurring nearly simultaneously on the two sides (Figure 5A). In contrast, at 20 hpf, the rebound excitation triggered a wave of activity first on one side and then, after a substantial delay, on the other side (Figure 5B). The firing then alternated back and forth between the two sides, similar to what was seen in spontaneous locomotor-like activity (Figure 1F and 2B, right). The delay between correlated events (two or more cells participating) on the left and right sides following light offset increased significantly between 18 and 21 hpf ($p < 10^{23}$, paired Student's t test, n = 6 fish; Figure 5D), suggesting that contralateral antagonism is strengthened during this period.

Developmental Transition Disrupted by Inhibition of Activity

To determine the influence of uncorrelated spontaneous activity on the formation of the correlated network and the locomotor CPG, we inhibited spontaneous events for 1 hr with NpHR during the period of transition from uncorrelated to correlated activity (18 to 19 hpf), while imaging population activity with GCaMP3 (Figure 6). To prevent cumulative desensitization of NpHR during long-term activation, we applied a 500 msec pulse of blue light (410 nm) every 10 s [33, 19], concurrently with yellow light using a double bandpass filter to prevent rebound stimulation with yellow light off (Figure 6A). Light was applied to the full imaged region covering both sides of the cord and approximately six somites, centered at somites 5 and 6.

Activation of NpHR from 18 to 19 hpf with yellow/blue light resulted in a reduction in the frequency during the 18 to 19 hpf period in NpHR-positive fish as compared to three control groups: (1) NpHR-negative fish without yellow/blue light, (2) NpHR-negative fish with yellow/ blue light, and (3) NpHR-positive fish without yellow/blue light (Figure 6B). NpHR-induced inhibition reduced activity by 66% initially (18 hpf) and by 53% by the end of the illumination period (19 hpf) compared to GCaMP only (group 1) controls (Figure 6B). An intermediate decrease in the frequency of spontaneous events was observed in NpHR-positive fish that did not receive the yellow/blue light protocol (group 3). This effect

was attributed to the fact that the 488 nm imaging light overlaps with the NpHR excitation spectrum and activates the pump by approximately 18% [19]. To eliminate potential effects of the imaging light on the frequency of spontaneous events, we imaged the population patterns only at the end of the experiment (22 hpf) for NpHR without yellow/blue light controls.

We observed a substantial reduction in pairwise ipsilateral correlation in the experimental fish (NpHR-positive fish receiving the yellow/blue light protocol) when compared to controls (Figure 6C), though the four groups did not differ at baseline at 18 hpf (ipsilateral correlation one-way analysis of variance [ANOVA], $p = 0.22$). This reduction in correlation became evident at 20.5 hpf and continued through 22 hpf (Figure 6C). Additionally, the three controls were similar at 22 hpf, indicating that neither NpHR expression alone, possible NpHR constitutive activity alone, nor yellow/blue light alone disrupts the emergence of correlated activity.

An examination of the activity in control and experimental fish showed that by 22 hpf, the experimental fish had a larger proportion of active cells with immature phenotypes (Figure 7B). As shown above (Figures 1–3) and in control fish (Figure 7A), most active cells were part of an ipsilateral, correlated network in the older embryo, with a small minority of the cells showing long-duration, uncorrelated events, and usually residing more medially in the spinal cord (Figures 1D and 1E; Figure 7A, asterisks). In contrast, in experimental fish, approximately 50% of the active cells were uncorrelated, with long-duration events (Figure 7B, asterisks; Figure 7C), displaying the more immature activity pattern that we observed in our single-cell tracking (Figure S2). Associated with this perturbed pattern of activity, we found that in the experimental animals, a larger fraction of the active cells were located closer to the midline of the spinal cord (Figure 7B, asterisks; Figure 7D), where more immature cells, like BrdU-incorporating progenitor cells, have been shown to reside [24]. Groups did not differ in events kinetics (width at half maximum one-way ANOVA, $p = 0.30$) nor the location of active cells (distance to midline one-way ANOVA, $p = 0.28$) at 18 hpf before activity manipulation. The number of active cells per field of view was not significantly different between experimental and control fish (Figure S6), suggesting that the optical inhibition of activity in motor neurons and VeLDs perturbed the developmental transition by reducing the efficiency with which cells that originated at the midline joined the lateral correlated network.

Discussion

Rapid Emergence of Ipsilateral Correlation

Optical measurements of spontaneous activity in genetically selected ventral spinal neurons in live zebrafish revealed a rapid transition from uncorrelated, sporadic slow activity to ipsilaterally correlated fast activity. The transition to correlated activity could be accounted for by the formation of electrical connections, which initially couple nearby

neurons into local microcircuits and then merge to include the majority of active ipsilateral neurons into a single coupled network.

Our observations in vivo are consistent with observations made previously. In *Xenopus*, cell-autonomous calcium events are seen in dissociated spinal cultures and in the isolated spinal cord, with short-duration calcium events becoming correlated between small groups of neurons later in development [7]. In isolated spinal cord of rodent [34] and chick [35], spontaneous events, which are correlated between motor neurons and interneurons, propagate between multiple spinal segments [35]. In the zebrafish spinal cord, cell-autonomous calcium events have been detected in axon-less cells of the 19–26 hpf embryo in imaging experiments but likely overlap minimally with the events we detected due to their very slow kinetics [36]. Correlated depolarizations have been observed between pairs of ventral neurons in dual-cell electrophysiological recordings in 20–24 hpf zebrafish embryos [21], which likely correspond to the correlated calcium events we observed with GCaMP. During swimming, waves of activity propagate down the ipsilateral spinal cord, resulting in nearby motor neurons being more correlated than distant ones [14, 28]. A similar, though slower, rostral to caudal propagation is observed in spontaneously active motor neurons of 24 hpf zebrafish embryos [16]. We observed that nearby spinal neurons became correlated before distant neurons, suggesting that more mature rostral to caudal relationships are established as the first connections are formed between neurons.

The changes in global activity patterns that we observed were associated with a rapid strengthening of functional connectivity between ipsilateral neurons, as seen from the change in the spread of NpHR inhibition and rebound excitation to nonilluminated cells, suggesting that early activity is cell autonomous and later activity depends on network interactions. The initiation of rhythmic spontaneous events in the rodent and chick spinal cord has been shown to depend on recurrent excitation between GABA-, glycine- and glutamatergic interneurons and cholinergic motor neurons [1, 9]. The ipsilateral network interactions that we observed in the zebrafish appear to be mediated via electrical synapses, as shown in previous studies [26, 21], though chemical synapses may also play a role. Gap junctions also appear to play an integral role in the propagation of correlated spontaneous activity in the spinal cord of rodents [9] and chicks [37] and appear to form some of the first connection in the developing retina [38], cortex [39], and hippocampus [6].

Contralateral Antagonism Emerges Concurrently with Ipsilateral Correlation

We found that as the coupled ipsilateral network was established there also emerged a superstructure in which the spontaneous activity alternated from side to side, a fundamental characteristic of the CPG, which has been shown to involve contralateral inhibition through chemical synapses [14]. Earlier lesion studies have indicated that spontaneous activity and left/right alternation in the spinal cord of embryonic zebrafish

does not rely on input from the brain [25, 40], suggesting that the network mediating this rhythmic activity is endogenous to the spinal cord. Given that, among the cells expressing in our Gal4 line, only KAs and VeLDs project within the spinal cord, and, of these, only the VeLDs are active in the first day of development; it therefore appears that the VeLDs, and neurons that they drive, can account for a minimal circuit for locomotor-like activity and behavior.

In rats and mice, spontaneous events are at first synchronized between both sides of the spinal cord and begin to alternate between sides around birth when the activation of $GABA_A$ and glycine receptors become hyperpolarizing [8, 9]. We did not observe a period of synchronized spontaneous events between the left and right sides of the spinal cord in the zebrafish. Rather, the first coordinated patterns consisted of both ipsilateral correlation and contralateral alternation (Figures 2B and 2C). We observed similar patterns of alternating activity with bilateral rebound activation with NpHR. The similarity between spontaneous and NpHR rebound-evoked alternation suggests that a bilateral drive may be responsible for triggering the earliest alternating bursts of locomotor-like activity in the embryonic zebrafish.

Activity-Dependent Emergence of the CPG

Inhibition of activity for 1 hr with NpHR during the transition from sporadic to patterned activity disrupted the emergence of correlated, short duration, rhythmic activity, indicating that early activity is either instructive or permissive for the maturation of the spinal network. In the normal development of the spinal cord, our imaging revealed that cells first display long-duration, uncorrelated events before transitioning to brief, correlated activity as they establish functional connectivity with other neurons. This transition occurred in neurons that became active early (e.g., Figure S2A) and in neurons that matured and integrated into the network at a later stage (e.g., Figure S2B). Light-driven reduction of activity with NpHR reduced the overall ipsilateral correlation by reducing the fraction of cells that made the transition to brief, correlated activity. As seen in control fish experiencing normal activity, the uncorrelated cells tended to be located more medially in the spinal cord, except that in the fish whose activity had been inhibited by light, they went from being a small minority to being roughly half of the active cells (Figure 7).

These effects are striking given that the inhibition of activity is only by approximately half, it lasts for only 1 of the 3 hr of the developmental transition, and it occurs in only a subset of ventral spinal neurons: the VeLD interneurons and motor neurons (the KAs, also targeted in the $Gal4^{s1020t}$ line, have not been shown to display rhythmic spontaneous activity [21]). These observations imply that early spontaneous activity in VeLD interneurons and/or motor neurons, or in neurons that they drive, is required for the integration of less mature neurons into the correlated network and for the acquisition of normal patterns of population activity. The effect that we observe from inhibiting activity between 18 and 19 hpf was not present until 20.5 hpf, suggesting that inhibition of activity

in the few cells that are active early likely alters the integration of other neurons that mature later.

Previous studies have shown that calcium fluctuations play an essential role in developmental processes such as cell migration [41], axon guidance [42], and the expression of the membrane proteins that control cell excitability [43]. It is possible that some or all of these mechanisms underlie the effect of activity manipulation that we observe. For example, a lateral position could be required for integration into the correlated network, and blocking migration to this position could subsequently reduce the number of coupled cells. It has recently been shown that endogenous patterns of spontaneous activity are required for the proper development of coordinated patterns of activity in the motor system of an invertebrate [44]. Here we show that early uncorrelated spontaneous activity is required for the formation of coordinated motor circuits in a vertebrate.

Conclusion

Correlated, rhythmic spontaneous activity is a common feature of developing networks and is essential for normal circuit maturation. By applying noninvasive optical tools to image activity, we observed a rapid transition from sporadic, long-duration, uncorrelated activity to fast, correlated, and rhythmic spontaneous activity in the spinal cord of the intact developing zebrafish. Correlated activity between neurons on the same side of the cord was found to emerge through the formation of small local microcircuits and their subsequent coalescence into a single ipsilateral network, at the same time as side-to-side alternation emerged. This transition to patterned locomotor-like population activity is perturbed by optical inhibition of motor neurons and VeLD interneurons during the transition period, impeding the integration of maturing neurons into the coordinated network. These results indicate that the formation of the spinal CPG is dependent on activity that occurs before functional connectivity is robustly established in the network.

Experimental Procedures

The following transgenic lines were used for experiments (naming according to official zebrafish nomenclature): Et(−0.6hsp70l:Gal4-VP16)s1020t (a.k.a. Gal4s1020t) [22]; Tg(UAS-E1b:Kaede)s1999t/+ (a.k.a. UAS:Kaede) [22]; and Tg(UAS:NpHRmCherry) s1989t (a.k.a. UAS:NpHR) [20], as well as UAS:GCaMP3 [18]. Animal experiments were done under oversight by the University of California institutional review board (Animal Care and Use Committee).

Embryo Preparation and GCaMP imaging

Embryos of the Tubingen genetic background were raised in E3 embryo medium at 28.5ºC until 60% epiboly, and at 25ºC thereafter to delay development for experimentation. GCaMP positive progeny of UAS:GCaMP3 and Gal4s1020t fish were mounted in 1.4% agar and paralyzed with injections of 750μg/ml ∝-bungarotoxin

(Invitrogen) into the tail once before imaging (at 17-17.5 hpf). Embryos were aged by somite counting and were in a 28.5ºC heated chamber for time-lapse experiments (including NpHR rebound experiments, Fig. 5) so that they could develop at a normal rate. NpHR functional connectivity experiments (Fig. 4, 5) were performed at room temperature. Morphology images of UAS:Kaede/ Gal4s1020t fish were taken on a Zeiss 510 Meta confocal microscope. Functional imaging was performed on a 3i Marianas system (Intelligent Imaging Innovations) with a spinning disk confocal (Yokagawa) mounted on a Zeiss microscope and using a 488nm laser and 20x water-immersion objective (numerical aperture = 1.0). For time-lapse experiments, 4 minute movies were acquired every half hour at 4 Hz. Imaging was acquired at 2 Hz for all NpHR experiments to reduce potential activation of NpHR by imaging light.

Photomanipulation of activity

Photostimulation of NpHR and Kaede was accomplished through a digital micro-mirror device (DMD) illumination system (Photonic Instruments) coupled to the imaging microscope. Activating light was provided by a Xenon lamp (Sutter Instruments) filtered to 573-613nm and was 19mW/mm2 at the sample. Spatial and temporal control of the yellow light was achieved through integration software (Intelligent Imaging Innovations). NpHR experiments were performed on UAS:NpHR-mCherry/ UAS:GCaMP3/ Gal4s1020t fish displaying both red and green fluorescence. For functional connectivity experiments (Fig. 4), the experimental protocol consisted of 1 minute NpHR activation with yellow light to the targeted region (e.g. single cell, two somite section or two somite-sized light control off of cord) followed by 1 minute of rest while calcium activity was simultaneously imaged at 2 Hz. Experimental epochs were preceded and followed by 2 minute baseline periods for frequency normalization of individual cells. Single cell manipulations were restricted to CaP primary motoneurons for consistency. For bilateral rebound excitation experiments (Fig. 5), light was applied in 15 second intervals with 15 seconds of rest in between and repeated four times per embryo per time point. For chronic manipulation of activity (Fig. 6A), 9.5 seconds of 19mW/mm2 593 nm light alternated with 500 msec of yellow/blue light using a double bandpass filter for 410 nm and 568 nm to provide continuous yellow light illumination and pulses of blue light for resensitization of NpHR. GCaMP3 movies were taken during light manipulation to test effectiveness of inhibition.

Analysis of calcium imaging movies

All analysis for time-lapse and NpHR experiments was performed using Matlab (Mathworks). ROI and time course extraction: Drift during image acquisition was corrected using the DIPimage package (www.diplib.org) for all time-lapse and NpHR movies. The CellSort toolbox was used to automatically detect active cell bodies, identified as contiguous pixel islands, each with a distinctive time course of response. ROIs that were redundant (i.e. corresponding to the same cell) were manually merged; ROIs corresponding to axons or moving cells were manually removed. Traces plotted in Figs. 1, 4 and 7 and Supplemental Figs. 1F, 2 and 5 were normalized by taking the zscore of the ΔF/F values (plots display these standard deviation values) to best visualize the event contours in all cells. All other traces shown are ΔF/F. See Supplemental Fig. 1G for a comparison of traces pre- and post-normalization. Event detection and characterization: Each intensity trace was scanned for instances when the rise in fluorescence over a 1-

second interval exceeded an empirically determined threshold. The resulting estimated timing and amplitudes of the events were used to initialize a parameterized model of the trace, which was subsequently refined using a nonlinear, least-squares fitting algorithm (lsqnonlin, Matlab). The model consisted of three components: a cubic spline that accounted for any slow drifts in baseline; a double exponential kernel to match each cell's unique, stereotyped calcium transient (e.g. Fig. 1B, E); and the timing and amplitude of each event detected as described above. The convergence of the resulting fits was manually verified. Events were identified as spurious if the estimated magnitude was exceeded by its confidence interval. The amplitudes and timings of all remaining events encoded the time course of a cell's activity (e.g. Fig 1C, F) and were used for all subsequent analysis. Characterization of synchronous events: To identify time-coupled events in a given movie, binary traces encoding the occurrence of events in all cells were filtered with a 2-second wide Gaussian window and summed. Peaks in the resulting trace that exceeded an empirically-determined threshold were marked as "synchronous" events. Cells were identified as participating in an event when they were active within 1 second of a peak (in other words, synchrony allowed for a little temporal jitter between cells). For these time-coupled cells, lag times between when a particular cell was active and the event peak were determined. The response amplitudes of n cells during m population events (0 if a cell was inactive during the event) were compiled into an n x m matrix. This was used to calculate an n x n correlation matrix, resulting in correlations across events (Figs. 2C, 3, 6C and for Supplemental Figs. 2 and 3). In contrast, the correlations presented in Fig. 2A, B were calculated for the entire activity trace, using the idealized traces filtered with a 1-second wide Gaussian. To identify correlated ensembles of cells within a network for Fig. 3 and Supplemental Fig. 3, cell pairs were marked as belonging to the same group if their correlation across synchronous events was greater than 0.2 for Fig. 3 or 0.5 for Supplemental Fig. 3. Separate groups were then identified using the components function within the Matlab mesh partitioning toolbox4. NpHR experiments: For the analysis of NpHR functional connectivity experiments, frequency in the first 30 seconds after yellow light on- and off was compared to average frequency for pre- and post-experiment baseline epochs in paired Student's t tests. For NpHR rebound bilateral excitation experiments, synchronous events were determined as described above and left/right lag was determined by calculating the temporal difference between the first synchronous event (two or more cells) on the left versus the right side of the cord after light offset. Ipsilateral correlation for Fig. 6C was calculated as in Fig. 2C.

Statistical analysis: For chronic Halorhodopsin experiments, the effect of group (GCaMP, GCaMP/Light, GCaMP/NpHR, and GCaMP,NpHR,Light) on frequency x amplitude (Fig. 6B), mean correlation (Fig. 6C), mean event width (Fig. 7C), mean cell distance to midline (Fig. 7D), and number of active cells (Supplemental Fig. 6) was tested with one-way ANOVAs at each time point. Time points with significant effects of group ($p<0.05$) were further analyzed with a post-hoc comparison test with Bonferroni correction (at alpha = 0.05 and 0.01) to identify which group pairs were significantly different from one another. For all other analyses, statistical significance between mean data was calculated using the unpaired and paired two-tailed Student's t test.

Figure 1

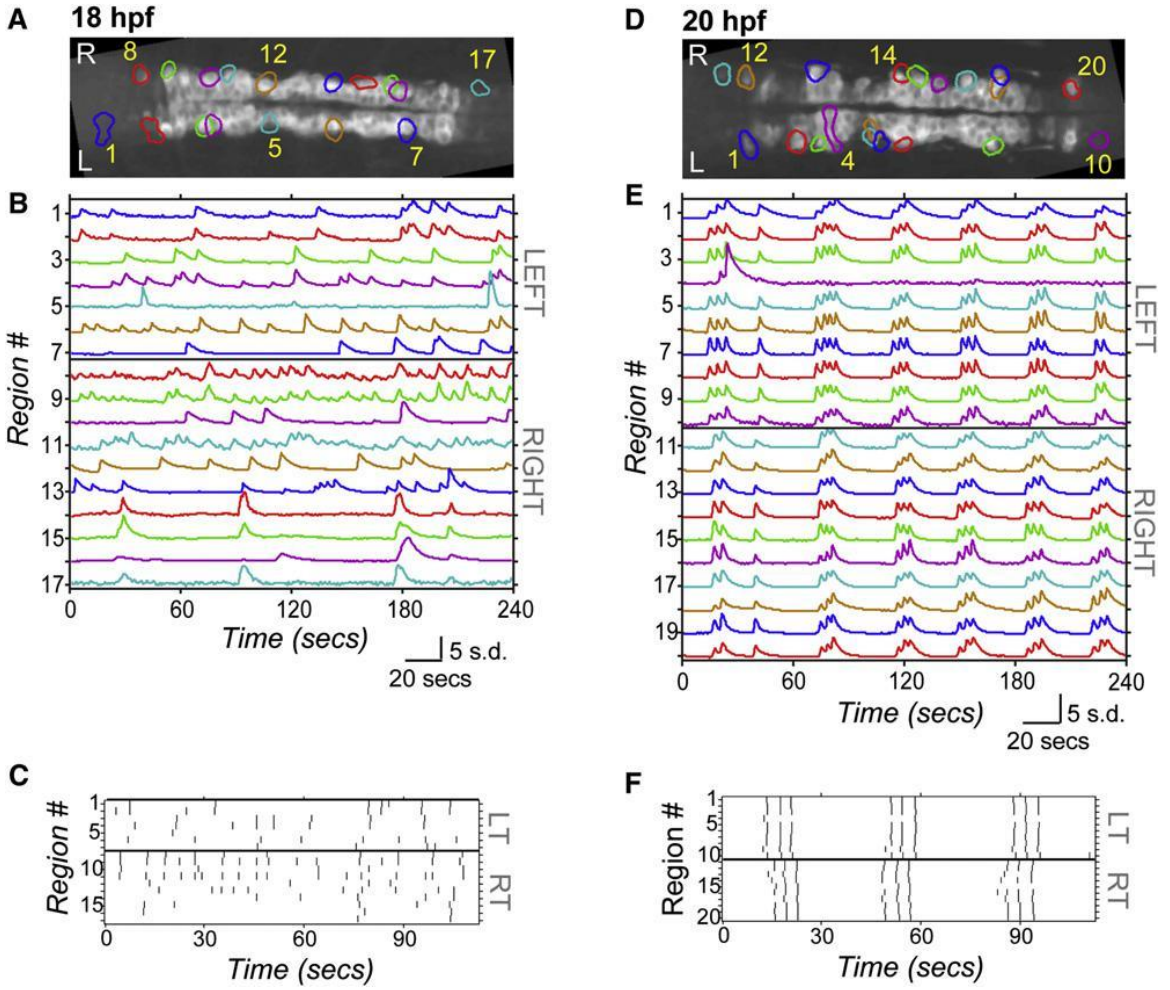

Figure 1. Spontaneous Calcium Activity in Spinal Neurons Progresses from Sporadic to Locomotor-Like During Embryonic Development. GCaMP3 activity in single neurons in one example embryo at 18 hpf (left) and 20 hpf (right). **A, D.** Dorsal views of GCaMP3 baseline fluorescence with active regions circled (rostral left; imaged area somites 4–8). **B,E.** Normalized intensity traces for active regions (identified on y axis) for the left and right sides of the cord, with amplitude corresponding to standard deviations (s.d.) of fluorescence away from baseline. **B.** At 18 hpf, ipsilateral neurons have little correlated firing, though some synchronization is observed (e.g., cells 8 and 9). **E.** At 20 hpf, ipsilateral neurons are tightly synchronized, with few exceptions (e.g., cell 4; note elongated shape extending to the midline). **C,F.** Raster plots of detected events for subsection of data in (B) and (E). **C.** At 18 hpf, population activity is uncoordinated. **F.** By 20 hpf, ipsilateral cells are synchronized, contralateral cells alternate, and a higher order left/right bursting organization is observed. See also Figure S1.

Figure 2

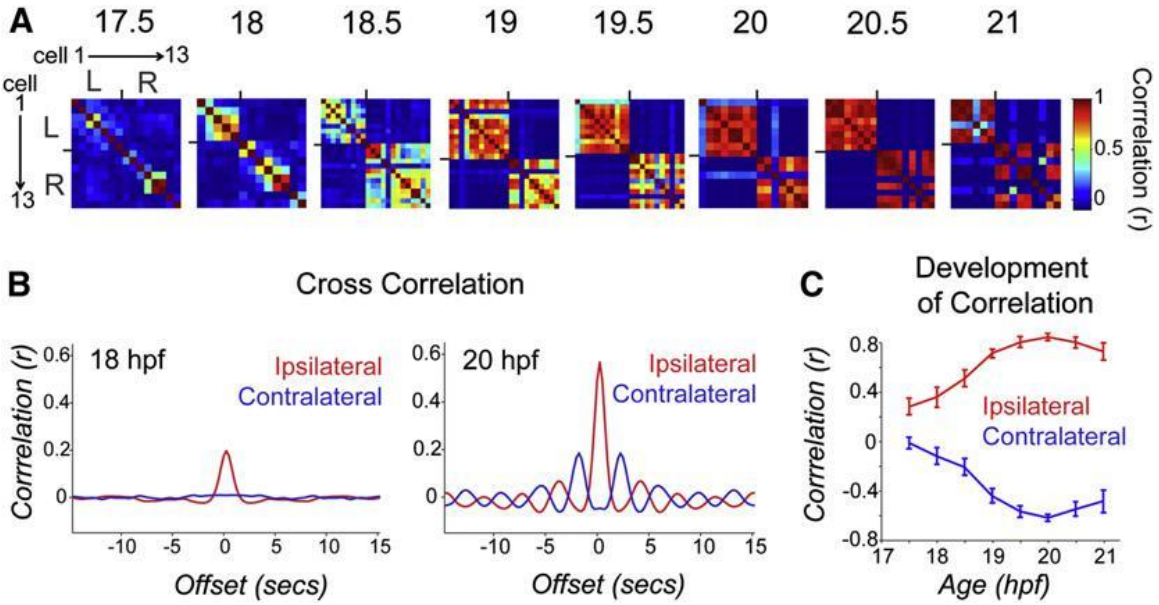

Figure 2. Pairwise Cell Relationships Progress from Independent to Ipsilaterally Correlated and Contralaterally Anticorrelated during a Short Period of Development. A. Correlation matrices of single-cell traces through the development of an example embryo. Each pixel represents a pairwise comparison between two cells, with high correlation values in red and perfect autocorrelation along the diagonal. Cells are sorted left to right and top to bottom as shown for 17.5 hpf. Ticks mark border between left and right cord and bound a high degree of ipsilateral correlation observed at later time points. **B.** Cross-correlation shows a strengthening of ipsilateral coupling between 18 and 20 hpf and acquisition of oscillatory rhythm by 20 hpf. Cross-correlation was calculated by averaging time-shifted correlation data for all ipsilateral and contralateral cell pairs in individual movies, pooled across nine different fish. **C.** Average pairwise correlations for synchronous events comparing ipsilateral and contralateral cell pairs from individual time-lapse movies acquired from fish ages 17.5 to 21 hpf and pooled across fish. We observed a significant difference between ipsilateral correlations in younger versus older embryos (18 hpf, $r = 0.272 \pm 0.082$; 20 hpf, $r = 0.761 \pm 0.031$; $p < 10^{-3}$, paired Student's t test; n = 9 fish) and a significant increase in the anticorrelation of contralateral cells (18 hpf, $r = 20.207 \pm 0.067$; 20 hpf, $r = 20.710 \pm 0.028$; $p = < 10^{-3}$, paired Student's t test; n = 9 fish). n = 9 fish for 18–21 hpf; n = 4 fish at 17.5 hpf. Error bars = SEM. See also Figure S2.

Figure 3

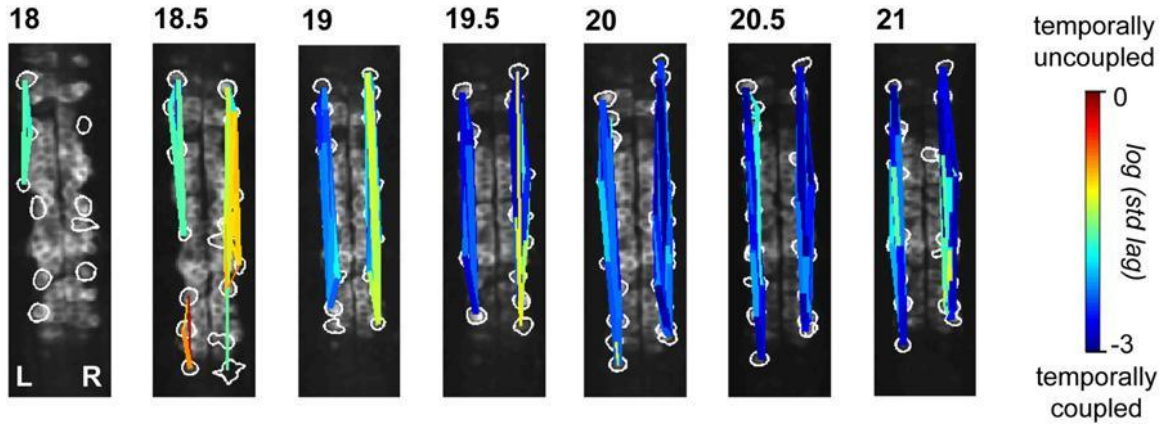

Figure 3. Ipsilateral Correlation Is Acquired through the Progressive Synchronization of Local Subgroups of Cells. Spatial maps of correlated groups in an example fish from 18 to 21 hpf show small local circuits containing a few cells at 18 and 18.5 hpf that expand into full correlation of each side at later stages. Correlations between all cell pairs were calculated and lines were drawn between cell pairs with correlations greater than 0.2, with thicker lines representing stronger correlation. Line color represents the log of the standard deviation of the lags between event start times of cell pairs and shows an overall increase in temporal precision between ipsilateral pairs as development progresses. See also Figure S3.

Figure 4

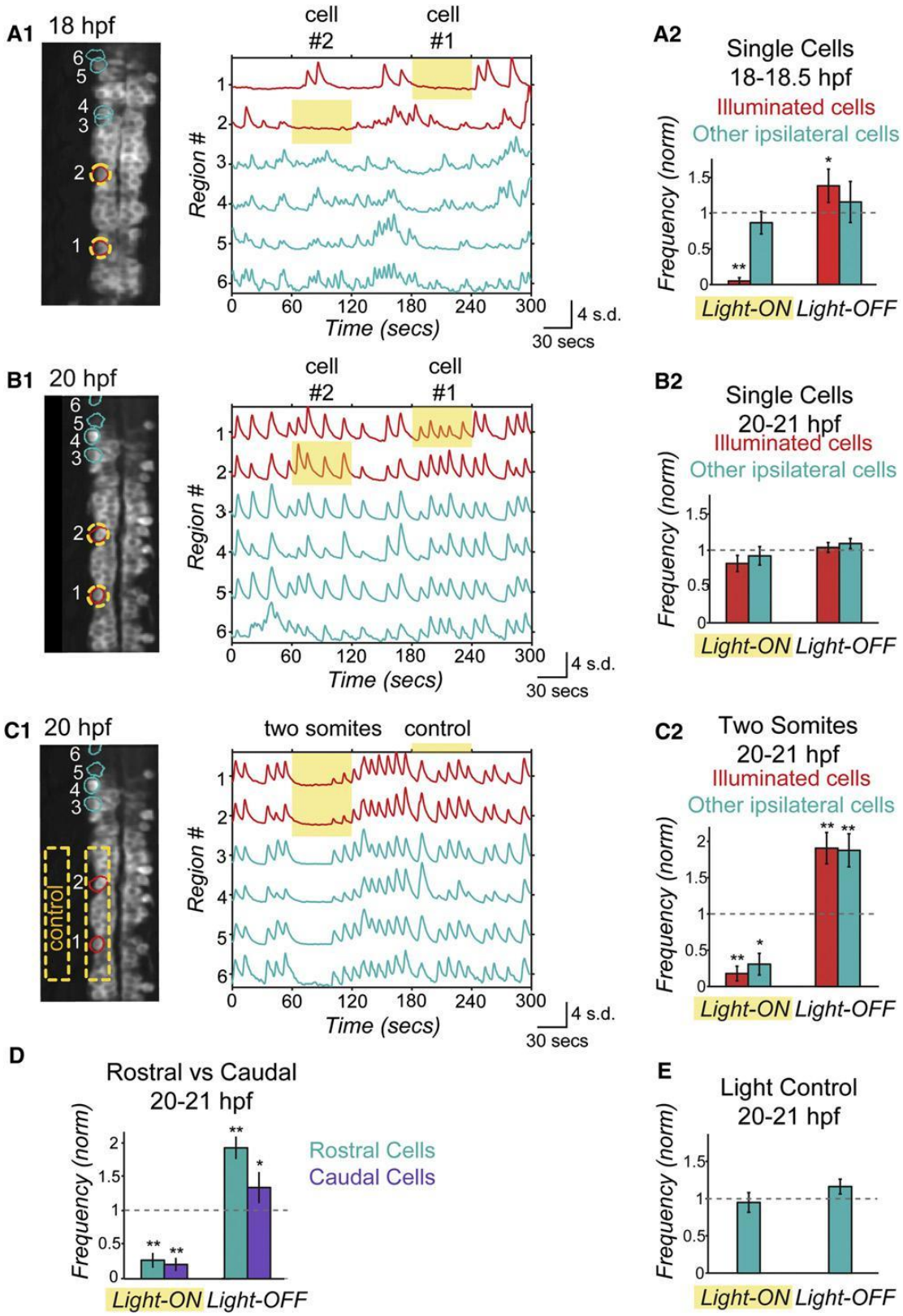
A1
18 hpf
cell #2
cell #1
Region #
Time (secs)
4 s.d.
30 secs
A2
Single Cells
18-18.5 hpf
Illuminated cells
Other ipsilateral cells
Frequency (norm)
Light-ON Light-OFF
B1
20 hpf
B2
Single Cells
20-21 hpf
C1
20 hpf
two somites
control
C2
Two Somites
20-21 hpf
D
Rostral vs Caudal
20-21 hpf
Rostral Cells
Caudal Cells
E
Light Control
20-21 hpf

Figure 4. Optical Manipulation of Targeted Network Components with NpHR Reveals Changes in Functional Connectivity between Ipsilateral Neurons during Development **A,B.** Single-cell optical manipulation of spontaneous activity with NpHR at 18 hpf (A) and 20 hpf (B). Illumination at 593 nm at 19 mW/mm^2 is targeted successively to two regions outlined in yellow (A1, left), while calcium population activity is simultaneously recorded (A1, right) in the illuminated cells (red) and in the other ipsilateral cells (teal), and here displayed as normalized traces (standard deviation, s.d.) with regions indicated on y axis. **A.** At 18 hpf, application of yellow light to a single cell (during yellow highlight bar) inhibits only the illuminated cell, while other cells remain active. Pooled results (n = 6 embryos) show inhibition during light-ON and activation at light-OFF to be limited to illuminated cells (red bars). **B.** At 20 hpf, single-cell illumination has no effect on activity of either the illuminated or nonilluminated cells (n = 7 embryos). **C.** At 20 hpf, illumination of one side of spinal cord in region spanning two somites (yellow outline in image, left) inhibits and rebound excites both the illuminated cells and other ipsilateral cells (n = 7 embryos). **D.** Reduction of activity and rebound due to NpHR activation at 20 hpf are observed in cells that are both rostral and caudal to the region illuminated. **E.** Control application of light aimed to the side of the cord but within the embryo (C1) does not perturb activity (n = 7 embryos), indicating that effect on unilluminated ipsilateral cells is not due to light scattering, though we acknowledge that light scattering may have different properties in this region. Rostral end points up in fluorescence images. Significance values from paired Student's t-test are *$p < 0.05$ and **$p < 0.01$. See also Figures S4 and S5.

Figure 5

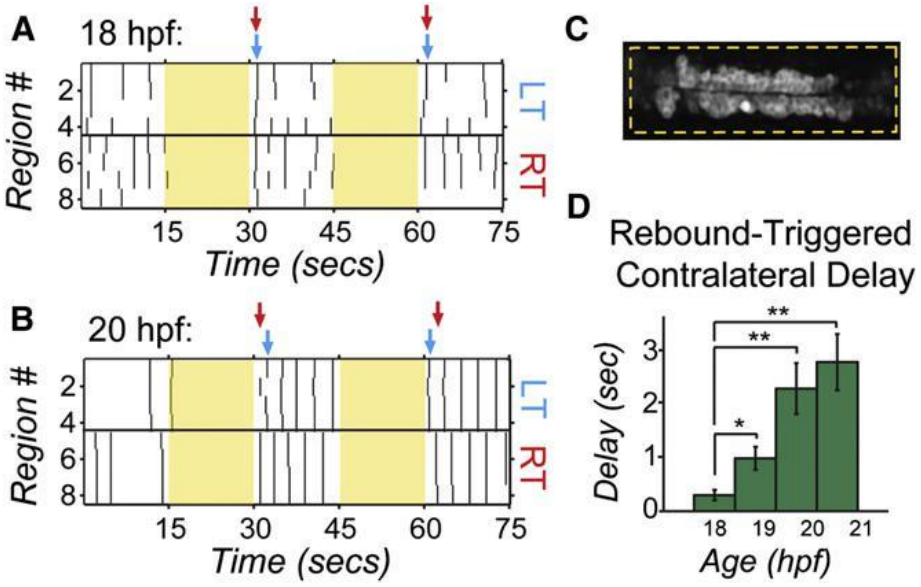

Figure 5. Bilateral Activation with NpHR Rebound Reveals Acquisition of Contralateral Antagonism during Development. Raster plots of spontaneous events of left and right cells in a single embryo at 18 hpf and 20 hpf during and following bilateral NpHR inhibition with 593 nm light (yellow bars) covering approximately four somites (C). **A.** Bilateral activation following NpHR inhibition at 18 hpf results in near simultaneous activation of left (LT) and right (RT) cells following light offset. Arrows indicate the time when two or more cells participate in an event following light offset for one side of the cord (left side, blue; right side, red). **B.** At 20 hpf, activation at light offset of bilateral illumination results in a burst of activity in which one side fires first, followed, after a delay, by firing on the other side and continuing in alternation of firing from side to side. In this example, the right side is active first in trial 1, but the left side is active first in the trial 2. **D.** The delay following offset of bilateral illumination between synchronous events on the left and right sides of the cord (two or more cells participating) increases during development, suggesting an increase in left/right antagonism. n = 5 fish (four trials per fish per condition); *p < 0.05; **p < 0.01, paired Student's t test. See also Figure S5.

Figure 6

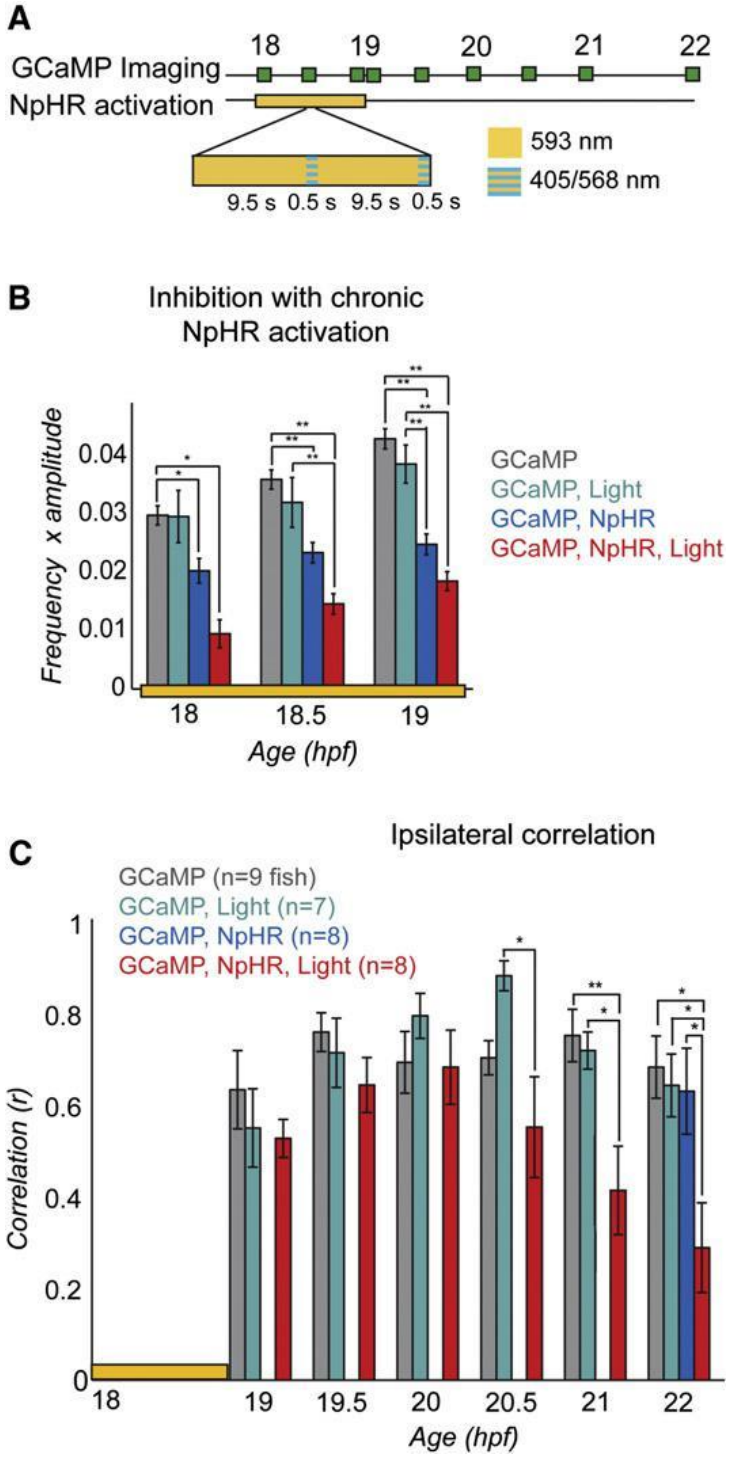
A
18
19
20
21
22
GCaMP Imaging
NpHR activation
593 nm
405/568 nm
9.5 s 0.5 s 9.5 s 0.5 s
B
Inhibition with chronic NpHR activation
Frequency x amplitude
0.04
0.03
0.02
0.01
0
18
18.5
19
Age (hpf)
GCaMP
GCaMP, Light
GCaMP, NpHR
GCaMP, NpHR, Light
C
Ipsilateral correlation
GCaMP (n=9 fish)
GCaMP, Light (n=7)
GCaMP, NpHR (n=8)
GCaMP, NpHR, Light (n=8)
Correlation (r)
1
0.8
0.6
0.4
0.2
0
18
19
19.5
20
20.5
21
22
Age (hpf)

Figure 6. Inhibition of Spontaneous Events with NpHR from 18 to 19 hpf Yields a Subsequent Decrease in Ipsilateral Correlation. A. Experimental protocol for chronic inhibition experiments. GCaMP movies were acquired during the light manipulation (at 18, 18.5, and 19 hpf) with 488 nm light to determine the effectiveness of the light protocol and at half-hour to hour intervals thereafter (until 22 hpf) to assess subsequent changes in network dynamics. Stimulation of NpHR was performed from 18 to 19 hpf with continuous 593 nm light at 19 nW/mm^2 interspersed every 10 s with 500 msec long pulses of light simultaneously at two wave-lengths: 405 nm to reduce desensitization of the NpHR and 568 nm to activate it. **B.** The frequency of calcium events from 18 to 19 hpf was quantified for experimental fish expressing NpHR and receiving the yellow light protocol (GCaMP, NpHR, Light) as well as for three kinds of control fish: (1) NpHR-negative fish without yellow/blue light (GCaMP), (2) NpHR-negative fish with yellow/blue light (GCaMP, Light), and (3) NpHR-positive fish without yellow/blue light (GCaMP, NpHR). Means were calculated per cell, n = 13– 385 cells per group. There was a significant effect of group at 18, 18.5, and 19 hpf (one-way ANOVA at each time point, $p < 0.05$), with greatest decreases in the experimental group (red bars; GCaMP, NpHR, Light). The reduction in activity in embryos that expressed NpHR but did not receive the light protocol can be attributed to the activation of NpHR by the 488 nm imaging light. **C.** Average ipsilateral pairwise correlations measured for experimental fish (n = 8) and the three control groups (n = 7 to 9) in movies acquired after the termination of the yellow/blue light protocol reveal a decrease in correlated activity in the experimental fish (GCaMP, NpHR, Light) at later time points compared to all of the controls. There was no difference between groups at 19, 19.5, and 20 hpf (one-way ANOVA at each time point, $p > 0.05$), with significant differences at 20.5, 21, and 22 hpf (one-way ANOVA at each time point, $p < 0.05$). Note that to avoid activation of NpHR in controls without yellow/blue light protocol, GCaMP imaging in this group was only done at 22 hpf. Error bars = SEM. Asterisks in (B) and (C) mark pairwise significance from post hoc comparison with Bonferroni correction (*$p < 0.05$; **$p < 0.01$).

Figure 7

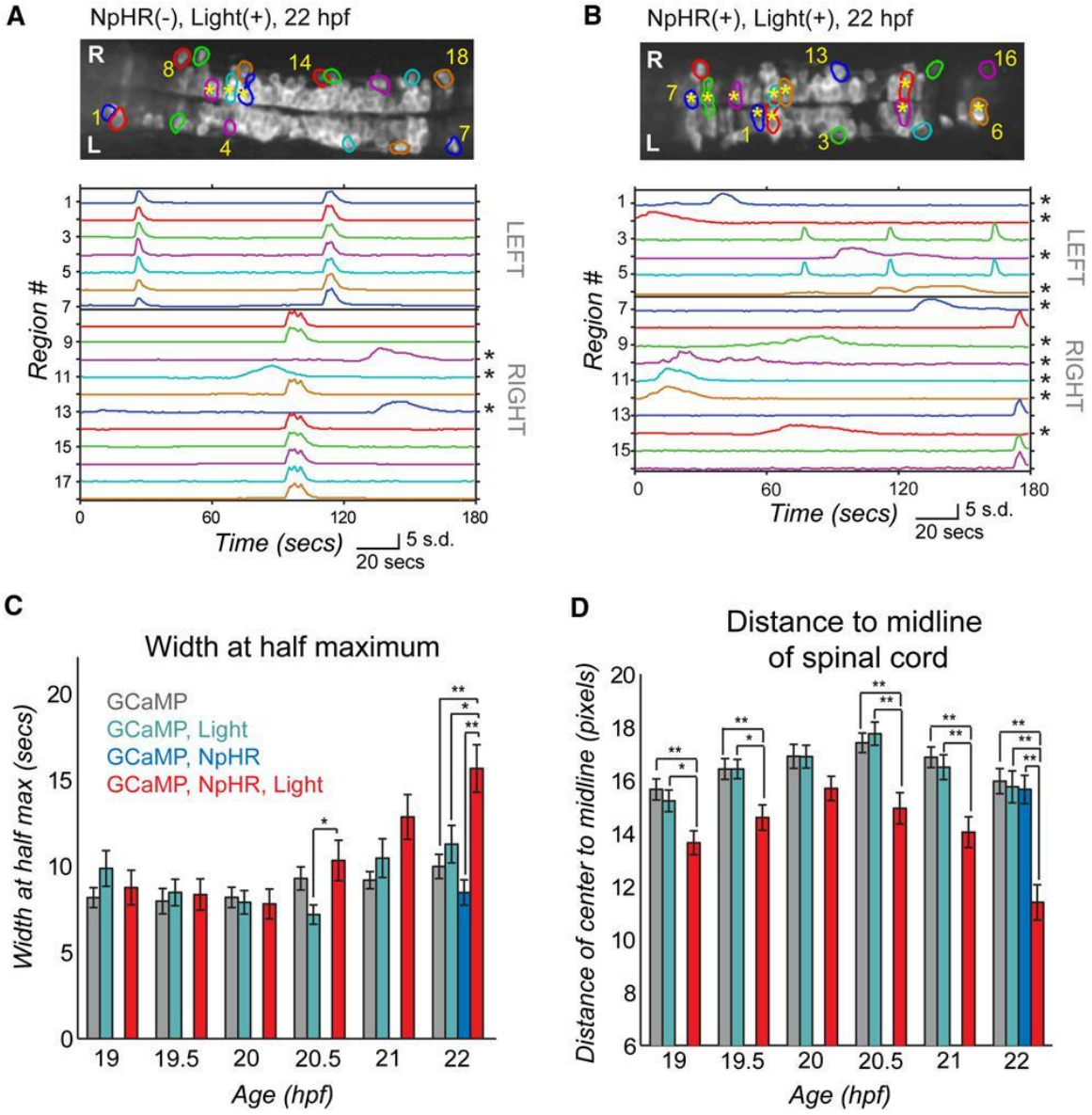

Figure 7. Light Inhibition Decreases the Number of Cells Joining the Correlated Network. A,B. Baseline GCaMP fluorescence images with active regions circled (top, rostral left) and associated normalized intensity traces (bottom; amplitude plots standard deviation, s.d.) in example control fish (without NpHR but illuminated with yellow/blue light protocol from 18–19 hpf) (A) and experimental fish (with NpHR and illuminated with yellow/blue light protocol from 18–19 hpf) (B) at 22 hpf. Asterisks mark cells with long-duration, uncorrelated events, which increase in number in the experimental fish (B, bottom) and can be seen to reside in the medial spinal cord (B, top). **C.** Average event

duration through development was quantified using width at half maximum for experimental fish expressing NpHR and receiving the yellow light protocol (GCaMP, NpHR, Light) and for the three sets of control fish: (1) lacking light and NpHR expression (GCaMP), (2) lacking NpHR expression (GCaMP, Light) or lacking light (GCaMP, NpHR). There was no difference between groups at 19, 19.5, 20, and 21 hpf (one-way ANOVA at each time point, $p > 0.05$), with significant differences at 20.5 and 22 hpf (one-way ANOVA at each time point, $p < 0.05$), when experimental fish showed increases in event duration. **D.** The distance from the cell center to the midline of the cord for active cells is reduced significantly in the experimental (GCaMP, NpHR, Light) fish compared to the three controls at all ages tested except for 20 hpf (one-way ANOVA at each time point, $p < 0.05$). In (C) and (D), means were calculated per cell (72–137 cells per group). Error bars = SEM. Asterisks in (C) and (D) mark pairwise significance from post hoc comparison with Bonferroni correction (*$p < 0.05$; **$p < 0.01$). See also Figure S6.

References

1. Blankenship, A.G., and Feller, M.B. (2010). Mechanisms underlying spontaneous patterned activity in developing neural circuits. Nat. Rev. Neurosci. *11*, 18–29.
2. Spitzer, N.C. (2004). Coincidence detection enhances appropriate wiring of the nervous system. Proc. Natl. Acad. Sci. USA *101*, 5311– 5312.
3. Torborg, C.L., and Feller, M.B. (2005). Spontaneous patterned retinal activity and the refinement of retinal projections. Prog. Neurobiol. *76*, 213–235.
4. Gust, J., Wright, J.J., Pratt, E.B., and Bosma, M.M. (2003). Development of synchronized activity of cranial motor neurons in the segmented embryonic mouse hindbrain. J. Physiol. *550*, 123–133.
5. Corlew, R., Bosma, M.M., and Moody, W.J. (2004). Spontaneous, synchronous electrical activity in neonatal mouse cortical neurones. J. Physiol. *560*, 377–390.
6. Cre´pel, V., Aronov, D., Jorquera, I., Represa, A., Ben-Ari, Y., and Cossart, R. (2007). A parturition-associated nonsynaptic coherent activity pattern in the developing hippocampus. Neuron *54*, 105–120.
7. Gu, X., Olson, E.C., and Spitzer, N.C. (1994). Spontaneous neuronal calcium spikes and waves during early differentiation. J. Neurosci. *14*, 6325–6335.
8. Nakayama, K., Nishimaru, H., and Kudo, N. (2002). Basis of changes in left-right coordination of rhythmic motor activity during development in the rat spinal cord. J. Neurosci. *22*, 10388–10398.
9. Hanson, M.G., and Landmesser, L.T. (2003). Characterization of the circuits that generate spontaneous episodes of activity in the early embryonic mouse spinal cord. J. Neurosci. *23*, 587–600.
10. Delpy, A., Allain, A.-E., Meyrand, P., and Branchereau, P. (2008). NKCC1 cotransporter inactivation underlies embryonic development of chloride-mediated inhibition in mouse spinal motoneuron. J. Physiol. *586*, 1059–1075.
11. Hanson, M.G., Milner, L.D., and Landmesser, L.T. (2008). Spontaneous rhythmic activity in early chick spinal cord influences distinct motor axon pathfinding decisions. Brain Res. Rev. *57*, 77–85.
12. Gonzalez-Islas, C., and Wenner, P. (2006). Spontaneous network activity in the embryonic spinal cord regulates AMPAergic and GABAergic synaptic strength. Neuron *49*, 563–575.
13. Myers, C.P., Lewcock, J.W., Hanson, M.G., Gosgnach, S., Aimone, J.B., Gage, F.H., Lee, K.F., Landmesser, L.T., and Pfaff, S.L. (2005). Cholinergic input is required during embryonic development to mediate proper assembly of spinal locomotor circuits. Neuron *46*, 37–49.
14. Grillner, S. (2006). Biological pattern generation: the cellular and computational logic of networks in motion. Neuron *52*, 751–766.

15. Tian, L., Hires, S.A., Mao, T., Huber, D., Chiappe, M.E., Chalasani, S.H., Petreanu, L., Akerboom, J., McKinney, S.A., Schreiter, E.R., et al. (2009). Imaging neural activity in worms, flies and mice with improved GCaMP calcium indicators. Nat. Methods *6*, 875–881.

16. Muto, A., Ohkura, M., Kotani, T., Higashijima, S., Nakai, J., and Kawakami, K. (2011). Genetic visualization with an improved GCaMP calcium indicator reveals spatiotemporal activation of the spinal motor neurons in zebrafish. Proc. Natl. Acad. Sci. USA *108*, 5425–5430.

17. Higashijima, S., Masino, M.A., Mandel, G., and Fetcho, J.R. (2003). Imaging neuronal activity during zebrafish behavior with a genetically encoded calcium indicator. J. Neurophysiol. *90*, 3986–3997.

18. Del Bene, F., Wyart, C., Robles, E., Tran, A., Looger, L., Scott, E.K., Isacoff, E.Y., and Baier, H. (2010). Filtering of visual information in the tectum by an identified neural circuit. Science *330*, 669–673.

19. Zhang, F., Wang, L.P., Brauner, M., Liewald, J.F., Kay, K., Watzke, N., Wood, P.G., Bamberg, E., Nagel, G., Gottschalk, A., and Deisseroth, K (2007). Multimodal fast optical interrogation of neural circuitry. Nature *446*, 633–639.

20. Arrenberg, A.B., Del Bene, F., and Baier, H. (2009). Optical control of zebrafish behavior with halorhodopsin. Proc. Natl. Acad. Sci. USA *106*, 17968–17973.

21. Saint-Amant, L., and Drapeau, P. (2001). Synchronization of an embryonic network of identified spinal interneurons solely by electrical coupling. Neuron *31*, 1035–1046.

22. Scott, E.K., Mason, L., Arrenberg, A.B., Ziv, L., Gosse, N.J., Xiao, T., Chi, N.C., Asakawa, K., Kawakami, K., and Baier, H. (2007). Targeting neural circuitry in zebrafish using GAL4 enhancer trapping. Nat. Methods *4*, 323–326.

23. Wyart, C., Del Bene, F., Warp, E., Scott, E.K., Trauner, D., Baier, H., and Isacoff, E.Y. (2009). Optogenetic dissection of a behavioural module in the vertebrate spinal cord. Nature *461*, 407–410.

24. Park, H.-C., Shin, J., and Appel, B. (2004). Spatial and temporal regulation of ventral spinal cord precursor specification by Hedgehog signaling. Development *131*, 5959–5969.

25. Saint-Amant, L., and Drapeau, P. (1998). Time course of the development of motor behaviors in the zebrafish embryo. J. Neurobiol. *37*, 622–632.

26. Saint-Amant, L., and Drapeau, P. (2000). Motoneuron activity patterns related to the earliest behavior of the zebrafish embryo. J. Neurosci. *20*, 3964–3972.

27. Mukamel, E.A., Nimmerjahn, A., and Schnitzer, M.J. (2009). Automated analysis of cellular signals from large-scale calcium imaging data. Neuron *63*, 747–760.

28. Masino, M.A., and Fetcho, J.R. (2005). Fictive swimming motor patterns in wild type and mutant larval zebrafish. J. Neurophysiol. *93*, 3177–3188.

29. Kimmel, C.B., Ballard, W.W., Kimmel, S.R., Ullmann, B., and Schilling, T.F. (1995). Stages of embryonic development of the zebrafish. Dev. Dyn. *203*, 253–310.

30. Bernhardt, R.R., Chitnis, A.B., Lindamer, L., and Kuwada, J.Y. (1990). Identification of spinal neurons in the embryonic and larval zebrafish. J. Comp. Neurol. *302*, 603–616.

31. Kuwada, J.Y., and Bernhardt, R.R. (1990). Axonal outgrowth by identified neurons in the spinal cord of zebrafish embryos. Exp. Neurol. *109*, 29–34.

32. Deliagina, T.G., Zelenin, P.V., and Orlovsky, G.N. (2002). Encoding and decoding of reticulospinal commands. Brain Res. Rev. *40*, 166–177.

33. Hegemann, P., Oesterhelt, D., and Bamberg, E. (1985). The transport activity of the light-driven chloride pump halorhodopsin is regulated by green and blue light. Biochimica et Biophysica Acta (BBA) - Biomembranes *819*, 195–205.

34. Ren, J., and Greer, J.J. (2003). Ontogeny of rhythmic motor patterns generated in the embryonic rat spinal cord. J. Neurophysiol. *89*, 1187– 1195.

35. O'Donovan, M., Ho, S., and Yee, W. (1994). Calcium imaging of rhythmic network activity in the developing spinal cord of the chick embryo. J. Neurosci. *14*, 6354–6369.

36. Ashworth, R., and Bolsover, S.R. (2002). Spontaneous activity-independent intracellular calcium signals in the developing spinal cord of the zebrafish embryo. Dev. Brain Res. *139*, 131–137.

37. Milner, L.D., and Landmesser, L.T. (1999). Cholinergic and GABAergic inputs drive patterned spontaneous motoneuron activity before target contact. J. Neurosci. *19*, 3007–3022.

38. Syed, M.M., Lee, S., Zheng, J., and Zhou, Z.J. (2004). Stage-dependent dynamics and modulation of spontaneous waves in the developing rabbit retina. J. Physiol. *560*, 533–549.

39. Yuste, R., Peinado, A., and Katz, L.C. (1992). Neuronal domains in developing neocortex. Science *257*, 665–669.

40. Downes, G.B., and Granato, M. (2006). Supraspinal input is dispensable to generate glycine-mediated locomotive behaviors in the zebrafish embryo. J. Neurobiol. *66*, 437–451.

41. Komuro, H., and Rakic, P. (1996). Intracellular Ca2+ fluctuations modulate the rate of neuronal migration. Neuron *17*, 275–285.

42. Gu, X., and Spitzer, N.C. (1995). Distinct aspects of neuronal differentiation encoded by frequency of spontaneous Ca2+ transients. Nature *375*, 784–787.

43. Desarmenien, M.G., and Spitzer, N.C. (1991). Role of calcium and protein kinase C in development of the delayed rectifier potassium current in Xenopus spinal neurons. Neuron *7*, 797–805.

44. Crisp, S.J., Evers, J.F., and Bate, M. (2011). Endogenous patterns of activity are required for the maturation of a motor network. J. Neurosci. *31*, 10445–10450.

CHAPTER 3

Information transfer and forebrain recruitment underlie experience-dependent learning in larval zebrafish

Submitted to Current Biology

LINKER STATEMENT

In this chapter, I studied how experience of prey affects hunting behavior and underlying neural activity. I developed a paradigm to assess the effect of prior hunting on prey capture behavior and showed that experienced fish initiate more captures than their naïve counterparts. I next established that experience does not affect the ability to see prey. Rather, experience increases the probability that activity in visual areas will evoke a capture initiation. This is accomplished by increasing the impact of information transfer from visual to motor areas, possibly due to increased activity in forebrain areas for experienced fish.

Information transfer and forebrain recruitment underlie experience-dependent learning in larval zebrafish

Oldfield CS[1], Huth AR[1], Chavez M[2,3,4], Carroll EC[5], Prendergast A[2,3,4], Qu T[5], Hoagland A[5], Wyart C[2,3,4], Isacoff EY[1,5,6].

[1] Helen Wills Neuroscience Institute and Graduate Program, University of California Berkeley, Berkeley CA, 94720; [2] Institut du Cerveau et de la Moelle épinière (ICM), Hôpital de la Pitié-Salpêtrière, 75013, Paris, France; [3] CNRS-UMR-7225, 75005 Paris, France; [4] INSERM UMRS 1127, 75013 Paris, France; [5] Department of Molecular and Cell Biology, University of California Berkeley, Berkeley CA, 94720; [6] Bioscience Division, Lawrence Berkeley National Laboratory, Berkeley CA, 94720.

Author Contributions: CSO, CW and EYI designed the project. CSO, EC and TQ collected data. AP generated the NeuroD transgenic line. CSO, ARH, MC and AH analyzed the data. CSO, CW and EYI wrote the paper.

Acknowledgements: We thank Kait Kliman, Mel Boren, Sonia Castillo and Allison Kepple for mainting fish lines at UC Berkeley; and Natalia Maties, Bodgan Buzurin and Sophie Nunes Figueiredo for maintaining transgenic lines at the ICM zebrafish facility. Holly Aaron, Jen Lee from the Berkeley MIC, and Intelligent Imaging Innovations provided invaluable advice and assistance with the optical system. We thank Carlos Pantoja, Amy Winans and Victoria Chou for thoughtful feedback on the manuscript. Vincent Guillemot from the ICM Biostatistics/Bioinformatics core facility, and Chris Holdgraf from UC Berkeley for providing advice on statistics. This work received support from the ERC starting grant Optoloco (#311673), a Research-in-Paris postdoctoral fellowship as well as an EMBO postdoctoral fellowship # ALTF 549-2013 for AP. CSO received a Boehringer Ingelheim Fonds fellowship. CSO, CW and EYI received a Chateaubriand fellowship for this project.

Summary

Experience strongly influences behavior, but little is known about how changes in neural activity are implemented at a network level to improve performance. Here we investigate how experience impacts brain circuitry and behavior in zebrafish larval prey capture. We find that experience of live prey increases capture success by increasing capture initiation frequency. Strikingly, response to “virtual prey” depends on prior experience of live prey. Simultaneous behavior monitoring and whole-brain calcium imaging in head-restrained animals was used to examine how experience shapes neural activity and behavior. Regularized regression to construct encoding models shows that retinotopic responses to prey in visual areas are indistinguishable between experienced and naive animals, suggesting that experience does not affect the ability to see prey. Granger-causality analysis shows that information transfer from pretectum to both cerebellum and hindbrain strongly predicts prey capture initiation, and that experience lowers the threshold for this drive to trigger capture. Moreover, experience increases the probability that activity in visual areas will evoke eye convergence. Finally, experienced fish, but not naïve fish, show greater activity in two forebrain areas - the telencephalon and the habenula - when pretectal events are associated with eye convergence. Our observations suggest that the forebrain operates as an experience-dependent switch that enhances the impact of information transfer from visual to motor areas for the initiation of prey capture.

Introduction

To transform sensory input into an optimal behavioral response, animals must extract relevant perceptual information from their environment, interpret it within their internal and external contexts, and translate it into a motor output. Prior experience modulates how this transformation occurs, and influences whether the response is successful. A large body of work has studied how enriching or depriving an animal’s sensory experience affects perceptual encoding in sensory areas with morphological and molecular changes [1]. Similarly, teaching an animal to fear or expect a sensory stimulus alters properties of the circuits recruited in response to the sensory cue (for example, [2,3]). However, most studies of experience-dependent changes rely on drastic manipulation such as depriving animals of all sensory input in one modality, inducing fear association with a noxious stimulus, or depriving animals of food or water to achieve sufficient motivation to assure a response. Few studies have addressed the question of how natural experience influences brain activity in the context of a native behavior.

One of the most critical native behaviors for survival in carnivores and omnivores is hunting for food. In most species, the basic hunting sequence is innate and is triggered in full by certain sensory cues. For example, predation can be evoked in toads and fish by the sight of small prey-like moving objects [4–8] and in barn owls by a ruffling prey-like noise [9]. The accomplishment of this goal directed behavior is highly flexible and is modulated by experience in animals as phylogenetically distant as mammals (the Etruscan shrew relies on tactile experience to develop efficient predation [10]) and

mollusks (*Limax* learn to avoid a food if they become sick after eating it [11]). Here we asked how experience-dependent brain plasticity is implemented by imaging whole-brain neural activity, taking advantage of larval zebrafish transparency and ability to initiate prey capture when semi-immobilized. Five days post fertilization, zebrafish without prior experience capture prey, such as paramecia, in a highly stereotyped manner: when a prey is in sight, the fish reorients its body towards the prey with a series of unilateral tail flicks (J-Bends), forward swims until it reaches a proximal striking zone, and then darts forward to engulf the prey in a final capture swim [12–15]. Notably, the onset of this sequence is characterized by gradual eye convergence as the fish gets closer to the prey, and the increase of visual field area covered by binocular vision has been suggested to improve the depth perception needed for precise targeting of the prey [5]. Restrained fish presented with virtual prey (a moving dot) on a screen respond with eye convergences and tail flicks, indicating that visual inputs are sufficient to initiate the prey capture sequence [5–7,16].

Prey capture in larval zebrafish has emerged as a model for understanding how sensory information translates into motor action [7,16–21]. Visual information about prey location flows from the retina to the pretectum and optic tectum (OT) on the contralateral side of the brain. Recently the pretectal area around the 7th arborization field of retinal ganglion cells (AF7, see [22]) was shown to be critical for detecting prey-like objects and triggering the prey capture sequence [7]. Ablation and optogenetic studies indicate that the OT is necessary for prey capture [17,19]. Assemblies of medial peri-ventricular tectal neurons activate prior to eye convergence, suggesting a role in inducing the motor response to the sight of prey [16]. How information from the pretectum and OT is combined, and the precise activation sequence downstream of the visual areas is currently unknown. Similar to the toad and goldfish, the signal is probably transmitted to reticulo-spinal neurons, which in turn could activate the hindbrain controlling the locomotor central pattern generators [4,17], and the mesencephalic reticular formation controlling eye movements [23].

Here we show that experience increases the initiation of prey capture in natural conditions and investigate the underlying changes in brain activity. We find that experience does not alter activity evoked in visual areas, but increases the reliability of capture initiation once the prey is in sight. Causality analysis of calcium signals from visual and motor brain areas reveals that the functional connectivity from the pretectum onto the cerebellum and hindbrain predicts prey capture initiation. Experience increases the impact of these connectivity links on prey capture initiation. Taken together our findings indicate that experience reduces the variability in neural activity in motor areas and acts as a gain control on the functional links between visual and motor areas to increase the initiation of a complex goal-directed behavior.

Results

Experience increases prey capture initiation in larval zebrafish

To assess the effect of experience on prey capture behavior and the underlying neural activity, we compared two groups of zebrafish larvae: one group ("experienced") was fed live paramecia for two days prior to the experiment (days 5 and 6 post-fertilization [dpf]), whereas the other ("naïve") group was fed inert food flakes (Figure 1A). At day 7 prey capture behavior was tested in both groups by quantifying behavioral steps of the prey capture sequence: a) pursuits that are aborted before a capture swim is attempted, b) capture swim attempts that fail, and c) successful captures (see Movie S1). We found that experienced fish have significantly more pursuits and successful captures than their naïve counterparts, but the same probability of attempting a capture once a pursuit was initiated (Figure 1B). Experience did not change the probability of success once a capture was attempted. This analysis suggests that experience increases initiation of prey capture, but not motor performance of the capture.

We next examined prey capture in a virtual environment [5–7,16]. We presented a single moving dot of varying contrast to a fish immobilized in agar with its eyes and tail free (Figure 1D) and identified initiation of prey capture as the coincidence of eye convergence and tail flick. We quantified performance using the discriminability index, d', calculated from response rates to a stimulus (hit) *versus* a blank screen (false positive) (see Supplementary Experimental Procedures). We found that experienced fish responded significantly more than naïve counterparts at higher contrast, whereas naïve fish showed no improvement at higher contrast (Figure 1E).

Differences in diet (live paramecium vs. inert flakes) could affect fish health and have consequences on prey capture performance. To rule out this possibility, we showed that fish length, spontaneous swimming velocity, and swimming velocity in the presence of prey did not differ with experience (Figure 1C). Similarly, swim distance and rest times between swims (Figure S1C),as well as rates of baseline tail flicks, eye saccades and eye convergences in the virtual environment did not differ between groups (Figure 1F). These results suggest that the differences in diet between experienced and naïve fish did not affect health but rather, improved prey capture performance from the paramecia "training" experience.

Spatio-temporal brain activity pattern associated with prey capture initiation

To establish the neuronal basis of the higher rate of prey capture initiation in experienced fish, we imaged neuronal activity in the form of calcium transients in the *Tg(neuroD:GCaMP6f)* [24] transgenic zebrafish line, which expresses the calcium indicator GCaMPf broadly in the central nervous system. Imaging was performed in 7 and 8 dpf fish, which were restrained in agar with eyes and tail free. We imaged fluorescent calcium signals from a single plane that included the pretectal area around AF7, which was previously shown to be involved in prey detection [7], while simultaneously imaging

eye and tail movements as well as prey trajectory (Figure 2A-C). For each fish, we used the baseline GCaMP6f fluorescence image (Figure 2D) to identify the major brain areas for imaging activity (Figure 2E). Consistent with our assays on semi-immobilized fish, above (Figure 1D-F), tail flicks were similar between experienced and naïve fish but experienced fish exhibited a higher eye convergence frequency when exposed to the prey (Figure 2F).

We began recording spontaneous neural activity and associated tail and eye movements in absence of prey for a period of 7 minutes. We then added a single paramecium to a well in front of the fish and recorded for 11 additional minutes. In experienced fish, brain activity centered on eye convergence events at their strongest vergence angle included strong activation of visual areas in the pretectal neurons around AF7 and the optic, as well as motor areas in the cerebellum and hindbrain known to play roles in swim behavior (Figure 2G, H). Within the tectum, there were responses in the rostral neuropil and in periventricular neurons, which include output neurons [25], but not in the caudal neuropil. The regionalization of tectal neuropil activity is consistent with the fish initiating prey capture sequences when the paramecium is in front, because retinal ganglion cells receiving input from the nasal visual field project to the rostral tectum [26]. In addition, we observed responses in two areas that were not previously implicated in prey capture: the telencephalon and the habenula. The spatio-temporal patterns of spontaneous and evoked activity were similar, except that, in presence of prey, activity in the pretectum and tectal neuropil was asymmetric when evoked (more strongly activated contralateral to the paramecium), and symmetric when spontaneous (Figure S2B). Although naïve fish had fewer eye convergence events, the spatio-temporal pattern of the associated activity and the difference between spontaneous activity and paramecium-evoked activity were similar to what we observed in experienced fish (Figure S2B). In summary, although prey capture initiation occurred more frequently in experienced fish than in naïve fish, the general brain activation sequence around eye convergence was similar. This led us to hypothesize that experience either improves the ability to detect prey visually or increases the probability of prey capture initiation when prey is in sight.

Experience does not affect encoding of prey position in visual areas

To determine whether experience affects the ability of the fish's brain to detect and represent the location of its prey, we compared prey location encoding in visual areas of experienced *versus* naïve fish (Figure 3). Traditionally, visual responses are evaluated by repeatedly showing identical virtual stimuli, pooling trials and determining if responses in a given region of interest are reliable enough for it to be deemed “visually responsive”. Here, we used natural visual input where the fish was presented with its biological prey, a live paramecium. Since the locomotion of the paramecium is not experimentally controlled, we faced the analytic challenge of dealing with irregular visual stimulation. To address this, we applied a method developed recently for building predictive encoding

models of human brain activity that is elicited by natural scenes or language and detected by functional magnetic resonance imaging [27,28]. We used regularized regression to construct a separate encoding model for each pixel that predicts the pixel's fluorescence time series based on the location of the prey (Figures 3A-B). To validate the encoding models, we predicted fluorescence time series on held-out segments of the dataset that were not used for weight estimation, and then computed the correlation between predicted and actual time series. Pixel fluorescence can include information about prey position but also has intrinsic noise due, for example, to spontaneous activity and fluctuations of brain states. Despite the considerable spontaneous brain activity in absence of prey, the modeling approach achieved pixel activity / prey correlation (or predictions values) as high as 0.52 in the pretectum, 0.41 in the tectal neuropil and 0.46 in the tectal periventricular neurons, comparable to what was seen earlier [28].

For pixels where prediction performance was significantly above chance (False Discovery Rate, $q < 0.05$), we computed which prey position tended to elicit the largest response, and defined it as the pixel's "preferred angle" (Figure 3A-C). The encoding model weights, which were estimated using ridge regression, describe the spatial receptive field of the pixel (Figure 3C, see Supplementary Experimental Procedures). Pixels in the visual areas preferred positions on the contralateral side of the animal, consistent with retinal ganglion cell projections crossing the midline. We observed strong retinotopic gradients, with more rostral pixels responding to central positions of the prey and more caudal pixels preferring lateral positions of the prey in the pretectum and the optic tectum. Retinotopic maps were equally well defined in experienced *versus* naïve fish: we found no difference in encoding strength in the pretectum or the tectal neuropil (Figure 3D). In addition, both experienced and naïve fish showed well-separated bimodal distributions for angle preferences between left and right sides and no difference between the distributions of preferred angles of significantly predicted pixels in any of the visual areas (Figure 3E). The mean and standard deviation of preferred angle for each area were also similar between experienced and naïve fish (Figure S3A), reflecting similar tuning characteristics.

Finally, we asked whether the threshold of responses of the visual system changed with experience. We focused on the pretectum, because pretectum activity is strictly visual, whereas the optic tectum also processes tactile information, and because the pretectal area around AF7 has been suggested to be specifically involved in prey detection [7]. Indeed, we found that pretectum pixels had the highest correlation values with prey position of the visual areas in our field of imaging in both experienced and naïve fish (Figure 3D, for experienced fish, the 25^{th} and 75^{th} percentile for average pixel correlation values were 0.02 and 0.09, respectively, and for naïve fish 0.02 and 0.07, respectively). We observed no differences between experienced and naïve fish in the frequency or amplitude of calcium transients in the pretectum when fish were observing a prey (Figure S3B).

Together, these results indicate that experience does not affect encoding of prey position or threshold of prey detection within visual areas, suggesting that experience does not improve the ability of the brain to localize the prey.

Information transfer in visual areas during prey observation

In an effort to understand the communication between brain regions that are activated during the prey capture sequence, we applied Granger-causality analysis, a method for determining if a time series of events predicts (or Granger-"causes") a second time series [29,30]. It has been classically applied to neurophysiological recordings in both animals and humans [31,32] to study the influence of one brain area or neuron upon another (Figure 4A, and see Supplemental Experimental Procedures). In contrast to correlation analysis, Granger-causality provides directionality information, which is crucial in investigating functional connectivity across brain regions (compare Figures 4 and S4). It is important to note that Granger-causality describes the transfer of information from one area to another, but does not reveal either its physical basis or whether the transfer is monosynaptic or polysynaptic.

To validate the use of Granger-causality, we first applied it within the visual system where the basic circuitry is well characterized [25,33,34]. We compared baseline activity (without prey) to activity evoked by the presence of a prey in experienced and naïve fish (Figure 4B). We found that the tectal neuropil (Figure 4B and C, areas 3 and 4) drove activity in tectal PVNs (Figure 4B and C, areas 5 and 6), consistent with the neuroanatomical connections between the two regions (Figure 4D), in which the PVNs extend their dendrites in the neuropil where they receive input from upstream tectal neurons [25,33,34]. Similarly, the link between the pretectum and the tectal PVNs could be explained by pretectal neurons projecting to the superficial layers of the optic tectum, where PVN dendrites ramify [7,25,33].

In the presence of the prey, the strength of causal links between brain regions changed (Figure 4B, C). Specifically, we found higher connectivity between the pretectum and the optic tectum and between left and right hemispheres of the optic tectum, consistent with binocular vision being necessary for prey capture. Statistical comparison revealed no difference in connectivity in visual areas between experienced and naïve fish in spontaneous or prey-evoked conditions (Figure 4B), confirming that experience does not affect circuit connectivity in visual areas.

Pretectal drive to downstream areas and hunting propensity

To determine if communication between brain areas changes with experience of prey, we applied Granger-causality analysis to compare region-to-region couplings between experienced and naïve fish (Figure 5A, C). Consistent with what is known about physical

connectivity [25,33,35], the tectal neuropil drove the tectal PVNs, the PVNs drove the cerebellum, and the cerebellum drove the hindbrain in both experienced and naïve fish. Other significant links included the tectal PVNs driving the tectal neuropil, consistent with the presence of peri-ventricular interneurons that project back into the tectal neuropil [33], the cerebellum driving the tectal PVNs, as suggested anatomically with the observation that cerebellar output neurons project back to the optic tectum [36], and the hindbrain driving the tectal neuropil as shown in *Xenopus tadpole* [37] that optic tectum integrates multisensory inputs.

We found no statistical difference in connectivity strength between visual and motor areas between experienced and naïve fish, however the link from tectal PVNs to telencephalon was significantly greater in experienced fish (Figures 5A,C and S5B). We also found that connectivity differed within groups, between fish that initiated prey capture often ("strong" hunters) *versus* rarely ("weak" hunters). Among experienced fish, strong hunters showed enhanced drive from pretectum to the tectal neuropil, tectal PVNs, cerebellum and hindbrain, but not to the telencephalon or habenula (Figures 5B,C and S5B). These results suggest an important role of the pretectum and its connectivity to downstream visual and motor areas in determining the frequency of prey capture initiation, and a possible implication of the tectal PVN to telencephalon connection in mediating experience.

Experience increases the probability of transitioning from sight of prey to capture initiation

Having observed an augmented pretectal drive to downstream brain areas in strong hunters (Figure 5), we asked if experience affects the relationship between Granger-causality links from pretectum to downstream areas, and prey capture initiation. We found a linear relationship between eye convergence frequency and Granger-causality strength from pretectum to tectal neuropil, tectal PVNs, cerebellum and hindbrain (Figure 6A). Granger-causality strength explained up to 54% of variance in behavior ($0.28 < R^2 < 0.54$). We also found a significant interaction between experience and Granger-causality strength in predicting prey capture performance for links from pretectum to cerebellum and hindbrain (3 to 4-fold increase in regression slope for experienced), and tectal PVNs (2-fold increase in slope) (Figure 6B). These results show that experience is associated with a larger impact on performance of functional connectivity from the pretectum to a downstream visual area and motor areas.

While Granger-causality analysis captures the general information flow from one region to another throughout the whole recording, we also wanted to examine what happens during the bursts of activity that occur in the brief temporal windows when the visual system is activated. To do this, we examined brain activity that is associated with transients in the pretectum when the animal is in the presence of a prey. As above, the pretectum with the larger fluorescence peak was deemed to be "contralateral", and its

signal was used to align calcium activity temporally over a 10 minute recording period in the optic tectum, cerebellum and hindbrain (Figure S6 and Supplementary Experimental Procedures). In both experienced and naïve fish, the average pretectal transient was associated with an increase of activity in the optic tectum, cerebellum and hindbrain (Figure S6A), and there were no differences between experienced and naïve fish in transient amplitude for any area (Figure S6B).

Similar to the Granger-causality links, we also asked if experience affected the relationship between prey capture initiation and pretectum-associated calcium transients in visual and motor areas (Figure 7D, E). In experienced and naïve fish, tectal PVNs and cerebellum were both good predictors for eye convergence frequency, suggesting that increased activity in those areas following a pretectal event drives eye convergence. Consistent with results above, a notable difference between experienced and naïve fish was the slope of the relationship between amplitude of the calcium signal in a given area and eye convergence. For example, for a given average level of activity in the cerebellum following pretectal transients, eye convergence frequency was higher in experienced fish, suggesting that the system is sensitized and more likely to trigger a capture initiation. We also observed that R^2 values tended to be lower in experienced fish, except in the cerebellum, suggesting that in experienced fish additional factors influence the level of activity, and further supporting the notion that the key drive for prey capture initiation is the cerebellum.

We next examined the switch that occurs between a pretectal event that did not lead to any motor output compared to those associated with eye convergence. Spatio-temporal patterns of brain activity revealed that activity could only be detected in the cerebellum and hindbrain when there was a motor output for both experienced and naïve fish (Figure 7A-C). In contrast, pretectal activity was high in both eye convergence and pretectum-only events (Figure 7B), although pretectal activation lasted longer during eye convergence events (Figure 7B, C). Strikingly, in experienced fish but not naïve fish, activity in the telencephalon and habenula was greater during eye convergence events than during pretectum-only events (Figure 7C, F). This difference was driven by an increase in sustained activation around eye convergences in experienced compared to naïve fish (quantified with integral similar to Figure 7F; telencephalon, $p = 0.002$; habenula, $p = 0.005$), but not around pretectum-only events (telencephalon, $p = 0.44$; habenula, $p = 0.12$).

Taken together, these observations suggest that an apparently similar pretectal event can lead to an eye convergence, or “remain” confined in the visual areas. The “switch” could possibly be driven by enhanced activity in the telencephalon and/or habenula. Patterns of activity downstream of the pretectum looked similar in experienced and naïve fish in both states, however the probability of a pretectal event being followed by an eye convergence was larger in experienced fish (Figure 7E).

Discussion

Experience improves hunting success in larval zebrafish

After larval zebrafish hatch from their chorion and finish using the nutrient reserves from their yolk, they are left to their own devices to survive, avoid predators and capture prey. Prey capture is generally thought to be an innate behavior in zebrafish because larvae are capable of successfully capturing prey as early as their first attempts [12–14]. We compared hunting of paramecia between larvae with two days of experience with these live prey, and sibling naïve fish that are exposed to paramecia for the first time. We found that experience increases the frequency of successful captures, indicating that practice improves performance of this innate behavior. The improvement after training can be measured both in freely swimming fish as well as when fish are semi-immobilized for imaging, and observing a live prey. Moreover, we find that experience of paramecia generalizes to increase responsiveness to a virtual prey, even though this small black dot moving at uniform speed on a screen is quite distinct from the erratic 3D movement patterns of a translucent paramecium. Remarkably, responsiveness to the virtual prey is only seen in the experienced fish. While dependence of virtual prey capture on experience of live prey has not been previously described, we note that studies on prey capture in a virtual environment consistently report feeding the fish paramecia prior to testing [5–7,16]. This finding is reminiscent of studies in snails where food triggers an appetitive response only if the animal has previously successfully eaten [38]. Thus, experience may contribute to the ontogeny of prey capture behavior, where older (and therefore more experienced) fish have more fluid capture maneuvers and are able to hunt prey from a wider angular range [39].

Genetically encoded circuits extract information relevant to predation at multiple levels of the visual information processing stream. Different groups of retinal ganglion cells and optic tectum neurons respond preferentially to small prey-like objects, or looming predator-like objects in zebrafish [7,19,34,40], and frogs [4], similarly to small target motion detector neurons in insects [41,42]. This information is relayed in the tectum, whose optogenetic activation has been shown to trigger the prey capture motor response [20]. These findings convincingly demonstrate that the prey-capture circuit is hard-wired in the novice hunter’s brain. Nonetheless, experience may shape the circuit as shown here, as well as for juvenile fish raised in the dark learn to forage using their lateral line system [43].

Activation of visual areas during prey observation and capture initiation

Our behavioral analysis showed that once a prey capture sequence is initiated, experienced and naïve fish perform equally well. Instead, we found that the improvement with experience is associated with an increase in the probability of initiation of the prey capture sequence. This observation led us to test whether experience enhances the early step of prey visualization, or the later step of decision to pursue. To distinguish between these possibilities, we imaged neural activity in semi-immobilized experienced and naïve

fish that were exposed to a live prey. Regression analysis of calcium signals revealed receptive fields to live prey, and retinotopic maps that encode prey position in two visual areas, the pretectum and optic tectum. We observed no difference in the maps between experienced and naïve fish, suggesting that the prey capture learning lies in a step subsequent to visualization of prey.

We examined brain activity around eye convergences, the hallmark of prey capture initiation events [5]. In agreement with an earlier finding that AF7 responds specifically to prey-like objects and is important for mediating the capture response [7], we observed that activation of pretectal neurons, likely surrounding AF7, consistently preceded eye convergence (Figure 2). We found that activation of tectal neuropil and PVNs preceded eye convergence, consistent with previous observations showing that optic tectum function is necessary for prey capture [17–19], and that assemblies of tectal neurons activate specifically when an eye convergence occurs, possibly representing the seat of prey recognition [16]. The amplitude and timing of activity observed in the visual areas in the presence of prey, whether it elicited an eye convergence or not, was similar in experienced and naïve fish. Thus, neither the mapping of prey-evoked activity in visual areas, nor strength or timing of the visual responses, appeared to be altered by experience. We therefore next turned to an analysis of the motor areas inducing prey capture initiation.

Circuit activation during prey capture initiation

When fish initiate a prey capture sequence they converge their eyes and flick their tail in a characteristic forward capture swim. Consistent with this, prey capture initiation events were associated with activation of motor areas such as the reticulo-spinal neurons of the hindbrain (Figure 2), presumably controlling the locomotor central pattern generators. We also observed strong activation of the cerebellum and hindbrain around eye convergence events, consistent with an important role in controlling the motor response to the sight of prey. Similar to mammals, the teleost cerebellum is compartmentalized into the vestibulocerebellar and the non- vestibulocerebellar systems that control balance and locomotion respectively [44], which undoubtedly play a big role in the successful outcome of a capture sequence. To understand how information flows from the visual areas to these motor areas, we used Granger-causality analysis [31]. We established that the strength of the functional links from pretectum to optic tectum, cerebellum, and hindbrain determined how frequently a fish initiated a hunting sequence (Figure 6).

Our results suggest that experience increases the gain of information flow from the pretectum to motor areas to initiate prey capture. Whole-brain activity imaging suggested that the mechanism by which this gain is set depends on the forebrain rather than visual and motor areas. In experienced fish, but not naïve fish, we observed greater activity in the telencephalon and habenula when prey-evoked visual activity was followed by eye convergence (Figure 7). We also determined that experience increases information flow from the tectal PVNs to the telencephalon. Forebrain regions that are activated by the

visual system's response to prey may therefore play a role in setting the gain of information flow through the prey capture circuit, with experience sharpening the contrast between visual events that do or do not trigger capture behavior.

To our knowledge, the telencephalon and habenula have not been implicated in prey capture before. While it is accepted that teleost telencephalon comprises subdivisions homologous to mammalian amygdala, hippocampus and piriform cortex, the exact anatomical location of the homologous regions and their roles in behavior have not been studied in detail in either adult or larval zebrafish [45]. The dorsal habenula in teleosts is homologous to the mammalian medial habenula and has been shown to modulate fear responses, and social conflict outcome in adult zebrafish [46,47], integrating olfactory and optical cues in larval zebrafish [48].

It should be noted that other brain areas may also contribute to gain control. Previous studies identified the nucleus of the medial longitudinal fasciculus (nMLF) as an important relay for motor signals controlling the prey capture circuit [17]. Some pretectal neurons have direct projections to the nMLF and the hindbrain [7]. The nMLF is situated more ventral than the focal plane we used for imaging, so we could not assess its activity or functional connectivity with the pretectum. The mesencephalic reticular formation, a region controlling eye movements and convergence in goldfish [23] was also missing from our imaging plane. Other areas that could contribute to gain control are the serotonergic raphe nucleus, which modulates responsiveness and arousal in fish [49] and mammals [50], the dopaminergic system that encodes stimulus valence and regulates motivation [3], the noradrenergic locus coeruleus which is thought to modulate arousal in rodents [51], or even the hypocretin neurons of the hypothalamus thought to control a variety of motivational functions like arousal and feeding [52]. Neuromodulatory systems are thought to control brain states [53]. It has recently been reported that the serotonergic system modulates prey-approach behavior depending on hunger levels of the fish [54].

In conclusion, we found that hunting experience boosts prey capture performance by increasing the impact of information transfer from visual to motor areas in the larval zebrafish brain, thus lowering the threshold to trigger a capture initiation. Our results suggest that two structures in the forebrain, the telencephalon and habenula, may play a role in gating this process, with experience sharpening contrast between visual events to create a "go" / "no-go" signal for initiating this complex motor behavior.

Experimental Procedures

Zebrafish care

Animal experiments were done under oversight by the University of California Berkeley institutional review board (Animal Care and Use Committee). Adult AB and and Tüpfel long fin (TL) strains of *Danio Rerio* were maintained and raised on a 14/ 10 hour light cycle and water was maintained at 28.5°C, conductivity at 500μS and pH at 7.4. Embryos

were raised in blue water (3 g of Instant Ocean® salts and 2 mL of methylene blue at 1% in 10 L of osmosed water) at 28.5°C. For imaging experiments, fish were screened for GCaMP expression at 2 or 3 dpf. We focused our study on early larval stages (5 to 8 dpf) when the neural circuitry of prey detection has been well studied in visual areas, and when animals are more tractable for neural activity imaging due to their transparency and small brain size.

Transgenic lines

To generate the *Tg(NeuroD:GCaMP6f)*^{icm05}, GCaMP6F fragment was amplified by PCR from pGP-CMV-GCaMP6F (Addgene) and used to generate pME-GCaMP6F in a BP recombination reaction (Invitrogen). Subsequently, p5E-NeuroD [55] ,pME-GCaMP6F, p3E-poly(A), and pDest-pA2 were recombined in a 3-fragment LR reaction to generate NeuroD:GCaMP6F. This construct was injected into zebrafish embryos at the 1-cell stage in the following mixture--35 ng/µL Tol2 transposase mRNA, 25 ng/µL NeuroD:GCaMP6F, 0.1 M KCl, 0.2% phenol red. The resulting F0 generation was raised and selected for single insertion of the transgene and best expression. The *Tg(ath5:mRFP)* line [56] was used to compare labelling in the NeuroD line with retinal ganglion cell projections.

Diet and freely swimming behavior assay

Healthy wild type TL larval zebrafish were selected based on the inflation of the swim bladder at 4 dpf. Fish were split into two groups either fed a diet of paramecia or of fish flakes (Hikari USA inc) with 20 animals per dish. Fresh paramecia were prepared every day. We found that feeding the fish for a minimum of 6 hours per day insured that spontaneous swimming was the same across fish with different diets (Figure S1). Fish were fed twice a day, in the morning at 9 -10 am, and in the afternoon at 1-2 pm. Dishes were cleaned out between each feed and fish were transferred to a new dish every evening at 5-6 pm. At 7 dpf, one by one, fish were transferred to a 35 mm diameter dish and left to acclimate for 1 minute under white light. Spontaneous swimming was recorded for 5 minutes with a uEye CCD camera (IDS Imaging Development Systems GmbH) at 30 Hz using dark field illumination. 500µL of fresh paramecium culture was then added to the dish and prey capture behavior was recorded for 5 minutes. Fish that did not move at all during the spontaneous swimming test were excluded. We also compared spontaneous swimming of our two experimental groups to a third group fed pureed brine shrimp and flakes, our fish facility diet (Figure S1).

Virtual prey capture assay

We adapted virtual prey capture assays previously described in the literature [5,6]: larval zebrafish that were fed paramecia or flakes were embedded in low-melting point agar at the end of their 6th day. Agar around the eyes and tail was carefully removed so that only the area around the swim bladder was restrained. Fish were kept in the incubator to acclimate overnight. At 7 dpf fish were transferred to our imaging setup, a diffusive filter was fixed to the side of the dish acting as a screen ~ 10 mm away from the mid-point

between the eyes. All stimuli were generated in MATLAB (Mathworks, USA) using the Psychophysics Toolbox extensions [57]. All fish were first tested for a robust optokinetic reflex evoked by moving gratings to ensure that the visual system was functional. Fish were then left to acclimate on the setup for 10 minutes. Small moving dots were projected at eye level onto the screen in front of the fish using an M2 Micro Projector (AAXA, USA). Optimal stimulus properties were chosen to maximize prey capture responses: 1 mm diameter dots of varying contrasts on a white background appeared in front of the fish and moved to the left or the right of the screen at 30 degrees / sec. Changes in speed of the stimulus due to the curvature of the screen were corrected for programmatically. The contrast of the dot was varied from 20% (light grey on white) to 100% (black on white) in 20% increments. Dots of different contrasts were presented in blocks. Fish were kept in the dark between trials (12 sec inter-trial interval), the white background screen appeared progressively 3 seconds before the onset of the trial, and at trial onset the stimulus appeared on the screen and moved to the left or to the right for a duration of 3 sec. Each contrast was tested 8 times (with 4 in each direction), and 20 blank trials were interweaved randomly with the (8 x 5 contrast types) target trials throughout the experiment, a total of 60 trials per fish. Contrast blocks were also ordered randomly. Fish were illuminated from the side with a custom-built red LED light source and behavior was imaged with a 2.5x/0.06 air objective (Carl Zeiss, Inc.) using a high-speed CMOS camera (Mikrotron Eosens 1362) at 250 Hz. Behavior image acquisition and stimulus projection was synchronized by the software controlling the behavior camera (Piper, Stanford Photonics).

Behavioral data analysis and statistics

All data was analyzed using custom-written software in MATLAB unless otherwise indicated. All pairwise comparisons were made using permutation tests using the difference in means as a test statistic [58] unless otherwise indicated. Permutation tests do not make any assumptions about the underlying distribution, do not require equal variances or equal sample size. We rearranged labels (i.e. experienced or naïve) on observed data points and calculated the new test statistic 100,000 times thus creating a null distribution (under the null hypothesis, labels are interchangeable). We then computed the p-value by calculating the probability of obtaining the observed test statistic (the difference in means between the actual experimental groups) under the null distribution. We used a significance level $\alpha = 0.05$ (or a 5% chance of incorrectly rejecting the null hypothesis). Raw data from individual fish is plotted along with a boxplot summarizing the distribution statistics of the group: the central bar is the median, the bottom and top edges of the box indicate the 25^{th} and 75^{th} percentiles respectively, and the whiskers extend to the most extreme data points not considered as statistical outliers. Behavioral units of the prey capture sequence (pursuits, capture attempts and successful captures) were counted manually (Figure 1). Swimming velocity and percent of time resting were determined using custom tracking code. In the virtual environment setup, eye convergence events and tail flicks were also detected manually. A hit was defined as

an eye convergence event when a stimulus was presented and a false alarm was an eye convergence when a blank stimulus was presented. Hit rate was defined as the number of hits divided by the number of stimulus trials and false alarm rate was estimated as the number of false alarms by blank stimulus trials. Blank stimuli were interleaved with stimulus trials throughout the experiment so we used the same false alarm rate for all contrast levels. To measure eye convergence rates compared to baseline for a given fish at each contrast level, we calculated the discriminability index $d' = Z(\text{hit rate}) - Z(\text{false alarm rate})$, where Z is the inverse of the cumulative Gaussian distribution. d' distributions for experienced and naïve fish were compared using a 2-way anova test.

Imaging calcium activity induced by a live paramecium

Transgenic *Tg(NeuroD:GCaMP6f)* fish were embedded in agar and were placed under a one-photon spinning disc confocal microscope to acclimate for 10 minutes. They further acclimated for one minute with the laser light (488nm) on continuously before the onset of image acquisition to avoid detecting the strong initial activation of visual response in response to light onset. The laser was on continuously throughout the acquisition session (no synchronization with frame acquisition) to avoid distracting the animal with flashing light. For speed considerations, we limited our imaging to a single plane that contained the pretectal area around AF7 [7], recording at 5x magnification at 3.6 Hz. Systems that would have allowed us to achieve the desired type of speed and record volumes are not yet commercially available [59,60]. Spontaneous activity was recorded for 1500 frames (about 7 min). A single paramecium was then added to a small well cut out in the agar in front of the fish [61]. The well was sealed with a small lid of agar to keep the paramecium in front of the fish, and avoid evaporation. A Logitech C525 webcam (Logitech, USA) was placed under the fish to film the position of the paramecium using dark field illumination with an IR light source. A uEye CCD camera (IDS Imaging Development Systems GmbH) was attached to the microscope side port to record eye position. A notch filter 488nm (Chroma, USA) was placed in front of the webcam to block out the imaging laser light, a 488 band pass filter (Chroma, USA) was used to image GCaMP6f fluorescence and a dichroic mirror (T470lpxr, Chroma, USA) reflected wavelengths below 470 nm and above 750 nm to the uEye camera while transmitting green photons to the fluorescence camera. The webcam and the uEye camera were controlled by custom written software written in MATLAB so that a webcam and uEye frame were acquired every time a fluorescence frame was acquired. Acquisition was synchronized by sending a TTL pulse from the fluorescence imaging software Slidebook (3I, USA) to MATLAB.

It has recently been suggested that the light intensities used for 1p light-sheet microscopy stimulate the blue and UV cones of the retina which compromises visual perception [60]. At 5x magnification, light intensity at the focal plane was 50-75µW, which is substantially less than intensities used for light-sheet. Low magnification imaging resulted in enough scattered blue (488nm) light that the fish was able to see the paramecium in front of it and we supplemented visible blue LED to provide side illumination and maximize paramecium sightings.

Calcium and behavior imaging data pre-processing

Movies were registered using rigid body transformation (dftregistration from the Matlab File Exchange). Regions of interest (ROI) were drawn manually around the left and right telencephalon, habenula, pretectum, tectal neuropil, tectal PVNs, cerebellum, parallel fibers of the crista cerebellaris [35] and the hindbrain. Images were bleach corrected by fitting a single or double exponential (depending on the best goodness-of-fit) to the mean baseline fluorescence of each ROI excluding outliers and subtracting it from each pixel's fluorescence time series. Fluorescence time-series of each pixel was then normalized by z-scoring. For analysis of fluorescence around pretectum transients (Figure 4) we detected pretectal peaks by thresholding the traces at 2 standard deviations from the mean, and correcting for any aberrations manually. For each transient we considered the contralateral pretectum (to the prey) to be one the side with the highest amplitude at peak time. We could not use prey position to determine contralateral identity because the prey was often on the midline and both eyes could detect it, and the prey moved faster than calcium transients rose to maximum meaning that a prey might evoked a transient while on one side of the fish, and already be on the other side by the time the transient has reached its peak. We extracted the average fluorescence in pretectum, optic tectum, cerebellum and hindbrain around 30 frames (~ 8 seconds) before and 30 frames after each pretectal peak. We calculated a baseline for each trace by averaging the fluorescence of the first 13 frames (~3.5 seconds).

To detect eye angle, for each frame eye contours were identified using custom written software, and an ellipse was fit to the contours. Eye angle was considered to be the angle of the major axis of the ellipse relative to the midline of the fish. Eye vergence was the angle between the two eyes. Eye convergences were detected semi-automatically by identifying frames where both eye moved sharply towards the midline, thresholding vergence at 30° [5], and correcting any aberrant detections manually. Speed of acquisition did not enable us to track fast changes in tail angle, so tail movements were detected by calculating pixel intensity changes on either side of the tail, subtracting a baseline rolling average over 20 frames. Pixel intensity changes matched tail bend amplitudes remarkably well when we scored movies by eye. Tail flick time points were detected semi-automatically by thresholding at 2 standard deviations from the mean and corrected for aberrations.

Quantifying prey position for the encoding model.

We preprocessed prey-position movies by subtracting a baseline rolling average over 20 frames. Prey position was quantified using a polar representation of space around the fish. We defined 19 angle bins (or angle basis functions) of prey position relative to the fish midline. Each bin was represented by a von Mises distribution (which is an approximation of the circular normal distribution) with centers evenly spaced from –pi to pi and the width parameter kappa set to 20. When the prey was close to the center of a bin, that angle was weighted strongly, whereas when the prey was in between two bins,

the angles at the centers of those bins were weighted equally, generating a more continuous representation of prey-space. Similarly, we also defined 5 radial basis functions, which describe distance of the prey from the fish, using Gaussian distributions with centers evenly spaced from 0 to ~ 5 mm and width parameter sigma set to 40. We then took the product of each angle basis function and each radial basis function, yielding a total of 95 two-dimensional spatial basis functions that vary in both angle and radius. Each frame of the prey video was then projected onto each of these basis functions, producing 95 prey location time series. For a particular prey location time series the value is high for times when the prey is near the specified angle and radius and zero at other times.

Pixel-wise encoding model estimation and validation.

Linearized finite impulse response (FIR) encoding models [27,28] that predict pixel fluorescence based on the location of prey were estimated for each pixel in each fish. For each pixel **1) we constructed the stimulus input matrix that represents prey location over time**: To account for calcium indicator kinetics, and neural response delays relative to movement of the prey, each of the 95 prey-location time series were delayed from -5 to + 15 frames (-1.4 sec to 4.2 sec), yielding a total of 1900 features that were used to predict pixel fluorescence. The shifted prey location time series were concatenated, and the mean of each 1900 feature time series was then subtracted to avoid fitting an intercept term in the regression. **2) We used ridge regression to estimate the model coefficients** that quantify the relationship between prey location and pixel fluorescence**.** To enable unbiased assessment of model prediction performance we used a 10-fold cross-validation (the outer-layer validation) approach to fit and validate the encoding models. First, the full dataset for each fish was divided into 10 sequential temporal segments. For each fold, one segment was reserved for model validation and the other 9 segments were used to estimate the model weights by way of L2-regularized linear regression (ridge regression). 3) **We estimated the regularization parameter** for each of the 10 outer-layer folds using a second lever of cross-validation. We tested 20 regularization parameters α, log spaced between 1 and 1,000. For each parameter α, the following procedure was repeated 50 times: we randomly selected and removed 400 time points (10 blocks of 40 consecutive time points each) from the model estimation dataset. Model weights were then estimated using the remaining time points and used to predict responses in the 400 selected time points. After this procedure was repeated 50 times a regularization-performance curve was obtained for each outer-fold layer by averaging the 50 prediction performance values for each regularization parameter. The regularization parameter with the best prediction performance was selected. **4) We re-computed model weights using the entire model estimation dataset** (consisting of the 9 segments of data for this cross-validation fold). **5) We predicted fluorescence for the held-out segment of data** using the estimated weights. Both weights and predicted fluorescence were saved. **6) We repeated steps 3 to 5** for each of the 10 outer-layer cross-validation folds**. 7)** After all 10 folds had been completed **the predicted segments**

were concatenated to form a complete prediction dataset of the same size as the original fluorescence data. The Pearson correlation between the complete predicted time series and actual fluorescence time series was then computed for each pixel. For further analysis of pixel selectivity **8) we averaged together the estimated model weights** from each of the 10 cross-validation folds. **9) Statistical significance of predictions was computed** by comparing estimated correlations to the null distribution of correlations between two independent Gaussian random variables of the same length. Resulting p-values were corrected for multiple comparisons within each fish using the false discovery rate (FDR) procedure [62].

All model fitting was performed using custom software written in Python (https://github.com/alexhuth/ridge).

Granger-causality from calcium fluorescence imaging data

On the basis of our previous study [32], we studied the Granger-causality between neuronal GCaMP6f fluorescence signals with the framework described below. According to the concept of Granger-causality [63,30] we say that a variable F_1 is causing F_2 ($F_1 \rightarrow F_2$) if the prediction of F_2 is improved when information from F_1 is included in the prediction model for F_2. GC measure is typically based on autoregressive (AR) models. In a bivariate AR modeling, a stationary signal $x_2(t)$ can be expressed by a linear regression of its past values according to the formula:

$$F_2(t) = \sum_{k=1}^{q} a(k)F_2(t-k) + e_1(t)$$

where $a(k)$ are the regression coefficients of the univariate AR model, *q* is the model order, and $e_1(t)$ is the respective prediction error. By introducing the information from the stationary signal $F_1(t)$, the formula can be rewritten as:

$$F_2(t) = \sum_{k=1}^{q} b_2(k)F_2(t-k) + \sum_{k=1}^{q} b_1(k)F_1(t-k) + e_2(t)$$

where $b_1(k)$ and $b_2(k)$ are the new regression coefficients of the bivariate AR model, and $e_2(t)$ is the new prediction error obtained by including also the past of $F_1(t)$ in the linear regression of $F_2(t)$. The GC between $F_1(t)$ and $F_2(t)$ was evaluated by the log ratio of the prediction error variances for the bivariate and univariate model:

$$GC_{1\rightarrow 2} = ln\left(\frac{var[e_2(t)]}{var[e_1(t)]}\right)$$

By construction, GC is a positive number; the higher $G\square I_{1\rightarrow 2}$, the stronger the influence of $F_1(t)$ on $F_2(t)$ is. Such influence is often considered to reflect the existence of an information flow outgoing from the system $F_1(t)$ towards the system $F_2(t)$ [63,30]. Finally,

GC is generally an asymmetric measure (i.e. $GCI_{1\to2} \neq GCI_{2\to1}$), which allows inferring causal or driver-response relationships.

The regression coefficients of the AR models are generally computed according to the ordinary-least-squares minimization of the Yule-Walker equations [63,64]. The model order *q* can be selected according to the Akaike criterion [65]. This criterion tries to find the optimal q that minimizes the following cost function $(q) = \ln(det(\Sigma_2)) + \frac{8q}{T}$, where Σ_2 is the noise covariance matrix of the bivariate AR model and *T* is the number of samples of the time series. Basically, this cost function balances the variance accounted for by the AR model against the number of coefficients to be estimated.

We estimated the GC between GCaMP6f fluorescence signals in spontaneous (without prey) and evoked (with prey) conditions over 1500 frames (7 min) and 2500 frames (11 min) respectively (normalized to zero mean and unitary variance). Each zebrafish brain was thus characterized by a full connectivity pattern by quantifying the *GC* influences between all the identified ROIs. The statistical significance of the obtained influences was established by means of of a parametric significance test (F-test) under the null hypothesis $GC_{1\to2} = 0$ [63,64] According to this procedure, only the *GC* values corresponding to percentiles inferior to a statistical threshold of $\alpha = 0.05$ Bonferroni corrected for multiple comparisons, were retained.

Here, the information propagation was estimated by means of bivariate AR models of Granger-causality as described above. Although other methods based on information theory or multivariate autoregressive models (MVAR) could be used to assess directionality [see [64] and references therein], practical evidence shows that they require generally longer data and strong assumptions on the absence of latent variables that could introduce spurious connectivity [66]. In our previous study [32], we could verify that these assumptions are marginally satisfied in GCaMP3 fluorescence signals and that using MVAR leads to unreliable connectivity patterns.

Robust multi-variate linear regression to relate prey capture initiation to Granger-causality links

We used multivariate linear regression to model the relationship between prey capture initiation frequency (response variable), and Granger-causality links strength and experience (two predictor variables). We used the “robust” option in the MATLAB *fitlm* function, which reiteratively weights each data point to reduce the effect of outlier response points on the fit. A bisquare function was used for re-weighting.

Figure 1

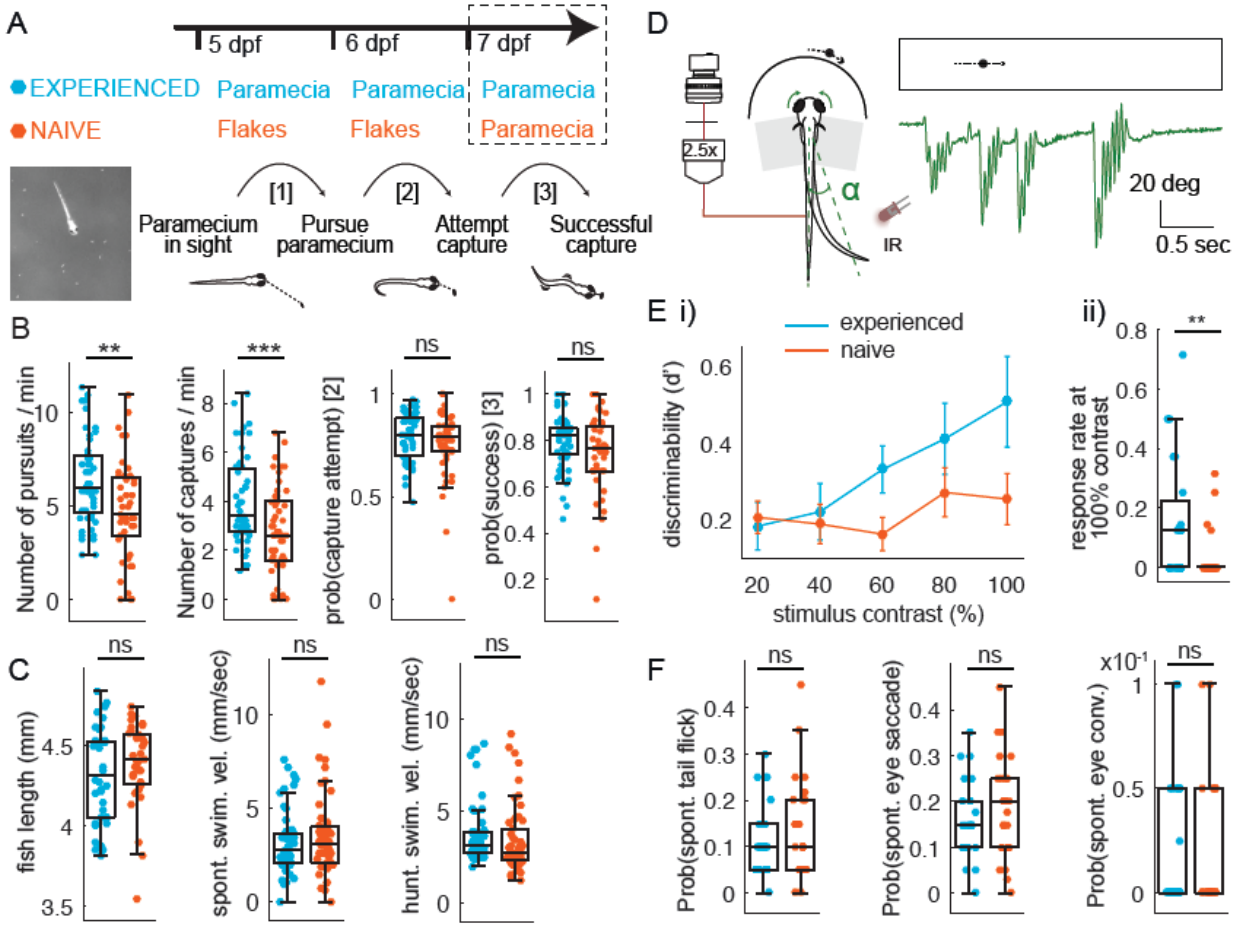

Figure 1: Larval zebrafish improve at capturing their prey with experience. A-C) Prey capture in freely swimming fish. A) Fish fed paramecia ("experienced") or flakes ("naïve") at 5 and 6 dpf were given paramecia at 7 dpf (top time line) and prey capture performance was assessed by imaging single fish and paramecia (white specks) (lower left image) to count: [1] pursuits aborted without a capture attempt, [2] failed capture attempts, and [3] successful captures (summary behavior scheme, lower, right). B) Summary of performance. Raw data (one symbol per fish) and a boxplot of group statistics show that experienced fish have higher frequencies of total pursuits (successful or not, p=0.0015), and successful captures ($p=7x10^{-4}$), but statistically indistinguishable probabilities of transitioning from pursuit to a capture attempt (p = 0.14), or of transitioning from capture attempt to successful capture (p = 0.06). Statistical comparisons used a permutation test (see Experimental Procedures) with N = 51 each experienced and naïve fish. C) No difference in health or swim behavior due to differences in diets: statistically indistinguishable fish length (p=0.14), spontaneous swim velocity (p=0.85), and swim velocity in presence of prey (p=0.20). D-F) Virtual prey capture. D) Setup: immobilized fish face a screen on which small moving dots are projected. Tail flicks and eye angle imaged from above at 250 fps. Example tail track during presentation of moving dot shown. E) i. Population average of

discriminability (d') across contrast levels for experienced (n = 23) and naïve (n = 25) fish. (2-way anova, interaction between experience *versus* lack of experience and contrast, p = 0.03). ii. Eye convergence rates differ significantly (p = 0.003) at highest contrast between experienced *versus* naïve fish. F) No difference between experienced and naïve fish in spontaneous tail flicks, eye saccades or eye convergences in absence of virtual prey stimulus (p=0.76, p=0.85, p=0.36, respectively).

Figure 2

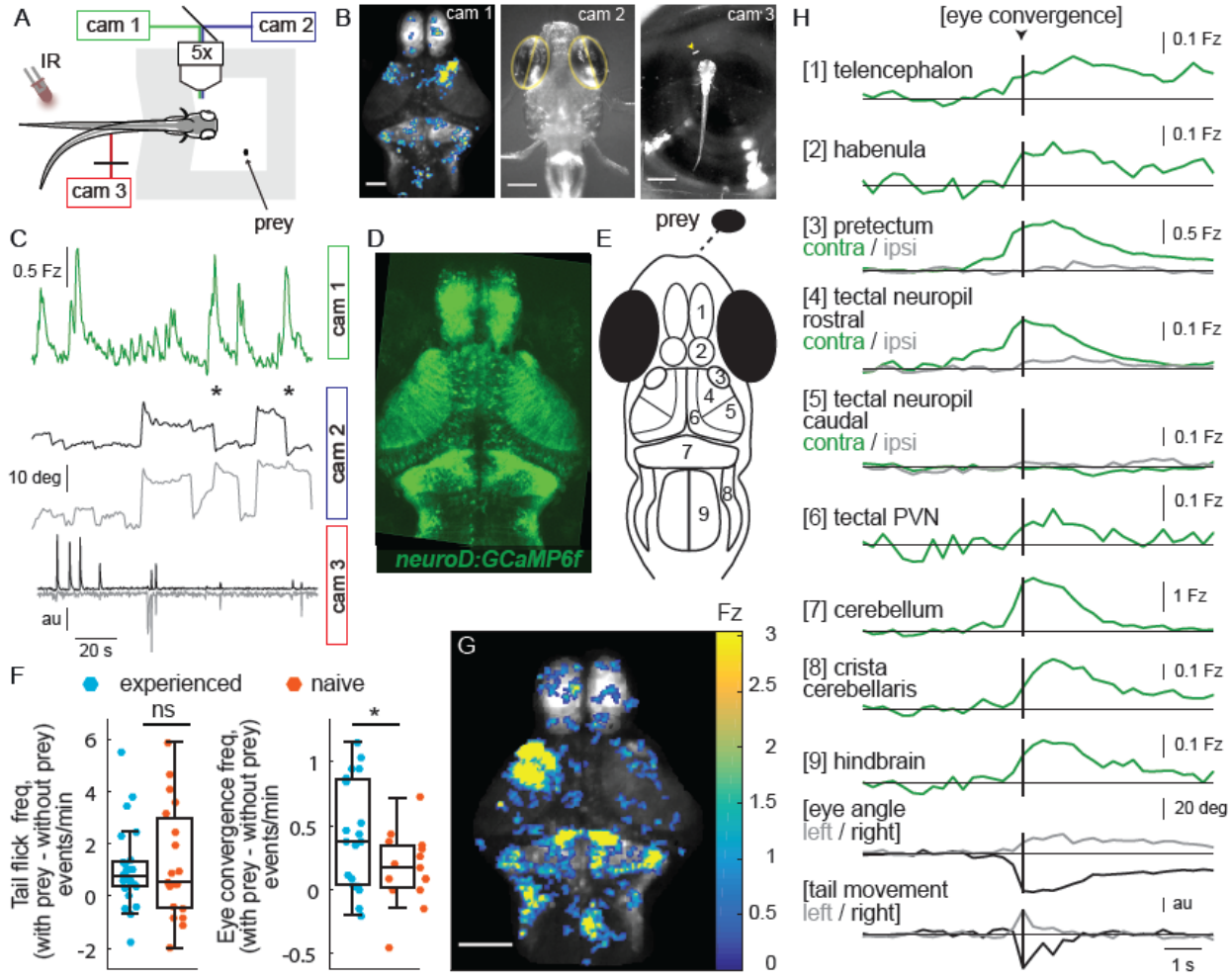

Figure 2. Whole brain imaging of prey capture initiation. A, B) Imaging setup (A) and images (B). Camera 1 (cam 1): neural activity in a plane of the whole brain while the fish observes prey, scale bar = 200μm. Camera 2 (cam 2): eye angle, scale bar = 200μm. Camera 3 (cam 3): prey position and fish tail position, scale bar = 1 mm. Cameras synchronized at 3.6 Hz. C) Example 3 minute traces from one fish of cam 1 fluorescence in the right pretectum (smoothed with a Lowess filter, span = 7) and corresponding eye angles (cam 2: left eye, grey; right eye, black; convergence events, stars; smoothed with a Lowess filter, span = 9) and cam 3: tail movement (left side, grey; right side, black, see Experimental Procedures). D) *Tg(neuroD:GCaMP6f)* 7 dpf fish brain. E) Schematic of anatomy in observation plane. Numbered areas as defined in (H). F) Experienced and naïve fish have statistically indistinguishable evoked (with prey – without prey) frequency of tail flicks (left, p = 0.3), but experienced fish have a significantly higher eye convergence frequency (right, with prey – without prey, p = 0.02). G, H) Neural activity in an experienced fish around eye convergences with prey (n = 12 eye convergences). This fish showed no spontaneous eye convergences preceding addition of paramecium, suggesting that averaged activity was purely evoked by the paramecium. G) Spatial distribution of summed calcium activity over 4.2 seconds (5 frames before and 10 frames after eye convergence) when the prey was to the right side

(average of 6 convergences). Scale bar = 100μm. H) Time-course of calcium activity for each brain area (average of 12 convergences; convergence time is vertical black line). Pretectum with largest response deemed “contralateral” (see Experimental Procedures). For eye angle and tail movement, black is contralateral, and grey is ipsilateral.

Figure 3

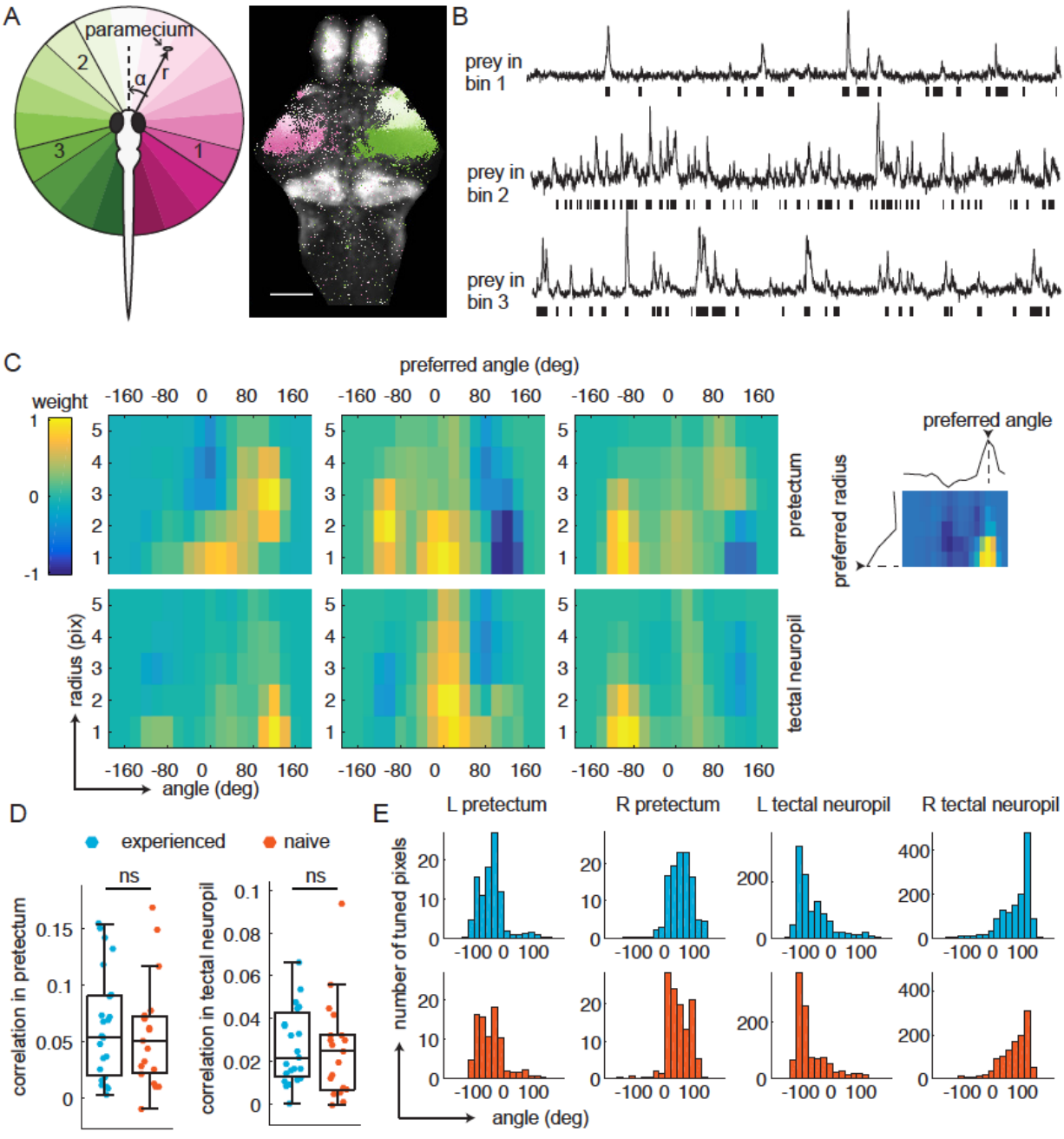

Figure 3. Experience does not affect detection prey-associated activity in visual areas. A) Left, schematic of prey location relative to the fish in polar coordinates (angle α, radius r). Right, example retinotopic map (fish #150910_6) generated by fitting an encoding model for each pixel to predict fluorescence intensity based on prey location. Significantly correlated pixels are in the color of their preferred angle. Scale bar = 200 μm. B) Fluorescence traces from pixels whose preferred angles are in bin 1 (120° to 101°, top), bin 2 (-30° to -49°, middle), or bin 3 (-104° to 126°, bottom). Bars below traces indicate time points when the prey was present in the preferred

angle bin. C) Example angular-radial receptive fields for 3 pixels in the pretectum (top row) and 3 pixels in the tectal neuropil (bottom row). X-axis: angle, y-axis radius; Color represents encoding model weight for that pixel. For each receptive field, color scale is normalized to the maximum weight and centered around 0. D) Average correlation values of visual area pixels in the pretectum (left) and the tectal neuropil (right) were not significantly different between experienced (N = 23) and naïve fish (N = 19), p = 0.27 for pretectum; p = 0.34 for tectal neuropil. E) Average distribution of pixels' preferred angles in each area (columns) in experienced (blue, top row) and naïve (red, bottom row) fish. There were no differences in average preferred angle distributions between the two groups of fish (two-sample Kolmogorov-Smirnov tests).

Figure 4

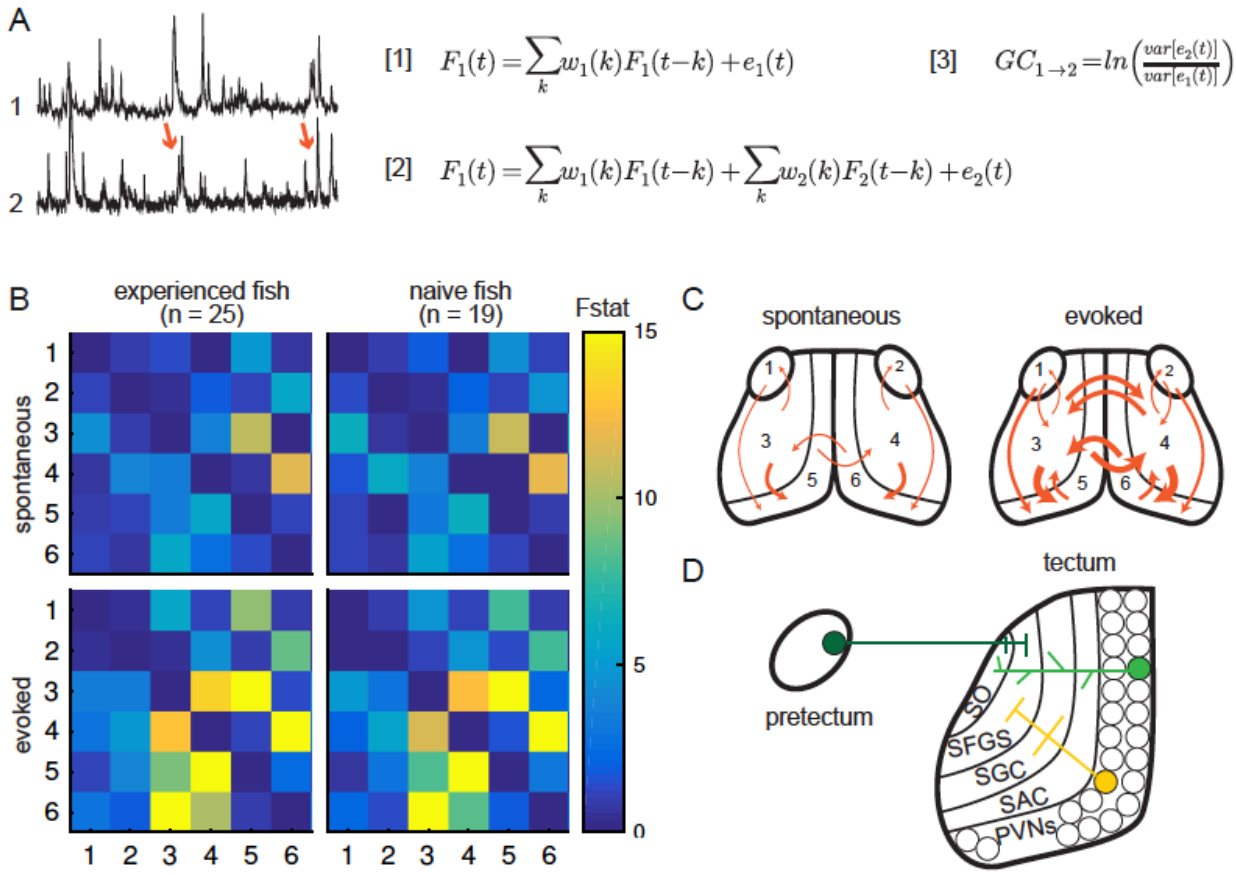

Figure 4. Experience does not affect functional connectivity in visual areas. A) Granger causality equations (right) to model fluorescence time-series 2 using information from time-series 1 (left). F(t) is fluorescence for time point t; w_1 and w_2 are the weights calculated for each time point; e denotes prediction error. Equations [1] and [2] are the autoregressive models for univariate and bivariate signals, respectively. Equation [3] is the Granger causality calculation. B) Granger causality within visual areas in spontaneous (no prey, top row) and evoked (prey present, bottom row) conditions, in experienced (left column) and naïve (right column) fish. Each box represents the F statistic which quantifies Granger causal link strength from the region identified by the row to the region identified by the column. F statistic values ranged from 0 to 23.7. Fstat values above 15 are yellow. 1, left pretectum; 2, right pretectum; 3, left tectal neuropil; 4, right tectal neuropil; 5, left tectal PVN; 6, right tectal PVN. Significant causality link for Fstat > 3.88. No significant difference between experienced and naïve fish in either spontaneous or evoked Granger causality matrices (pair-wise t-tests Bonferroni corrected for multiple comparisons; see Figure S5 for p-values). C) Schematics of functional links in visual areas in spontaneous (left) and evoked (right) conditions. Line width proportional to Granger connectivity value (evoked and spontaneous maps only indicate strongest links with Fstat > 5). D) Anatomy and known connections of the optic tectum. Dark green: input from pretectum to OT. Bright green: PVNs with dendritic arborization in tectal neuropil. Yellow: axonal projections from PVNs to different layers of OT.

Figure 5

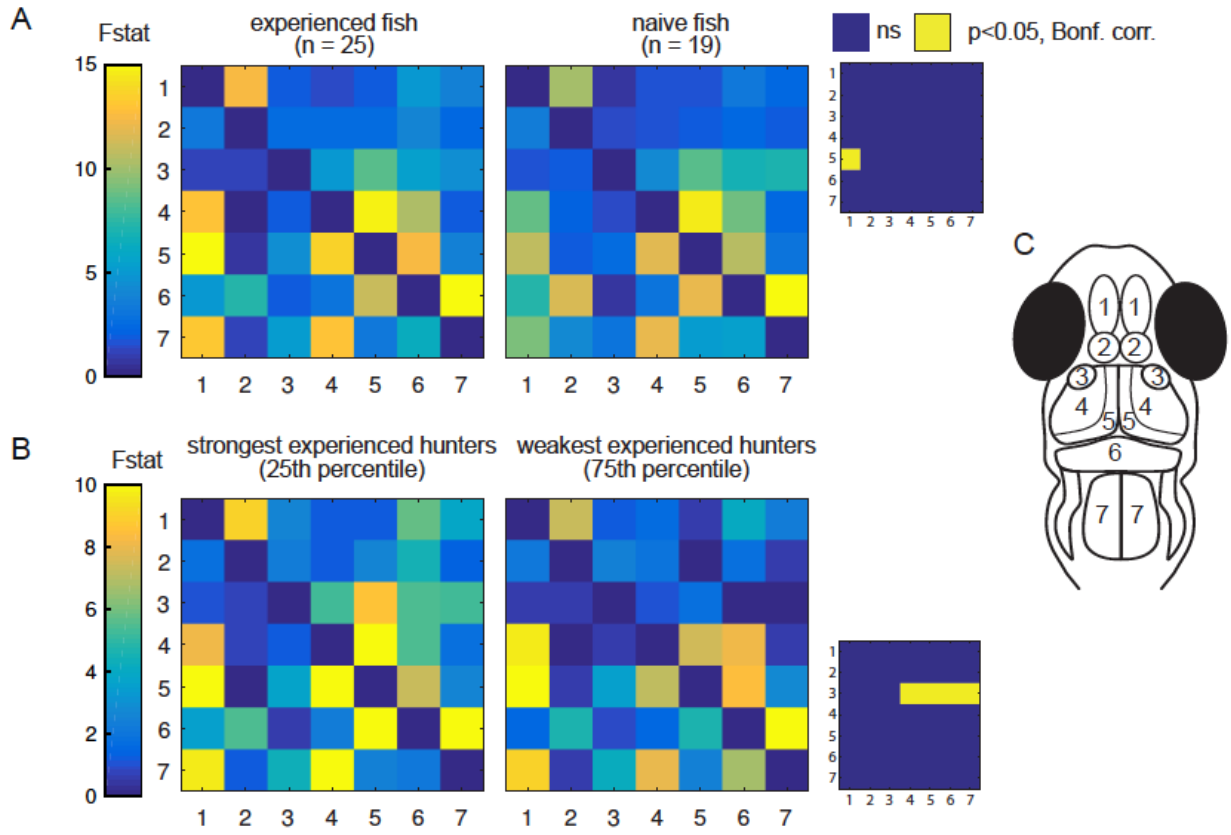

Figure 5. Functional connectivity of pretectum to visual and motor areas is increased in strong hunters. A) Granger causality between brain areas in experienced (left) and naïve (right) fish, as in Fig. 4. Activity from left and right sides averaged. F statistics ranged from 0 to 34.1. No significant difference between experienced and naïve fish in either evoked Granger causality matrices. Inset: Statistical comparison of all links. Significant links represented in yellow ($p < 0.05$, pair-wise t-tests, Bonferroni corrected; see Figure S5 for p-values). B) Experienced fish ranked by frequency of evoked eye convergence (with prey – without prey) into strongest quartile (left) and weakest quartile (right). Granger causality matrices for regions indicated in (C). Inset: Statistical comparison of all links (see Figure S5 for p-values). C) Anatomical schematic.

Figure 6

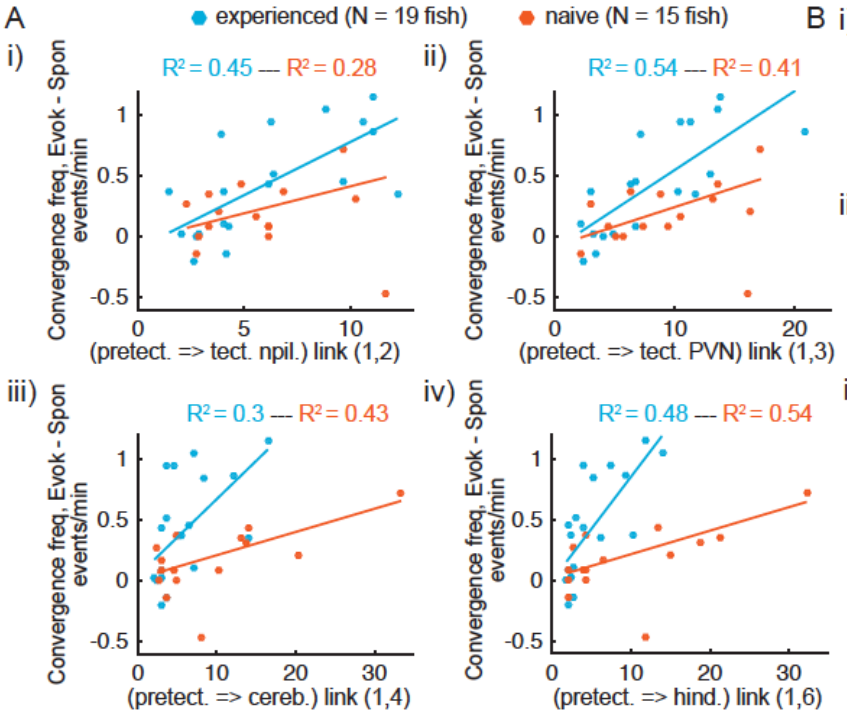

B i) preT => tect. npil. link (1,2)

source	tStat	pValue
Diet	0.52	0.61
GC (1,2)	4.50	**$9.5*10^{-5}$**
Diet*GC(1,2)	-1.53	0.14

ii) preT => tect. PVN link (1,3)

source	tStat	pValue
Diet	0.47	0.65
GC (1,3)	4.90	**$3.1*10^{-5}$**
Diet*GC(1,3)	-2.16	**0.04**

iii) preT => cereb. link (1,4)

source	tStat	pValue
Diet	-0.05	0.96
GC (1,4)	3.73	**0.0008**
Diet*GC(1,4)	-2.33	**0.03**

iv) preT => hind. link (1,6)

source	tStat	pValue
Diet	-0.08	0.94
GC (1,6)	4.98	**$2.5*10^{-5}$**
Diet*GC(1,6)	-3.53	**0.0014**

Figure 6. Prey capture probability depends on strength of pretectum connectivity to downstream areas and experience increases this dependence. A) Eye convergence frequency (evoked – spontaneous) is proportional to Granger-causality links in: i) pretectum→tectal neuropil; ii) pretectum→tectal PVN; iii) pretectum→cerebellum; iv) pretectum→hindbrain. Relationship is steeper in experienced (blue) than in naïve (red) fish. B) Robust linear regression model: [Convergence Frequency ~ 1 + Diet + GC + Diet*GC], where Convergence Frequency is (with prey – without prey), GC is Granger-causality Fstat, Diet is experienced or naïve fish (categorical variable), and Diet*GC is interaction. Models were significant for all links (link (1,2), Fstat=8.87, p=0.0002; (1,3), Fstat=10.6, $p=6.4x10^{-5}$; (1,4) Fstat=7.4, p=0.0007; (1,6), Fstat=12.1, $p=2.3x10^{-5}$). Significant terms are bolded, GC for all links, and (GC*diet) interactions for links (1,3), (1,4) and (1,6).

Figure 7

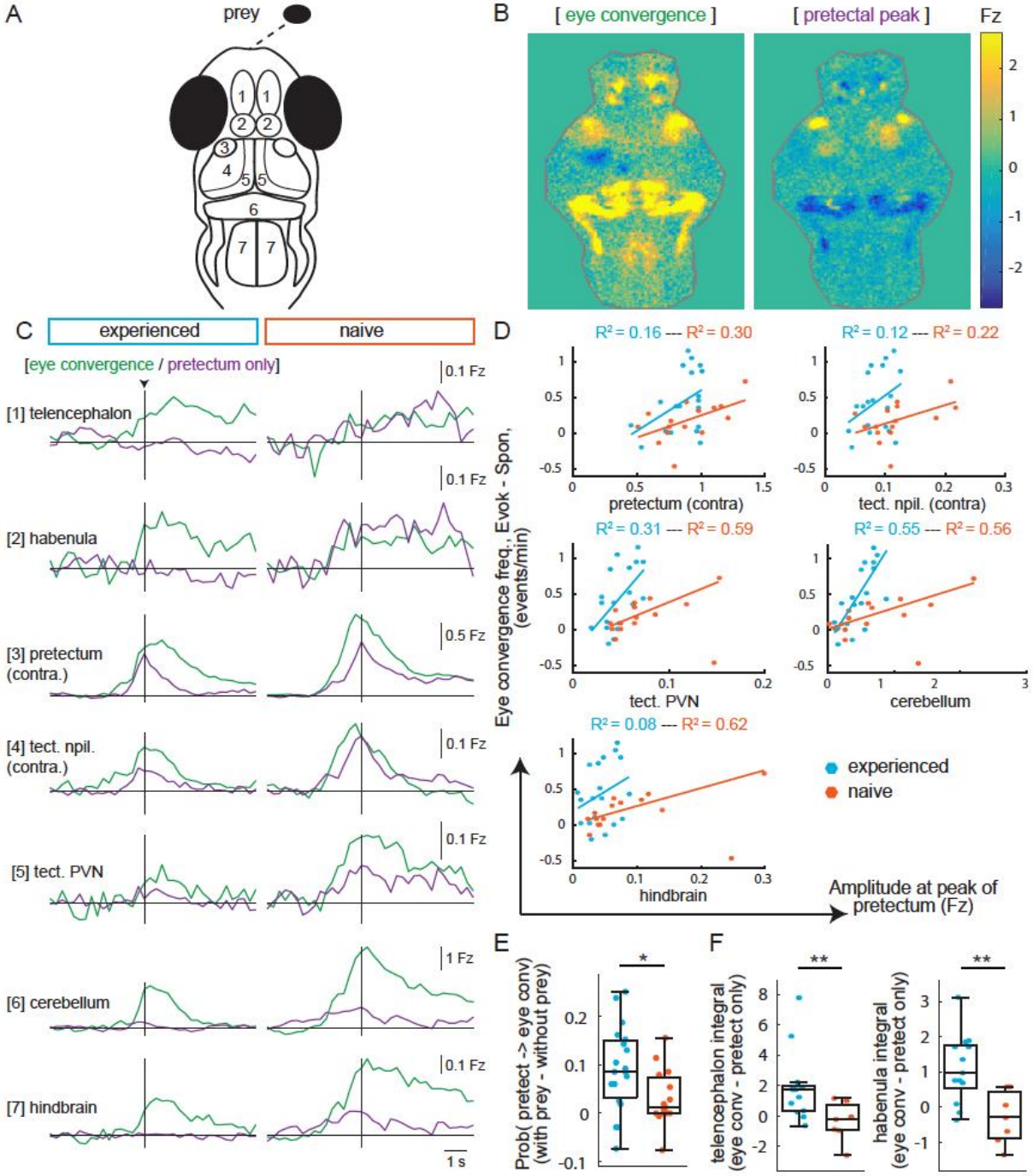
A
prey
1
2
3
4
5
6
7
B
[eye convergence]
[pretectal peak]
Fz
C
experienced
naive
[eye convergence / pretectum only]
[1] telencephalon
[2] habenula
[3] pretectum (contra.)
[4] tect. npil. (contra.)
[5] tect. PVN
[6] cerebellum
[7] hindbrain
0.1 Fz
0.5 Fz
1 Fz
1 s
D
R² = 0.16 --- R² = 0.30
pretectum (contra)
R² = 0.12 --- R² = 0.22
tect. npil. (contra)
R² = 0.31 --- R² = 0.59
tect. PVN
R² = 0.55 --- R² = 0.56
cerebellum
R² = 0.08 --- R² = 0.62
hindbrain
Eye convergence freq., Evok - Spon, (events/min)
experienced
naive
Amplitude at peak of pretectum (Fz)
E
Prob(pretect -> eye conv) (with prey - without prey)
F
telencephalon integral (eye conv - pretect only)
habenula integral (eye conv - pretect only)

Figure 7. Experience increases capture initiation-associated forebrain activity and lowers threshold for visual and motor activity to trigger capture initiation. A) Schematic of anatomical areas. B) Average brain activity maps for a representative experienced fish (#151210_6) in presence of prey, showing summed calcium activity over 4.2 seconds (5 frames before and 10 frames after) either eye convergence (prey left or right, n = 22) or pretectum transient that is not accompanied by behavior (n = 34). C) Time traces of activity in seven brain regions during either eye convergence (green) or pretectum transient with no behavior (purple) in representative experienced fish (left, fish #151120_3; n=12 convergences, n=42 pretectum-only events) and naïve fish (right, fish #151211_1, n=15 convergences, n=20 pretectum-only events). D) Evoked eye convergence frequency (frequency with prey – frequency without prey) as a function of fluorescence amplitude at pretectum peak (for all pretectal events) for pretectum, tectal neuropil, tectal PVNs, cerebellum and hindbrain. Each dot represents one fish, experienced in blue, naïve in red. Regression coefficients calculated using robust linear regression (see Supplementary Experimental Procedures). E) Probability of pretectum transient being associated with eye convergence (* indicates p = 0.01). F) Difference in fluorescence integral 5 frames before to 5 frames after event between eye convergences and pretectum-only events for experienced (blue) and naïve (red) fish in the telencephalon (left, p = 0.004) and the habenula (right, p = 0.0015). Fish with <5 eye convergences were excluded. ** indicates p < 0.01.

Figure S1

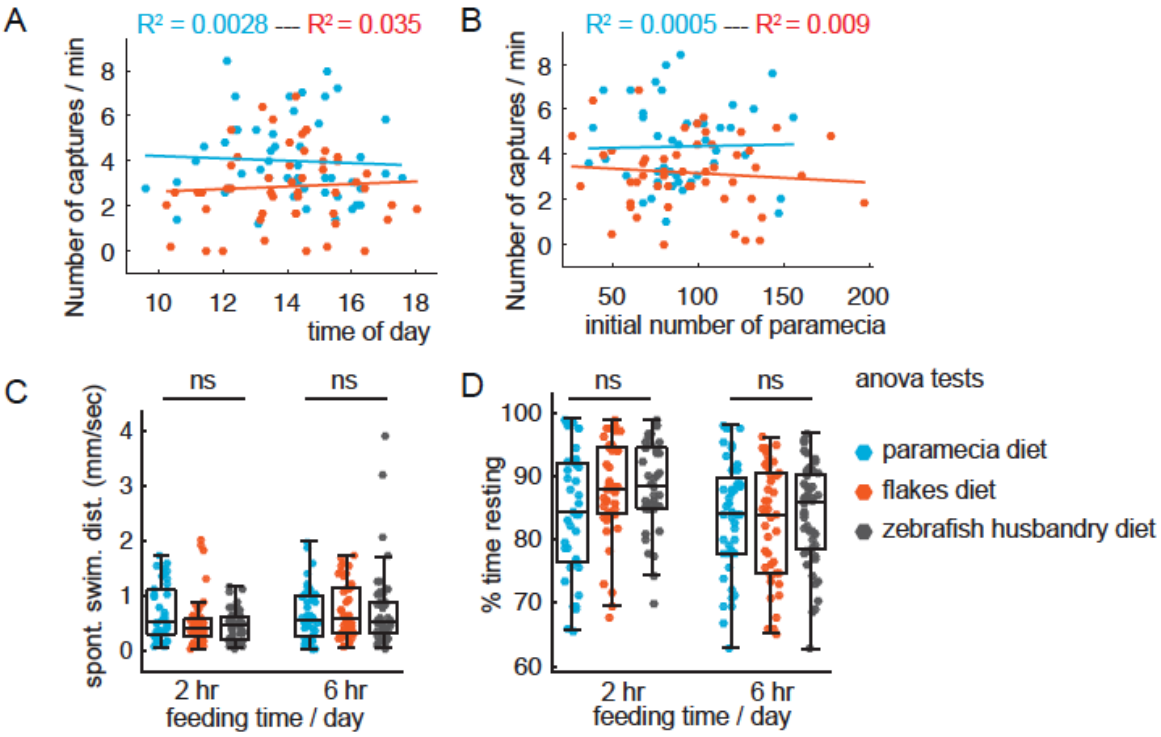

Figure S1. Lack of impact of other factors on prey capture performance. A, B) No effect on prey capture performance of time of day (A) or initial number of paramecia (B). C, D) No effect of diet on swimming. Spontaneous swimming velocity and percent of time spent resting similar in fish fed paramecia, flakes or pureed brine shrimp + dry food (husbandry diet) for (C) 2 hours or (D) 6 hrs./day not significantly different (one-way anova tests: spontaneous swimming velocity 2 hrs, Fstat = 2.95, p = 0.06; spontaneous swimming velocity 6 hrs, Fstat = 0.19, p = 0.83; % time resting 2 hrs, Fstat = 2.95, p = 0.06; % time resting 6 hrs, Fstat = 0.29, p = 0.75).

Figure S2

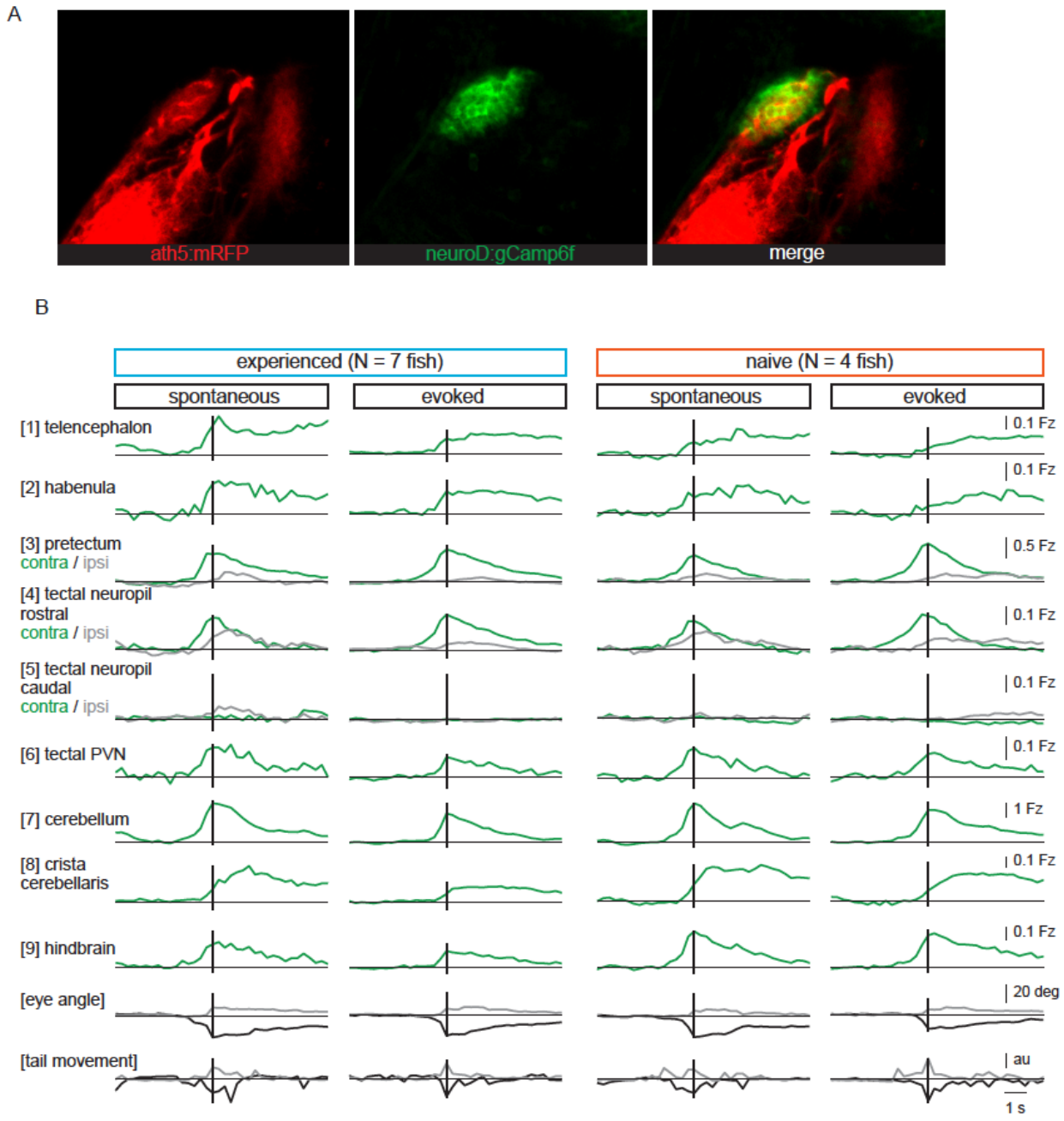

Figure S2. GCaMP6f expression pattern and time traces. A) Pretectum area of a 7 dpf *Tg(ath5:mRFP,neuroD:GCaMP6f)* fish. NeuroD-driven expression of GCaMP6f (green) includes pretectal neurons neurons in area AF7 that expresses mRFP (red) under the ath5 promoter. B) Composite GCaMP6f fluorescence time courses for experienced (N = 7) and naïve (N = 4) fish associated with eye convergence (vertical black line) for brain areas and behavioral measures shown in Figure 2H. Fish selected to have >10 eye convergences in presence of prey (evoked).

Figure S3

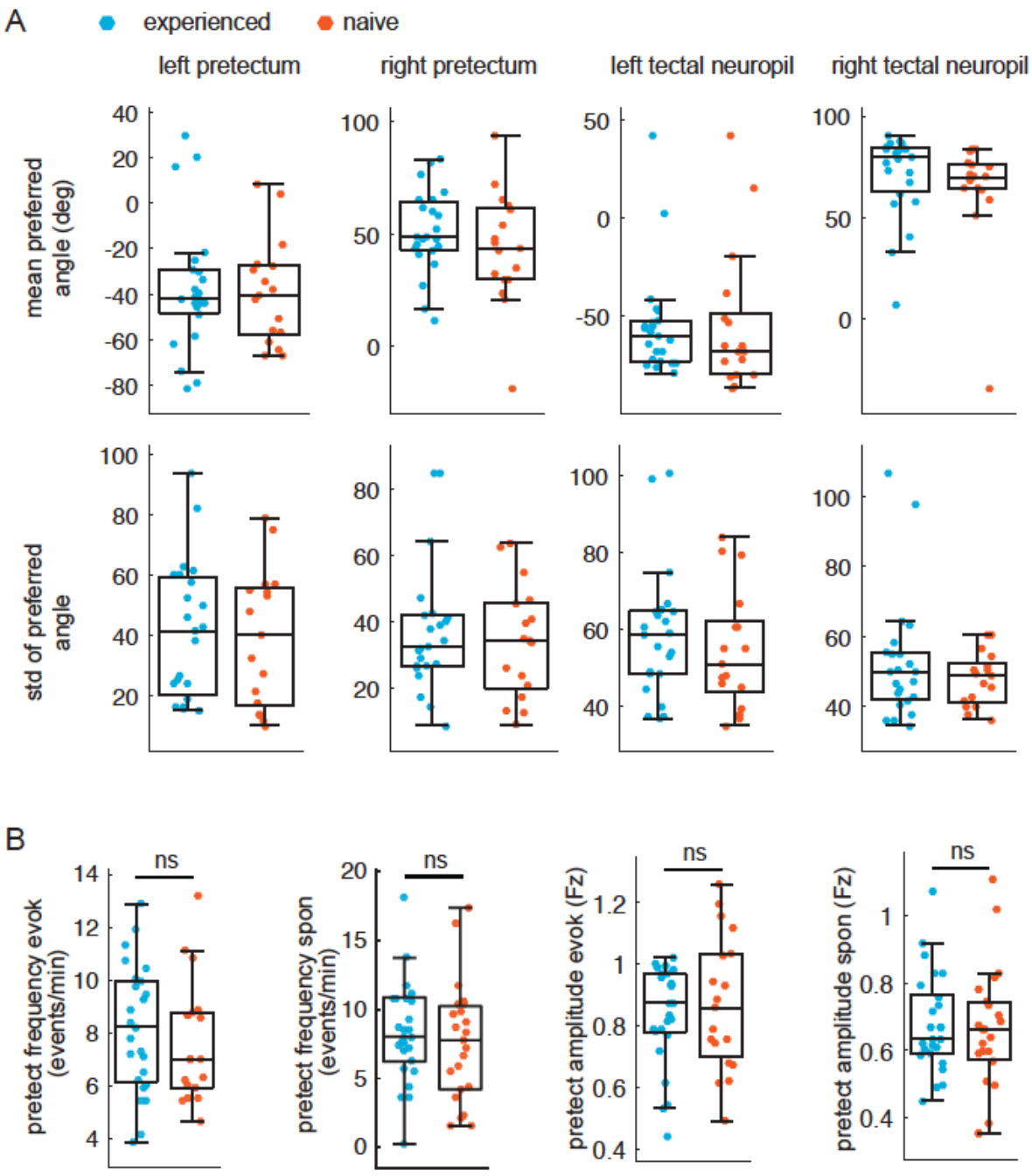

Figure S3. Similar retinotopic maps and pretectal events in experienced and naïve fish. A) The mean and standard deviation of the preferred angle distributions were indistinguishable between experienced and naïve fish. B) Average event frequency in left and right pretectums not different between experienced and naïve fish in either evoked (p=0.23, left) or spontaneous (p = 0.29, second from left) conditions. Average pretectum event amplitude was not different between

experienced and naïve fish in evoked (p = 0.73, second from right) or spontaneous (p = 0.34, right) conditions.

Figure S4

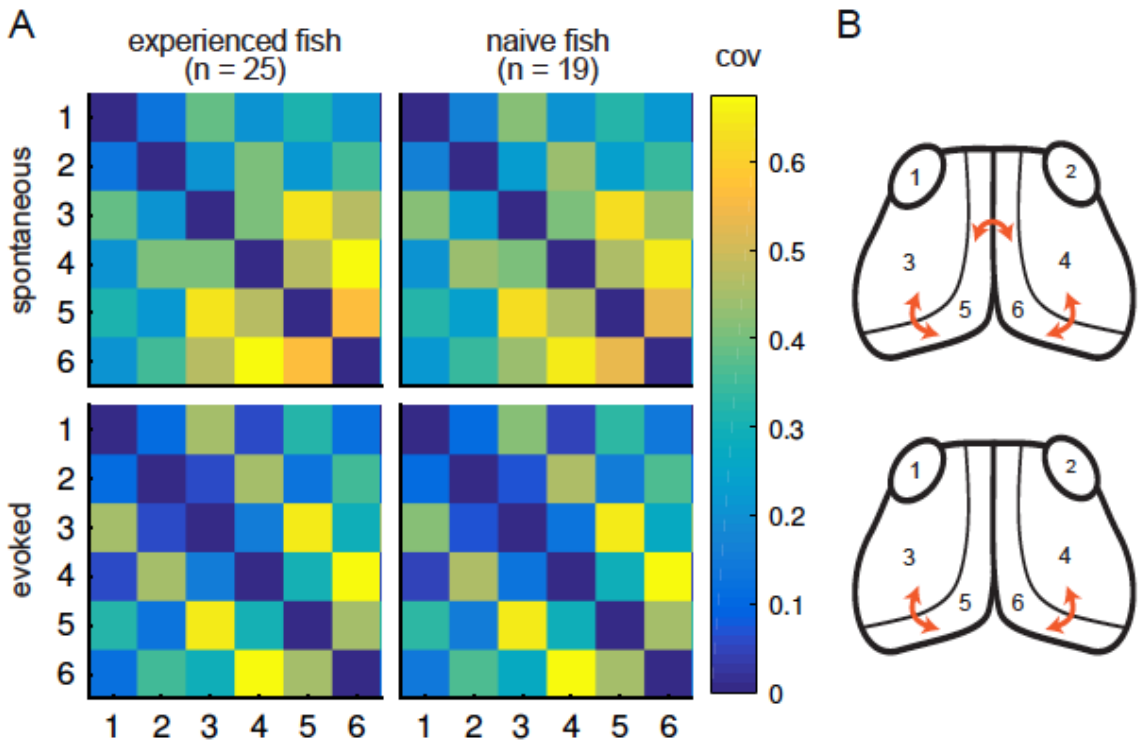

Figure S4. Experience does not affect circuit covariance in visual areas. A) Pair-wise covariance was calculated between the visual areas in spontaneous (top row) and evoked (bottom row) conditions and experienced (left column) and naïve (right column) fish. There were no statistical differences between experienced and naïve fish in the spontaneous or the evoked conditions (pair-wise t-tests, Bonferroni corrected). B) Links with linear correlation values higher than 0.5 for spontaneous (top) and evoked (bottom) conditions are represented by the orange arrows.

Figure S5

A

6 regions, Bonfferoni threshold for significance pThresh = 1.7.E-03

From Fig 4A: Experienced vs Naïve
Visual areas- spontaneous

	1	2	3	4	5	6
1		0.49	0.31	0.47	0.42	0.22
2	0.40		0.49	0.40	0.50	0.20
3	0.11	0.44		0.39	0.41	0.30
4	0.06	0.09	0.37		0.13	0.45
5	0.24	0.02	0.42	0.40		0.39
6	0.44	0.47	0.34	0.46	0.34	

From Fig 4A: Experienced vs Naïve
Visual areas - evoked

	1	2	3	4	5	6
1		0.27	0.22	0.48	0.18	0.46
2	0.32		0.12	0.45	0.19	0.36
3	0.21	0.30		0.32	0.49	0.12
4	0.15	0.32	0.24		0.31	0.33
5	0.17	0.19	0.26	0.26		0.26
6	0.23	0.26	0.41	0.18	0.16	

B

7 regions, Bonfferoni threshold for significance pThresh = 1.2.E-03

From Fig 5A: Experienced vs Naïve
Whole-brain circuit - evoked

	1	2	3	4	5	6	7
1	0.50	0.13	0.02	0.44	0.37	0.15	0.13
2	0.43	0.50	0.07	0.18	0.24	0.12	0.34
3	0.23	0.22	0.50	0.28	0.49	0.27	0.14
4	0.01	0.01	0.32	0.50	0.48	0.27	0.36
5	8.E-04	0.07	0.04	0.24	0.50	0.15	0.34
6	0.04	4.E-03	0.05	0.50	0.32	0.50	0.20
7	0.02	3.E-03	0.04	0.39	0.14	0.24	0.50

From Fig 5C: Strong vs Weak hunters
Whole-brain circuit - evoked

	1	2	3	4	5	6	7
1		0.29	0.10	0.33	0.32	0.27	0.23
2	0.40		0.49	0.37	0.08	0.09	0.29
3	0.31	0.46		5.E-04	2.E-06	3.E-04	4.E-05
4	0.21	0.16	0.28		0.09	0.12	0.26
5	0.42	0.16	0.44	0.16		0.30	0.47
6	0.11	0.29	0.37	0.28	0.01		0.02
7	0.43	0.29	0.48	0.30	0.49	0.06	

Figure S5. Statistical comparisons of Granger-causality links. A) p-values related to Figure 4. B) p-values related to Figure 5. Threshold for significance was divided by the number of pairwise comparisons being made.

Figure S6

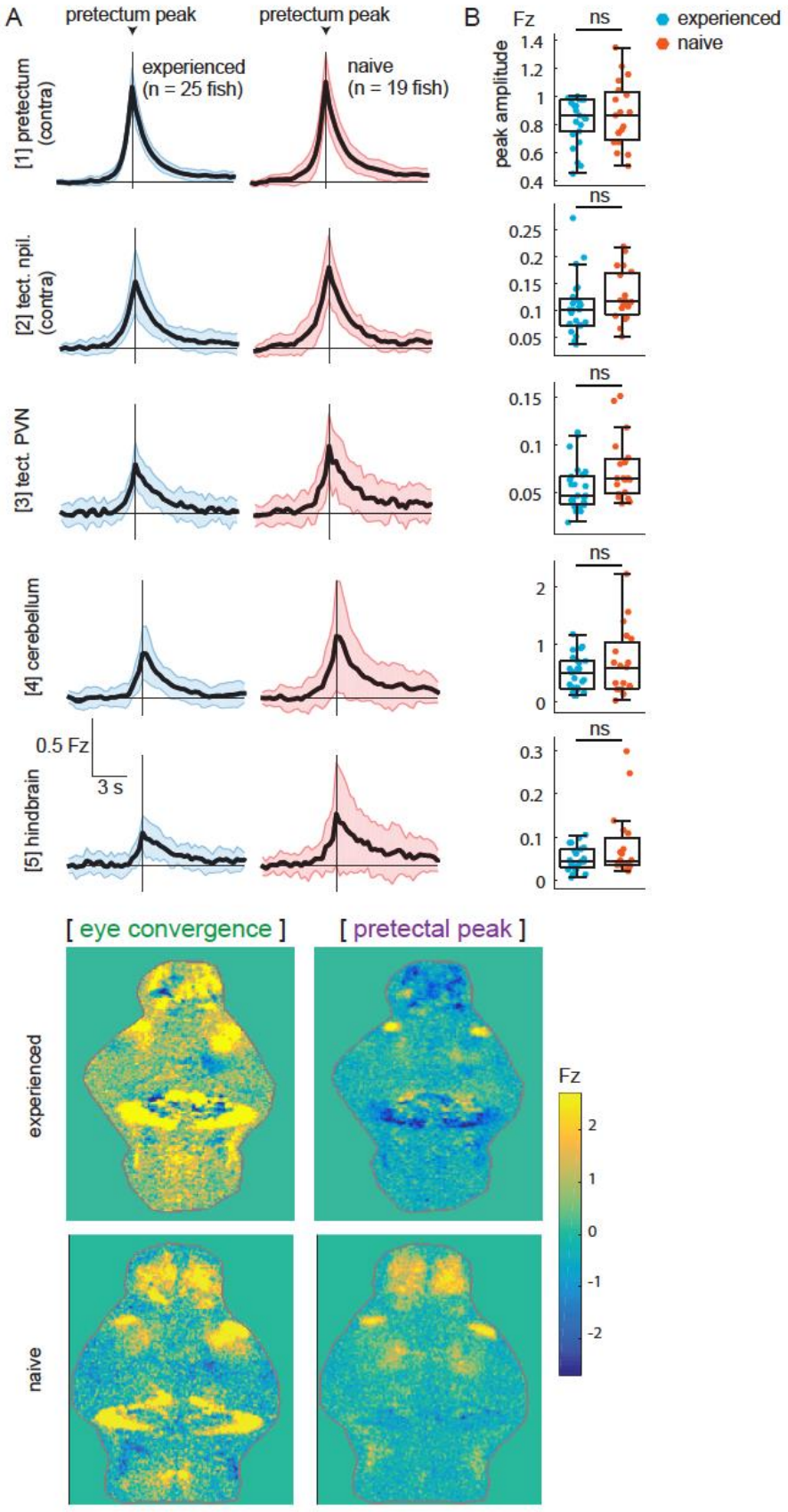
A
pretectum peak
pretectum peak
experienced
(n = 25 fish)
naive
(n = 19 fish)
[1] pretectum (contra)
[2] tect. npil. (contra)
[3] tect. PVN
[4] cerebellum
[5] hindbrain
0.5 Fz
3 s
B
Fz
ns
experienced
naive
peak amplitude
[eye convergence]
[pretectal peak]
experienced
naive
Fz

Figure S6. Comparison of pretectal-associated events in experienced and naïve fish. A) Composite fluorescence traces associated with all pretectum transients (combined with and without eye convergence) in the presence of prey in experienced fish (n=25, left column) and in naïve fish (n=19, right column). Mean fluorescence (black) and standard deviation across fish (shaded area, see Experimental Procedures). B) Mean peak amplitude of fluorescent events was not different between experienced and naïve fish. No significant differences after Bonferroni correction (threshold for significance = 0.01), permutation tests, pretectum p=0.23; tectal neuropil p=0.08; tectal PVNs p=0.02; cerebellum p=0.1; hindbrain p=0.05. C) Spatial distribution of summed calcium activity, as in to Figure 7B, for two additional representative fish. Experienced fish (top, fish #151210_2, n=16 eye convergences, n=31 tail flicks, n=35 pretectum-only events); Naïve fish (bottom, fish #151120_2, n=17 eye convergences, n=15 tail flicks, n=39 pretectum-only events).

References

1. Feldman, D.E. (2009) Synaptic mechanisms for plasticity in neocortex. Annu Rev Neurosci 32, 33–55.
2. Letzkus, J.J., Wolff, S.B.E., Meyer, E.M.M., Tovote, P., Courtin, J., Herry, C., et al. (2011) A disinhibitory microcircuit for associative fear learning in the auditory cortex. Nature 480, 331–5.
3. Matsumoto, M., Hikosaka, O. (2009) Two types of dopamine neuron distinctly convey positive and negative motivational signals. Nature 459, 837–41.
4. Ewert, J.P., Buxbaum-Conradi, H., Dreisvogt, F., Glagow, M., Merkel-Harff, C., Röttgen, A., et al. (2001) Neural modulation of visuomotor functions underlying prey-catching behaviour in anurans: Perception, attention, motor performance, learning. Comp. Biochem. Physiol. - A Mol. Integr. Physiol. 128, 417–61.
5. Bianco, I.H., Kampff, A.R., Engert, F. (2011) Prey capture behavior evoked by simple visual stimuli in larval zebrafish. Front. Syst. Neurosci. 5, 101.
6. Trivedi, C.A., Bollmann, J.H. (2013) Visually driven chaining of elementary swim patterns into a goal-directed motor sequence: a virtual reality study of zebrafish prey capture. Front Neural Circuits 7, 86.
7. Semmelhack, J.L., Donovan, J.C., Thiele, T.R., Kuehn, E., Laurell, E., Baier, H. (2014) A dedicated visual pathway for prey detection in larval zebrafish. Elife 4, 1–19.
8. Matsunaga, W., Watanabe, E. (2012) Visual motion with pink noise induces predation behaviour. Sci. Rep. 2, 1–7.
9. Payne, R.S. (1971) Acoustic location of prey by barn owls (Tyto alba). J. Exp. Biol. 54, 535–73.
10. Anjum, F., Brecht, M. (2012) Tactile experience shapes prey-capture behavior in Etruscan shrews. Front. Behav. Neurosci. 6, 1–8.
11. Elliott, C.J.H., Susswein, a J. (2002) Comparative neuroethology of feeding control in molluscs. J. Exp. Biol. 205, 877–96.
12. Borla, M.A., Palecek, B., Budick, S., O'Malley, D.M. (2002) Prey capture by larval zebrafish: Evidence for fine axial motor control. Brain. Behav. Evol. 60, 207–29.
13. McElligott, M.B., O'Malley, D.M. (2005) Prey tracking by larval zebrafish: Axial kinematics and visual control. Brain. Behav. Evol. 66, 177–96.
14. McClenahan, P., Troup, M., Scott, E.K. (2012) Fin-tail coordination during escape and predatory behavior in larval zebrafish. PLoS One 7, 1–11.
15. Patterson, B.W., Abraham, A.O., MacIver, M. a, McLean, D.L. (2013) Visually

guided gradation of prey capture movements in larval zebrafish. J. Exp. Biol. 216, 3071–83.

16. Bianco, I., Engert, F. (2015) Visuomotor Transformations Underlying Hunting Behavior in Zebrafish. Curr. Biol. 25, 831–46.

17. Gahtan, E. (2005) Visual Prey Capture in Larval Zebrafish Is Controlled by Identified Reticulospinal Neurons Downstream of the Tectum. J. Neurosci. 25, 9294–303.

18. Smear, M.C., Tao, H.W., Staub, W., Orger, M.B., Gosse, N.J., Liu, Y., et al. (2007) Vesicular Glutamate Transport at a Central Synapse Limits the Acuity of Visual Perception in Zebrafish. Neuron 53, 65–77.

19. Del Bene, F., Wyart, C., Robles, E., Tran, A., Looger, L., Scott, E.K., et al. (2010) Filtering of visual information in the tectum by an identified neural circuit. Science (80-.). 330, 669–73.

20. Fajardo, O., Zhu, P., Friedrich, R.W. (2013) Control of a specific motor program by a small brain area in zebrafish. Front. Neural Circuits 7, 67.

21. Muto, A., Kawakami, K. (2013) Prey capture in zebrafish larvae serves as a model to study cognitive functions. Front. Neural Circuits 7, 110.

22. Burrill, J.D., Easter, S.S. (1994) Development of the retinofugal projections in the embryonic and larval zebrafish (Brachydanio rerio). J Comp Neurol 346, 583–600.

23. Luque, M.A., Perez-Perez, M.P., Herrero, L., Torres, B. (2005) Involvement of the optic tectum and mesencephalic reticular formation in the generation of saccadic eye movements in goldfish. Brain Res. Rev. 49, 388–97.

24. Rupprecht, P., Prendergast, A., Wyart, C., Friedrich, R.W. (2016) Remote z-scanning with a macroscopic voice coil motor for fast 3D multiphoton laser scanning microscopy. Biomed. Opt. Express 7, 1656.

25. Scott, E.K., Baier, H. (2009) The cellular architecture of the larval zebrafish tectum, as revealed by gal4 enhancer trap lines. Front. Neural Circuits 3, 1–14.

26. Karlstrom, R.O., Trowe, T., Bonhoeffer, F. (1997) Genetic analysis of axon guidance and mapping in the zebrafish. Trends Neurosci. 20, 3–8.

27. Nishimoto, S., Vu, A.T., Naselaris, T., Benjamini, Y., Yu, B., Gallant, J.L. (2011) Reconstructing visual experiences from brain activity evoked by natural movies. Curr. Biol. 21, 1641–6.

28. Huth, A.G., Heer, W.A. De, Griffiths, T.L., Theunissen, F.E., Jack, L. (2016) Natural speech reveals the semantic maps that tile human cerebral cortex. Nature.

29. Friston, K.J. (1994) Functional and effective connectivity in neuroimaging: A synthesis. Hum. Brain Mapp. 2, 56–78.

30. Granger, A.C.W.J. (1969) Investigating Causal Relations by Econometric Models

and Cross-spectral Methods. Econometrica 37, 424–38.

31. Seth, A.K., Barrett, A.B., Barnett, L. (2015) Granger Causality Analysis in Neuroscience and Neuroimaging. J. Neurosci. 35, 3293–7.

32. De Vico Fallani, F., Corazzol, M., Sternberg, J.R., Wyart, C., Chavez, M. (2015) Hierarchy of neural organization in the embryonic spinal cord: Granger-causality graph analysis of in vivo calcium imaging data. IEEE Trans. Neural Syst. Rehabil. Eng. 23, 333–41.

33. Nevin, L.M., Robles, E., Baier, H., Scott, E.K. (2010) Focusing on optic tectum circuitry through the lens of genetics. BMC Biol. 8, 126.

34. Preuss, S.J., Trivedi, C.A., Vom Berg-Maurer, C.M., Ryu, S., Bollmann, J.H. (2014) Classification of object size in retinotectal microcircuits. Curr. Biol. 24, 2376–85.

35. Bae, Y.K., Kani, S., Shimizu, T., Tanabe, K., Nojima, H., Kimura, Y., et al. (2009) Anatomy of zebrafish cerebellum and screen for mutations affecting its development. Dev. Biol. 330, 406–26.

36. Heap, L.A., Goh, C.C., Kassahn, K.S., Scott, E.K. (2013) Cerebellar output in zebrafish: an analysis of spatial patterns and topography in eurydendroid cell projections. Front. Neural Circuits 7, 53.

37. Hiramoto, M., Cline, H.T. (2009) Convergence of multisensory inputs in xenopus tadpole tectum. Dev. Neurobiol. 69, 959–71.

38. Teyke, T. (1995) Food attraction conditioning in the snail, helix-pomatia. J. Comp. Physiol. 177, 409–14.

39. Westphal, R.E., O'Malley, D.M. (2013) Fusion of locomotor maneuvers, and improving sensory capabilities, give rise to the flexible homing strikes of juvenile zebrafish. Front Neural Circuits 7, 108.

40. Temizer, I., Donovan, J.C., Baier, H., Semmelhack Correspondence, J.L., Semmelhack, J.L. (2015) A Visual Pathway for Looming-Evoked Escape in Larval Zebrafish. Curr. Biol. 25, 1823–34.

41. Barnett, P.D., Nordstrom, K., O'Carroll, D.C. (2007) Retinotopic Organization of Small-Field-Target-Detecting Neurons in the Insect Visual System. Curr. Biol. 17, 569–78.

42. Wiederman, S.D., Shoemaker, P. a, O'Carroll, D.C. (2013) Correlation between OFF and ON channels underlies dark target selectivity in an insect visual system. J. Neurosci. 33, 13225–32.

43. Carrillo, A., McHenry, M.J. (2016) Zebrafish learn to forage in the dark. J. Exp. Biol. 219, 582–9.

44. Volkmann, K., Rieger, S., Babaryka, A., Köster, R.W. (2008) The zebrafish cerebellar rhombic lip is spatially patterned in producing granule cell populations of different functional compartments. Dev. Biol. 313, 167–80.

45. Mueller, T., Dong, Z., Berberoglu, M., Guo, S. (2011) The dorsal pallium in zebrafish, Danio rerio (Cyprinidae, Teleostei). Brain Res., 95–105.

46. Agetsuma, M., Aizawa, H., Aoki, T., Nakayama, R., Takahoko, M., Goto, M., et al. (2010) The habenula is crucial for experience-dependent modification of fear responses in zebrafish. Nat Neurosci 13, 1354–6.

47. Chou, M., Amo, R., Kinoshita, M., Cherng, B., Shimazaki, H., Agetsuma, M., et al. (2016) Social conflict resolution regulated by two dorsal habenular subregions in zebrafish 352, 599–602.

48. Jetti, S.K., Vendrell-Llopis, N., Yaksi, E. (2014) Spontaneous activity governs olfactory representations in spatially organized habenular microcircuits. Curr. Biol. 24, 434–9.

49. Yokogawa, T., Hannan, M.C., Burgess, H.A. (2012) The Dorsal Raphe Modulates Sensory Responsiveness during Arousal in Zebrafish 32, 15205–15.

50. Boulougouris, V., Tsaltas, E. (2008) Serotonergic and dopaminergic modulation of attentional processes. Prog. Brain Res. 172, 517–42.

51. Carter, M.E., Yizhar, O., Chikahisa, S., Nguyen, H., Adamantidis, A., Nishino, S., et al. (2010) Tuning arousal with optogenetic modulation of locus coeruleus neurons. Nat. Neurosci. 13, 1526–33.

52. Mahler, S. V, Moorman, D.E., Smith, R.J., James, M.H., Aston-Jones, G. (2014) Motivational activation: a unifying hypothesis of orexin/hypocretin function. Nat. Neurosci. 17, 1298–303.

53. Lee, S.H., Dan, Y. (2012) Neuromodulation of Brain States. Neuron 76, 109–222.

54. Filosa, A., Barker, A.J., Dal Maschio, M., Baier, H. (2016) Feeding State Modulates Behavioral Choice and Processing of Prey Stimuli in the Zebrafish Tectum. Neuron, 1–13.

55. McGraw, H., Snelson, C.D., Prendergast, A., Suli, A., Raible, D.W. (2012) Postembryonic neuronal addition in Zebrafish dorsal root ganglia is regulated by Notch signaling. Neural Dev. 7, 23.

56. Zolessi, F.R., Poggi, L., Wilkinson, C.J., Chien, C.-B., Harris, W. a. (2006) Polarization and orientation of retinal ganglion cells in vivo. Neural Dev. 1, 2.

57. Brainard, D.H. (1997) The Psychophysics Toolbox. Spat. Vis. 10, 433–6.

58. Good, P. (2005) Permutation, Parametric and Bootstrap Tests of Hypotheses. Springer; .

59. Vladimirov, N., Mu, Y., Kawashima, T., Bennett, D. V, Yang, C.-T., Looger, L.L., et al. (2014) Light-sheet functional imaging in fictively behaving zebrafish. Nat. Methods 11, 883–4.

60. Wolf, S., Supatto, W., Debrégeas, G., Mahou, P., Kruglik, S.G., Sintes, J., et al.

(2015) Whole-brain functional imaging with two-photon light-sheet microscopy MiXCR : software for comprehensive adaptive immunity profiling. Nat. Publ. Gr. 12, 379–80.

61. Muto, A., Ohkura, M., Abe, G., Nakai, J., Kawakami, K. (2013) Real-time visualization of neuronal activity during perception. Curr. Biol. 23, 307–11.

62. Benjamini, Y., Hochberg, Y. (1995) Controlling the False Discovery Rate : A Practical and Powerful Approach to Multiple Testing. J. R. Stat. Soc. 57, 289–300.

63. Bressler, S.L., Seth, A.K. (2011) Wiener-Granger Causality: A well established methodology. Neuroimage 58, 323–9.

64. Gourevitch, B., Le Bouquin-Jeannes, R., Faucon, G. (2006) Linear and nonlinear causality between signals: Methods, examples and neurophysiological applications. Biol. Cybern. 95, 349–69.

65. Akaike, H. (1974) A new look at the statistical model identification. IEEE Trans. Automat. Contr. 19, 716–23.

66. Kaminski, M., Liang, H. (2005) Causal influence: advances in neurosignal analysis. Crit. Rev. Biomed. Eng. 33, 347–430.

Chapter 4:

Conclusion and Discussion

For this dissertation I used advances in microscopy and neural activity imaging methods to probe how experience affects neural activity and behavior. In my first project in collaboration with others, I studied the motor neuron circuitry in the developing zebrafish spinal cord. It had previously been established that spinal cord neurons of vertebrates fire spontaneously early in the development of the motor system[1], and that later these neurons displayed patterns of correlated activity[2]. Our study revealed the transition of the whole network from slow, sporadic activity to fast, ipsilaterally correlated and contralaterally anticorrelated activity (Chapter 2). We determined that disrupting the emergence of synchronized activity impairs normal development of spinal cord circuits. In my second project, I studied how experience of prey alters prey capture behavior and underlying neural activity. Although larval zebrafish were previously thought to be incapable of learning[3], I demonstrated that experienced fish initiate more prey capture sequences than their naïve counterparts (Chapter 3). The motor steps of the behavior, as well as the ability to see the prey were not affected. Rather, incoming visual information to the pretectum was more likely to trigger a prey capture initiation event in experienced fish, possibly due to increased activity in the forebrain of those fish.

As discussed in the introduction, while learning and memory is well studied at the behavioral level, and cellular and molecular mechanisms that drive neural plasticity are well established, relatively little work has focused on how changes in different brain areas are integrated together to produce learning. In this project, by using a small animal model whose whole nervous system can be imaged in a single field of view, I was able to probe the effect of a naturally occurring learning experience, hunting, on the nervous system. To understand how behavior is encoded in the brain, there is a growing effort to image activity in as many neurons as possible, with the ultimate goal of recording from every single neuron in the brain. On the short- to medium term, an attractive way to achieve this goal is to image from small brains[4]. During the time of my PhD research, imaging techniques have vastly improved in particular for the larval zebrafish, popular for its small size and transparency. Using 1-photon light-sheet microscopy one can acquire a whole brain volume of spontaneous activity at up to 3Hz with cellular resolution [5,6], light-field microscopy imaged volumes can be reconstructed from single frames[7], or using traditional 2-photon microscopy one can reconstitute whole brain activity in response to a simple stimulus by acquiring multiple trials per plane and stitching data back together post-hoc [8,9]. Imaging systems that would have allowed us to achieve the desired type of speed and to record volumes for studying prey capture behavior are not yet commercially available[6,10]. However, future technical developments will undoubtedly continue to improve our ability to image volumetric brain activity underlying complex behaviors at cellular resolution.

Acquiring activity from individual neurons in whole brains over multiple minutes quickly generate datasets on the order of terabits, even for organisms with small brains such as the worm, fly and fish. Advances in microscopy are only advantageous because

they have been accompanied by equal strides in processing power of computers, and by integrating computational methods in the neurophysiologist toolkit[11]. For the two projects in this dissertation, we used a combination of dimensionality reduction, regression, and causality methods. Analyzing calcium imaging datasets presents much of the same challenges that functional magnetic resonance imaging (fMRI) encounters. The predictive encoding model method we used to analyze how pixel time series vary with prey position was first developed by a human fMRI laboratory. As for Granger causality, the method is classically applied in EEG and MEG in humans to determine how activity in one brain area predicts activity in another in order to establish functional links[12]. All of the analyses in this dissertation were made possible by collaborations with mathematicians and computational neuroscientists, an illustration of the importance of incorporating different expertises to advance in systems neuroscience.

Our study showed that experience increases the gain of pretectal activity on motor area activity: an increase cerebellum or hindbrain activity following a pretectal transient leads to a higher probability of evoking a prey capture initiation in experienced fish. The change in gain control could be driven by the forebrain. This effect is reminiscent of the role of the medial prefrontal cortex (mPFC) of mammals in controlling selective attention. It has recently been suggested that the mPFC acts as a filter for behaviorally relevant stimuli[13], receiving input from neuromodulatory systems, and exerting top-down control on stimulus saliency. My work opened new questions in investigating the role of the forebrain in controlling prey capture: are there specific sub-regions that are important? Are there also neuromodulatory systems that convey valence information to the forebrain? How does the forebrain act on downstream circuitry? How does control of hunting behavior relate to control of other behaviors? And how does it relate to control of behavior in mammals? Future experiments taking advantage of advances in microscopy, computational analysis, and optogenetics, will address these questions.

References

1. Gu, X., Olson, E. C. & Spitzer, N. C. Spontaneous neuronal calcium spikes and waves during early differentiation. *J. Neurosci.* **14,** 6325–6335 (1994).
2. Nakayama, K., Nishimaru, H. & Kudo, N. Basis of changes in left-right coordination of rhythmic motor activity during development in the rat spinal cord. *J. Neurosci.* **22,** 10388–10398 (2002).
3. Fero, K., Yokogawa, T. & Burgess, H. A. The behavioral repertoire of larval zebrafish. *Neuromethods* **52,** 249–291 (2011).
4. Ahrens, M. B. & Engert, F. Large-scale imaging in small brains. *Curr. Opin. Neurobiol.* **32,** 78–86 (2015).
5. Ahrens, M. B., Orger, M. B., Robson, D. N., Li, J. M. & Keller, P. J. Whole-brain functional imaging at cellular resolution using light-sheet microscopy. *Nat Methods* **10,** 413–420 (2013).

6. Vladimirov, N. *et al.* Light-sheet functional imaging in fictively behaving zebrafish. *Nat. Methods* **11,** 883–884 (2014).

7. Prevedel, R. *et al.* Simultaneous whole-animal 3D imaging of neuronal activity using light-field microscopy. *Nat. Methods* **11,** 727–30 (2014).

8. Ahrens, M. B. *et al.* Brain-wide neuronal dynamics during motor adaptation in zebrafish. *Nature* **485,** 471–477 (2012).

9. Portugues, R., Feierstein, C. E., Engert, F. & Orger, M. B. Whole-brain activity maps reveal stereotyped, distributed networks for visuomotor behavior. *Neuron* **81,** 1328–1343 (2014).

10. Wolf, S. *et al.* Whole-brain functional imaging with two-photon light-sheet microscopy MiXCR : software for comprehensive adaptive immunity profiling. *Nat. Publ. Gr.* **12,** 379–380 (2015).

11. Freeman, J. *et al.* Mapping brain activity at scale with cluster computing. *Nat. Methods* **11,** 941–950 (2014).

12. De Vico Fallani, F., Corazzol, M., Sternberg, J. R., Wyart, C. & Chavez, M. Hierarchy of neural organization in the embryonic spinal cord: Granger-causality graph analysis of in vivo calcium imaging data. *IEEE Trans. Neural Syst. Rehabil. Eng.* **23,** 333–341 (2015).

13. Popescu, A. T., Zhou, M. R. & Poo, M. Phasic dopamine release in the medial prefrontal cortex enhances stimulus discrimination. *Proc. Natl. Acad. Sci.* 201606098 (2016). doi:10.1073/pnas.1606098113